Establishing a Humanized Mouse Model to Study Prions

Dissertation
zur
Erlangung der naturwissenschaftlichen Doktorwürde
(Dr. sc. nat.)
vorgelegt der
Mathematisch-naturwissenschaftlichen Fakultät
der
Universität Zürich
von

Gregor Andrea Hutter
von
Diepoldsau SG

Promotionskomitee:
Prof. Dr. med. Dr. sc. nat. h. c. Adriano Aguzzi
(Leitung der Dissertation)
Prof. Dr. sc. nat. Burkhard Becher (Vorsitz)
Prof. Dr. sc. nat. Lukas Sommer
Prof. Dr. med. Roland Zimmermann
PD Dr. med. Roberto Speck

Zürich, 2008

Contents

Summary - Zusammenfassung **7**

I. Establishing a Humanized Mouse Model to Study Prions **11**

1. Introduction **13**
1.1. Prion diseases in humans, mice and cattle . . . 13
1.1.1. Historical perspective . . . 13
1.1.2. sCJD - clinical picture . . . 14
1.2. The nature of PrP^{Sc} and genetics . . . 17
1.3. Assigned functions to PrP^{C} . . . 18
1.4. Functions of PrP^{C} in the immune system . . . 19
1.4.1. Physiological function of PrP^{C} . . . 19
1.4.2. Peripheral immune system and prion disease . . . 21
1.5. Modeling a human adaptive immune system in mice for studying prion diseases . . . 22
1.5.1. Historical overview and perspectives . . . 22
1.5.2. A humanized model for prion disease . . . 24
1.6. Genetic background and experimental outcome . . . 24
1.7. Experimental plan and outline of the work . . . 25

2. Material and Methods **27**
2.1. Genetically modified mice, breeding strategy . . . 27
2.1.1. *Rag*$1^{-/-}$ and *Rag*$2^{-/-}$ mice . . . 27
2.1.2. "Zurich1"-*Prnp*$^{-/-}$ mice . . . 27
2.1.3. *Il2rg*$^{-/-}$-mice . . . 28
2.1.4. Tg*PRNP*129M mice . . . 28
2.1.5. Breeding strategy . . . 28
2.2. Genotyping of genetically modified mice . . . 29
2.3. Microsatellite mapping . . . 29
2.4. SNP mapping of chromosome 2 . . . 33
2.5. Sequencing of the human *PRNP* coding region for detection of polymorphism on codon 129 . . . 34
2.6. Sequencing of *Sirpa* exon 2 in different mouse strains . . . 34
2.7. Histology and immunohistochemistry . . . 34
2.8. Cord blood acquisition and preparation of CD34+ hematopoietic stem cells 35
2.9. Cell and tissue culture of hematopoietic stem cells . . . 35
2.10. Immunoblotting . . . 36

2.11. Flowcytometry 37

3. Results **41**
3.1. Breeding of genetically modified mice 41
3.1.1. *Rag*1$^{-/-}$ *Prnp*$^{-/-}$ *Il2rg*$^{-/-}$ mice 41
3.1.2. *Rag*2$^{-/-}$ *Prnp*$^{-/-}$ *Il2rg*$^{-/-}$ mice 42
3.1.3. Tg*PRNP*129M mice 44
3.1.4. STR-marker assisted backcrossing 45
3.2. CD34+ stem cell enrichment 52
3.2.1. Sequence analysis for human *PRNP* polymorphisms in the donor cord blood 52
3.3. Reconstitution with allogeneic bone marrow 54
3.4. Reconstitution with enriched stem cells 55
3.4.1. Reconstitution of BALB/c mice 55
3.4.2. Reconstitution of backcrossed mice 55
3.4.3. Reconstitution of backcrossed Tg*PRNP*129M mice 57
3.5. Reconstitution with expanded cells 60
3.6. Expression analysis of PrP in bone marrow 60
3.7. Additional SNP and STR on Chromosome 2 62
3.8. Analysis of signal regulatory protein alpha haplotypes and correlation to reconstitution outcomes 66
3.9. Meiotic recombination screening between *Sirpa* and *Prnp*, subsequent reconstitutions 66

4. Discussion **69**

5. Conclusion **75**

II. Global Gene Expression Analysis of PrP^{Sc} infected neuronal cells **77**

6. Introduction **79**
6.1. Introduction 80

7. Material and Methods **83**
7.1. Cell culture (N2aPK1 cells, CAD cells, GT1 cells) 83
7.2. Prion infection of cell lines (N2aPK1RML, CADRML, GT1RML cells) . . 83
7.3. Assessment of the infection ratio in RML infected cells (N2aPK1RML, CADRML, GT1RML cells) 83
7.4. Western blot detection of PrP^{Sc} 85
7.5. Preparation of labeled cRNA, microarray hybridization and data analysis 85
7.6. Quantitative Real-time PCR 86

8. Results **89**
8.1. In vitro cell culture models of prion infection 89

8.2. Transcriptional analysis 91
8.3. Gene expression in CAD cells 94
8.4. qPCR analysis results reported by others 94

9. Discussion **99**

A. List of figures **103**

B. List of tables **105**

C. Abbreviations **107**

D. Curriculum vitae Gregor Andrea Hutter **109**

E. Acknowledgments **113**

Bibliography **115**

Summary - Zusammenfassung

Transmissible spongiform encephalopathies (TSEs), also termed prion diseases, are lethal neurodegenerative diseases of humans and animals including bovine spongiform encephalopathy (BSE) in cattle, scrapie in sheep, chronic wasting disease (CWD) in deer and elk and Creutzfeldt-Jakob disease (CJD) in humans. Prion disease in humans (and animals) can occur by peripheral infection of the host (e.g. via an oral route of infection or iatrogenic transmission). According to the "protein-only" hypothesis the major component of the prion agent is an abnormal variant of the cellular prion protein (PrP^C), termed PrP^{Sc}. Intensive studies of prion pathogenesis suggest that the immnune system is a catalyst of prion replication/propagation long before the pathological agent finds its way into the brain.
In the first part of this thesis I will discuss the establishment of a "humanized mouse model" for prion diseases using human umbilical cord blood transplanted immunodeficient mice. This model might be employed to address many open questions in peripheral prion biology and would serve as an efficient in vivo test system for preclinical studies and diagnostic procedures. We were able to replicate a current model based on a publication of Traggiai et al. [119] and to induce a human adaptive immune system in BALB/c Rag2-Il2rg$^{-/-}$ mice. We therefore set out to modify this model by a complex strategy to generate "humanized mice" devoid of endogenous murine PrP^C and, in a later stage of the project, have re-inserted a human PrP transgenically to mimic further stages of disease progression beyond the immune system.

Interestingly, we did not succeed in engrafting immunodeficient mice devoid of PrP^C even though we employed a microsatellite based monitoring and backcrossing strategy to strongly control for the genetic background of the grafted recipient mice because currently unknown genetic factors modulate the innate response to xenografting. Littermates carrying at least one allele of *Prnp* were successfully engrafted whereas reconstitutability was abrogated in mice devoid of PrP^C. We show that PrP^C is highly expressed in homing compartments of the engrafted cells, especially in bone marrow macrophages and B-cell precursors indicating a possible function of *Prnp* in modulating xenogeneic stem cell engraftment. However, this phenomenon could not be rescued by mice expressing a human PrP transgene on a mouse PrP deficient background and exhibiting an equivalent STR marker profile as compared to reconstitutable mice, implicating that other genetic factors in the region of *Prnp* might be modulating the engraftment behaviour of xenogeneic cells. A more detailed STR analysis in the region around *Prnp* indicated that around 9 megabases of the *Prnp*- chromosome were still present in most of our backcrossed recipient mice. A recent publication of a polymorphic gene coding for signal regulatory protein alpha (Sirpa), very closely linked to *Prnp*, explained our observations to a great extent. A meiotic recombination screen finally led to a *Prnp*$^{-/-}$ mouse that is reconstitutable with human stem cells and serves as an ideal model since human *PRNP* expression is

restricted to the grafted cells.

The second part of this thesis describes a screen for genes that are differentially regulated upon prion infection in cell culture models of prion infection. A comparative transcriptional analysis revealed transcriptional stability of cultured neuroblastoma cells upon prion infection. Although highly infected, cells did not display consistent changes in transcriptional profiles as a response to prion infection. Several transcripts previously reported by others to be differentially expressed in prion-infected cells could not be confirmed in our assays. Most likely these discrepancies can be attributed to the technical stringency of the current study which was performed under conditions designed to minimize potential genetic drift. Therefore, it is concluded there are no universal transcriptional changes induced by prion infection of neuronal cells in vitro.

Zusammenfassung

Prionenerkrankungen sind obligat tödlich endende Erkrankungen des zentralen Nervensystems, welche bei Menschen und Tieren vorkommen. Die wichtigsten Entitäten sind die Creutzfeldt-Jacob Erkrankung (CJD) bei Menschen, die bovine spongiforme Enzephalopathie (BSE) bei Rindern, Scrapie bei Schafen und die Chronic Wasting Disease (CWD) bei Elchen. Prionenerkrankungen können durch Inokulation des Erregers in periphere Organe oder Organe des zentralen Nervensystems übertragen werden, z.B. peroral oder iatrogen. Gemäss der "protein-only" Hypothese besteht das pathogene Agens, PrP^{Sc}, hauptsächlich aus einer anders konformierten Variante eines zellständigen Proteins (PrP^{C}), welches sowohl im Immunsystem als auch im Nervensystem vorkommt. Zahlreiche Arbeiten über die Pathogenese von Prionenerkrankungen belegen, dass das Immunsystem ein Katalysator der Replikation von PrP^{Sc} darstellt, lange bevor das infektiöse Agens in das Nervensystem gelangt.

Im ersten Teil dieser Arbeit stelle ich die Etablierung eines "humanisierten Mausmodells" für Prionenerkrankungen vor. Hierbei benutzten wir haematopoietische Stammzellen aus Nabelschnurblut, welches wir in immundefiziente, neugeborene Mäuse transplantierten. Dieses Modell könnte sowohl für diagnostische Tests und praeklinische Studien als auch für grundlegende Fragen in der Prionenbiologie angewendet werden. Zunächst gelang es uns, ein bestehendes Modell, basierend auf der Methode von Traggiai et al. [119] zu reproduzieren, indem wir ein humanes adaptives Immunsystem in BALB/c $Rag2^{-/-}Il2rg^{-/-}$ Mäusen induzieren konnten. Wir entschlossen uns daher, dieses Modell dahingehend zu modifizieren, dass wir das endogene Maus-PrP^{C} mit einer komplexten Zuchtstrategie auf genetischem Wege entfernten und, in einer späteren Phase, ein humanes PrP-Transgen hineinkreuzten, um spätere Krankheitsstadien (Neuroinvasion) zu untersuchen. Jedoch gelang es uns nicht, *Prnp*-defiziente Mäuse mit humanen Stammzellen zu transplantieren, obwohl wir eine aufwändige, Mikrosatelliten-basierte Überwachung des genetischen Hintergrunds der Akzeptormäuse durchführten. Es ist bekannt, dass der genetische Hintergrund eine wesentliche Rolle bei immunologischen Experimenten spielt, jedoch schien in unserem Fall die Rekonstituierbarkeit in genetisch beinahen identischen Tieren *Prnp*-abhängig zu sein. Wir zeigen, dass PrP im Knochenmark, speziell in Makrophagen und B-Zell Vorläufern hoch exprimiert ist und daher evtl. eine modulierende Funktion auf das Anwachsen xenogener Stammzellen ausüben könnte. Jedoch konnten wir diesen Effekt mittels Re-Expression eines humanen *PRNP*-Transgens und in Absenz von Maus-*Prnp* nicht komplementieren, obwohl auch diese Tiere eine beinahe identische genetische Konstellation aufwiesen. Eine nähere Analyse in der Region um *Prnp* auf Maus Chromosom 2 zeigte, dass trotz zahlreichen Rückkreuzungen eine Region von ca. 9Mb die ursprüngliche Konstellation des $Prnp^{-/-}$ Chromosoms besass und somit auch andere genetische Faktoren diesen Effekt ausüben könnten. Tatsächlich hat vor

kurzem eine Gruppe ein polymorphes Gen, welches für das "Signal regulatory protein alpha" kodiert (Sirpa), publiziert, welches ganz nahe bei *Prnp* gelegen ist und aufgrund seiner Eigenschaften die Nicht-Rekonstituierbarkeit der $Prnp^{-/-}$ Mäuse erklärt [116]. Mittels eines meiotischen Rekombinationsscreens konnten wir schlussendlich eine mit menschlichen Stammzellen rekonstituierbare $Prnp^{-/-}$ Maus herstellen, welche ein ideales Modell für die periphere Replikation von Prionenerkrankungen im Menschen darstellt.

Der zweite Teil dieser Arbeit beschreibt die Suche nach differentiell exprimierten Genen nach subakuter Infektion mit Prionen in einem Zellkultur-Modell mittels Microarray und Taqman-Technologie. Überraschenderweise scheinen verschiedene neuronale Zelllinien keine nennenswerte Modulation ihres transkribierten Genoms aufzuweisen, obwohl alle untersuchten Zelllinien im Vergleich zu den Kontrollen zu beinahe 100% mit PrP^{Sc} infiziert waren. Diese Resultate widersprechen anderen Studien, welche einige hoch- oder herunterregulierte Gene identifiziert haben. Wir denken jedoch, dass unsere Resultate aufgrund des experimentellen Designs, welches die Entwicklung von genetisch unterschiedlichen Zellinienklonen verhindert, ein realistischeres Bild der Ereignisse bei Prioneninfektion in vitro widerspiegelt, und die zelluläre Antwort auf eine Prioneninfektion eher in posttranslationellen Modifikationen zu suchen ist.

Part I.

Establishing a Humanized Mouse Model to Study Prions

1. Introduction

1.1. Prion diseases in humans, mice and cattle

Prion diseases are a large but clinically homogenous group of lethal neurodegenerative disorders affecting both humans and animals. They are also called "Transmissible Spongiform Encephalopathies" (TSEs) because of the neuropathological picture of spongiform vacuolation classically seen in affected individuals and because of the transmissibility of this disease. Animal TSEs include sheep and goat scrapie, the prototypic animal TSE that was recognized more than 200 years ago, but also transmissible mink encephalopathy [50], chronic wasting disease of mule deer, antelope and elk (CWD) [127] and bovine spongiform encephalopathy (BSE) [124]. Human TSEs include familial, sporadic and variant Creutztfeldt-Jakob diseases (CJD), fatal familial insomnia (FFI), Gerstmann-Sträussler-Scheinker syndrome (GSS) and kuru. TSEs are either dominantly inherited, transmitted by infection or classified as sporadic if a known genetic or infectious transmission can be excluded. All TSE can be experimentally transmitted and can therefore be categorized as infectious diseases. However, the unusually long incubation time and the resistance to common means of sterilization such as high temperatures, formaldehyde treatment or UV light irradiation distinguish the prion from conventional bacterial or viral infectious agents. The Prion agent (from " infectious only") seems to be devoid of any informational nucleic acids, and prion infectivity is associated with PrP-scrapie (PrP^{Sc}), an "infectious" and proteinase resistant isoform of a physiological protein called PrP^{C} (cellular prion protein) [95].

1.1.1. Historical perspective

The first description of what would later be understood as a prion disease dates back to the 18th century and concerns scrapie, a natural neurological illness that occurs in sheep and goats. It was also called "tremblante" in French because of the tremor syndrome affecting these animals. Yet it was only in the 1930s that the transmissible nature of scrapie was demonstrated by transmission between sheep [21]. Scrapie was at that time considered to be a viral disease.
Spielmeyer introduced the term "Creutzfeldt-Jakob disease" in 1922 on the basis of cases described by Creutzfeldt and Jakob. Families with high incidences of CJD (familial CJD or fCJD) have been documented.
In the 1950s a great deal of attention was given to an epidemic of a neurodegenerative disease called Kuru among indigenous populations in the highlands of Papua New Guinea. It was soon suggested that Kuru was transmitted by ingestion of brain tissue during anthropophagic rituals. Transmission of human Kuru to chimpanzees by intracerebral inoculation of brain homogenates by Gajdusek during his expeditions to Papua New Guinea [34], [35] followed by transmission of CJD [37] and GSS [77] helped to categorize

these diseases as "transmissible dementias". In 1974, the first case of iatrogenic CJD (iCJD) was described in a 55-year-old woman whose symptoms began 18 months after corneal implant surgery - the donor had died of CJD [25]. Since then, other mechanisms of iatrogenic transmission have been identified including neurosurgical instruments, depth electrodes [14], human pituitary hormones [62] and human dura mater grafts [51]. To date, iCJD has developed in over 160 human growth hormone (hGH) recipients in a number of countries, mainly the US, the UK and France. All of these CJD transmissions have involved cross-contamination with material in or adjacent to the brain where the expected levels of prion accumulation would be highest. The route of inoculation has been parenteral, either by surgery or by intramuscular injection. Therefore, biosafety measures have been implemented including avoidance of cadaveric hGH and lyophilized dura and special sterilization methods for neurosurgical instruments since the infectious agent seems to be resistant to most of the common sterilisation methods [36]. A major impact on daily life came along in the UK in the late 1990s with the outbreak of "mad cow disease", bovine spongiform encephalopathy, and the suspected link to a CJD-like syndrome called variant CDJ (vCJD) in teenagers and much younger patients than usually affected [125]. To date, about 207 patients have succumbed to this type of prion disease, almost exclusively in the UK [126], http://www.cjd.ed.ac.uk/vcjdworld.htm. There is quite a body of evidence that vCJD might be caused by consumption of mainly neural bovine tissues from BSE-affected cattle, yet this has still to be proved. Human-to-human prion transmission of vCJD via blood transfusions has been reported and this has alerted health authorities worldwide to tighten the quality control of blood and blood products [68]. Thus, prion diseases still present a major challenge and danger to society.

1.1.2. Clinical phenomenology and course of sCDJ, diagnostics, neuropathology, treatment options

A common denominator of all these described entities is a quick and invariably fatal neurodegeneration which I would like to highlight by describing the clinical course and the most common diagnostic and pathological changes in CJD. The vast majority of CJD cases are sporadic (85 to 95 percent), while 5 to 15 percent are due to fCJD; iCJD generally accounts for fewer than 1 percent. Approximately one case of sporadic CJD occurs per 1,000,000 population per year with a worldwide distribution. In Switzerland, a recent rise in sCJD cases has been reported, likely because of better surveillance [40]. The mean age for the onset of disease is between 57 and 62 years, although rare cases in young adults and persons over 80 years of age have been described. The incidence of CJD is increased 30 to 100-fold in certain geographic regions including areas of North Africa, Israel, Italy, and Slovakia, mainly because of clusters of fCJD.

Clinical features

Rapidly progressive mental deterioration and myoclonus are the two cardinal clinical manifestations of sCJD. However, a number of variants or subtypes of disease have

been defined based upon focal neurologic findings reflecting predominant involvement of individual brain regions. Examples of these include forms with mainly visual, cerebellar, thalamic, and striatal features. Variants of sCJD have also been classified according to the genotype of the prion protein gene (*PRNP*) and the molecular properties of the pathological prion protein (PrP^{Sc}). Mental deterioration may be manifest as dementia, behavioral abnormalities, and deficits of higher cortical function. Concentration, memory, and judgment difficulties are frequent early signs. Mood changes such as apathy and depression are common; euphoria, emotional lability, and anxiety occur less frequently. Sleep disturbances, particularly hypersomnia, but also insomnia, are common and may be a presenting sign [40,41]. With disease progression, dementia becomes dominant in most patients and can advance rapidly. Death usually occurs within one year. Myoclonus, especially provoked by startle, is present in more than 90 percent of patients at some point during the illness but may be absent at presentation, even when dementia is profound. Extrapyramidal signs such as hypokinesia and cerebellar manifestations, including nystagmus and ataxia, occur in approximately two-thirds of patients and are the presenting symptoms in 20 to 40 percent [39]. Signs of corticospinal tract involvement develop in 40 to 80 percent of patients, including such findings as hyperreflexia, extensor plantar responses (Babinski sign), and spasticity.

Diagnostic procedures

Brain biopsy remains the gold standard diagnostic test for CJD. However, a number of tests can be helpful in providing clinical support for the diagnosis.

Neuroimaging: MRI is the imaging method of choice for diagnosing CJD. Abnormally increased T2 and FLAIR signal intensity in the putamen and head of the caudate nucleus is the most common finding on conventional MRI sequences in patients with CJD. Less commonly, areas of T2 and FLAIR signal hyperintensity are seen in the globus pallidus, thalamus, cerebral and cerebellar cortex and white matter. Laminar lesions in the cerebral cortex and cerebellum may be observed.

An *electroencephalogram (EEG)* can provide supportive but not definitive evidence for CJD. A characteristic EEG pattern of periodic synchronous bi- or triphasic sharp wave complexes (PSWC) is observed in 67 to 95 percent of patients with sCJD at some time during the course of the illness.

CSF biomarkers: A protein that is secreted into the CSF, the 14-3-3 protein, has been claimed to be a sensitive and specific diagnostic test for sCJD. In one study, a modified western blot technique for CSF 14-3-3 protein had a positive predictive value of 95 and 93 percent, respectively, for patients with definite and probable sCJD [52], but these results were challenged by other groups [38]. A variety of other CSF diagnostic tests have been reported in small series, including the S100 protein, neuron specific enolase, and tau protein, which are of unproven diagnostic utility at present. Therefore, the quest for good and non-invasive diagnostic markers is still ongoing.

Detection of extraneural PrP^{Sc}: Establishing the diagnosis of prion diseases by detecting abnormal prions outside the CNS remains a major research goal. Although a number of methods have been reported, none have been validated as diagnostic tests in human prion

diseases. One study in our lab by Glatzel [39] revealed extraneural PrP^{Sc} in skeletal muscle and spleen, and currently more sensitive assays are under development to detect minute levels of PrP^{Sc}.

Neuropathology

On macroscopic examination, most brains show some atrophy, which may include the deep gray structures such as the caudate nucleus, putamen, and thalamus. In contrast to Alzheimer's disease, the hippocampus is spared whereas the cerebellum may also show atrophy of the folia, usually due to loss of gray matter. The main histologic features of prion disease are spongiform change, neuronal loss (particularly of cortical layers III-V) without inflammation, gliosis and accumulation of the abnormal prion protein that is usually detectable by antibodies specific for PrP (Figure 1.1) and, most recently, with conjugated polyelectrolyte probes that distinguish between various molecular substrains of PrP^{Sc} on the basis of their biophysical properties [111].

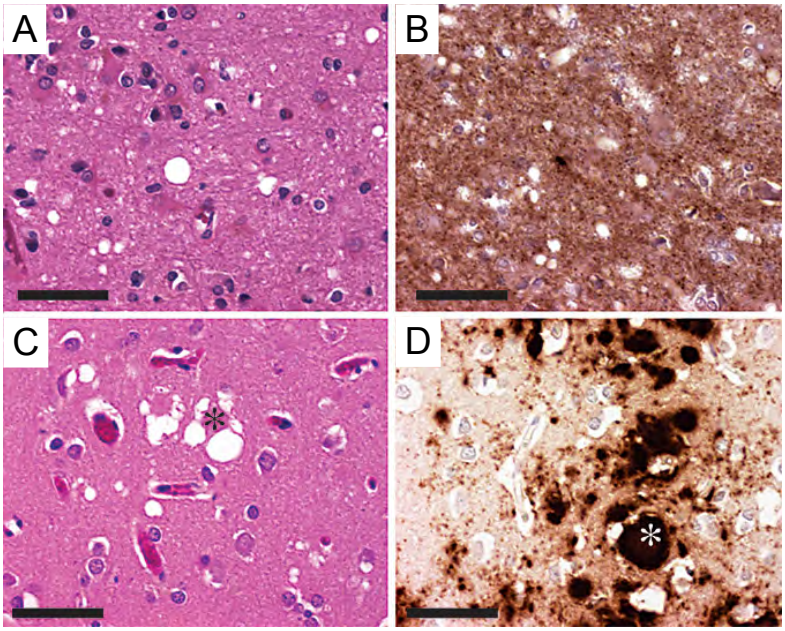

Figure 1.1.: Histologic features of prion diseases.
Central nervous system parenchyma of sporadic Creutzfeldt-Jakob disease (A and B) and variant Creutzfeldt-Jakob disease (C and D) showing astrogliosis and widespread spongiform changes. The protease-resistant forms of host-derived prion protein deposition are synaptic (A and B) and in the form of florid plaques (asterisk, C and D). A and C, hematoxylin-eosin, original magnification x400. B and D, immunohistochemical stainings for prion protein, original magnification x400. Scale bar = 50 μm. Adapted from Glatzel [41].

Post-mortem molecular typing

Varying clinical phenotypes of sporadic CJD have been associated with molecular subtypes determined by the *PRNP* gene codon 129 genotype and PrP^{Sc} type. The *PRNP* genotype is homozygous or heterozygous for methionine (M) or valine (V) at codon 129. The PrP^{Sc} type is determined by western blot analysis and classified in the Parchi/Gambetti nomenclature as type 1 or type 2 depending on the size and electrophoretic mobility of the protease resistant core fragment (PrPres) [88], [89], but this classification is currently widely debated [91].

Therapeutical strategies?

Despite the recent advances in research and the understanding of pathogenesis of prion diseases, no successful therapeutical strategies have been developed to date. Upon clinical manifestation, the destruction of the brain is already too far advanced to interfere with and therefore major efforts regarding diagnosis (i.e. development of early sensitive/specific markers) and peripheral pathogenetic mechanisms will be needed in the future.

1.2. PrP^{Sc} - the destructive agent and the discovery of its underlying gene Prnp

To date, compelling evidence speaks in favor of the protein-only hypothesis formulated by Prusiner [95] which represented a major new paradigm in infectious diseases. A possible viral nature of the "infectious" agent responsible for transmissible spongiform encephalopathies was questioned because of the absence of direct evidence of such a virus and the lack of a detectable immune response to the infectious agent, although some voices still claim a viral nature of this agent [75], [76]. Nevertheless, the resistance of the transmissible agent to procedures that inactivate nucleic acids (UV irradiation and nuclease treatment) suggested that the "infectious" agent was devoid of information-bearing nucleic acids [5] and led Griffith to define the "protein only hypothesis" in 1967 stating that the agent could well be a protein [43]. This hypothesis gained general acceptance after Stanley Prusiner purified the protease-resistant infectious protein, which he called PrP^{Sc} (scrapie-associated prion protein) in 1982 [95].
A very strong argument for the protein only hypothesis was the discovery of a gene coding for PrP^{C} (*PRNP* in humans, *Prnp* in mice) and subsequent gene-knockout studies. *Prnp* was cloned by Basler and Weissmann [10] based on partial sequencing of PrP^{Sc} and identification of a cDNA leading to a chromosomal gene encoding for a physiological protein. PrP^{C} is a highly conserved protein in mammals and paralogues, present in turtle [112], fish [101] and even amphibians [114]. The murine *Prnp* gene encoding the cellular isoform of the prion protein is located on chromosome 2 and the mature form of murine PrP^{C} consists of 210 amino acids [10]. The broad, diverse expression pattern of PrP^{C} with expression in skeletal muscle, kidney, heart, pancreas, secondary lymphoid organs and the CNS presumably points to a general, conserved function ([31]; [3]). PrP^{C} is a glycosyl phosphatidyl inositol (GPI)-linked glycoprotein, and can be

either un-, mono- or diglycosylated. After passing through the Golgi apparatus PrP is trafficked mainly to the cell surface, where its GPI anchor allows it to enter lipid raft domains preferentially. Pulse-chase labeling experiments have shown that the half-life of PrP^C in murine splenocytes is similar to that in neurons; about 1.5 to 2 h [20]. The three dimensional structure of mature PrP^C from mouse, humans, cattle and Syrian hamster shares common features e.g. a long, flexible N-terminal tail (residue 23-121), three α-helices, and a two-stranded anti-parallel β-sheet that flanks the first α-helix. The C-terminus is stabilized by a disulfide bond linking α-helices 2 and 3 [98]. PrP^C and PrP^{Sc} have the same amino acid sequence yet unlike PrP^{Sc}, PrP^C is protease sensitive and it is now known that PrP^{Sc} is a conformational variant derived from PrP^C. The mechanism of conversion from PrP^C to the much more aggregation-prone PrP^{Sc} is still a matter of intense debate. It is believed that PrP^C acts as a substrate for the conversion process of the abnormally folded PrP^{Sc}. The conversion from PrP^C to PrP^{Sc} is thought to rely on a physical interaction between host-encoded PrP^C and exogenous or spontaneously generated PrP^{Sc} as a template, resulting in the PrP^{Sc} conformation being imposed on PrP^C ("template-directed refolding model"). Another model suggests that PrP^C and PrP^{Sc} are in a constant equilibrium strongly favoring PrP^C, while stabilization of PrP^{Sc} due to unknown mechanisms and subsequent seed formation results in a cascade of infectious amyloid formation and fragmentation ("seeding model") as depicted in Figure 1.2. How PrP^C is turned into PrP^{Sc} remains elusive, but it can be stated nearly with certainty that genetic deficiency of a PrP^C will result in the inability of PrP^{Sc}-generation due to the lack of the appropriate template. Therefore, organisms that lack PrP^C will never develop disease [12].

1.3. Assigned functions to PrP^C

To date, the physiological function of PrP^C remains unknown. However, based on in vitro and in vivo studies, several possible though highly controversial "functions" have been assigned to it. These include regulation of the immune system, signal transduction, copper binding, being an antioxidant, synaptic transmission, inducing apoptosis or being anti-apoptotic or inducing circadian rhythms [18]. Furthermore, PrP^C positively regulates neural precursor proliferation during neurogenesis [113], but postnatal depletion of PrP^C in neurons does not result in neurodegeneration [73]. Interestingly, studies performed in PrP^C deficient mice have not elucidated a real phenotype associated with the deficiency of the protein, but mice expressing various PrP^C-deletion mutants show severe neurodegenerative and myelinotoxic phenotypes that are rescued with re-expression of a full-length *Prnp* wildtype copy as described by Shmerling and Baumann [107], [11]. In old age, however, Zrch1-$Prnp^{-/-}$ mice can develop a demyelinating phenotype as well, even in "near-normal" Zrch1-$Prnp^{-/-}$ mice. Frank Baumann claims that PrP^C might interact with a yet unknown receptor which exerts myelin survival signals. In the total absence of PrP^C, residual activity of the putative receptor might still be present whereas in case of deletion of certain domains of the protein it might be stabilized in a dominant-negative conformation and therefore lose its signaling to maintain myelin integrity [11]. The quest for possible PrP^C-interaction partners or for the composition of

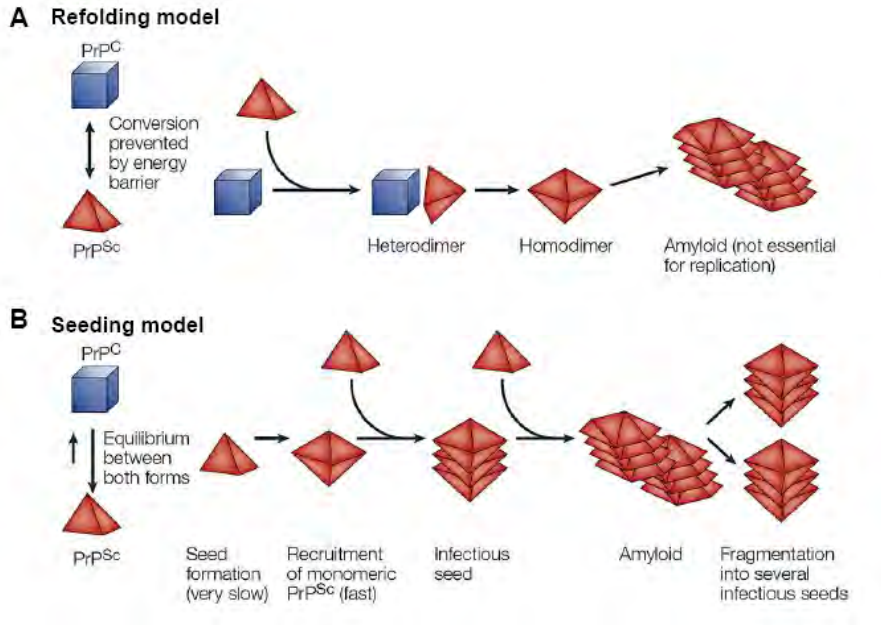

Figure 1.2.: Hypothetical models of conversion from PrP^C to PrP^{Sc}. Schematic of the refolding or template-directed assistance model (A) and the seeding or nucleation-polymerization model (B); adapted from [4].

a putative PrP^C-complex is ongoing and might soon shed light on a function of PrP^C in the nervous system and elsewhere.

1.4. Functions of PrP^C related to the peripheral immune system in physiological and pathological conditions

The relationship between PrP^C, PrP^{Sc} and the immune system is complex in both physiological and diseased states. The absence of a measurable adaptive immune response in prion disease is assumed to be due to tolerance to PrP^{Sc}. Further, the immune system contributes to peripheral pathogenesis by replicating or accumulating prions in lymphoid compartments before the infectious agent finds its way into the brain.

1.4.1. Proposed functions of PrP^C in immune regulation and hematopoiesis

Although studies in $Prnp^{-/-}$ mice were not very enlightening at first about the functions of Prp^C in the immune system, very recent analyses of hematopoietic development and the immune system in $Prnp^{-/-}$ mice have revealed fine tuned regulations. Steele et al. report that PrP^C is expressed on the surface of long-term (LT) hematopoietic stem cells (HSC) and HSC from $Prnp^{-/-}$ mice exhibited impaired self-renewal in serial transplantation of lethally irradiated mouse recipients in both the presence and the absence of competitors. Furthermore, when treated with a cell cycle-specific myelotoxic

agent, the animals reconstituted with *Prnp*$^{-/-}$ HSC exhibited increased sensitivity to hematopoietic cell depletion [130].

Comparison of lectin induced mitogenesis and selected cell signaling pathways in splenocytes from wild-type BALB/c and Zrch1-*Prnp*$^{-/-}$ mice has revealed that activation was significantly reduced in *Prnp*$^{-/-}$ splenocytes, most prominently early in activation [78].

Other groups compared the phagocytic activity of *Prnp*$^{-/-}$ macrophages to that of their wildtype counterparts and found a downregulation of macrophage activity in case of *Prnp*-deficiency [22]. Additionally, PrP^C seems to be involved in the phagocytic machinery used by *Brucella abortus* to invade macrophages [122], although this finding has been challenged [30].

Clues to the function of PrP^C may be gained by examination of cell-specific expression patterns. CD34+ hematopoietic stem cells express PrP^C, but, although lymphocytes and monocytes at least maintain PrP^C expression throughout their differentiation, PrP^C is downregulated upon differentiation along the granulocyte lineage [23]. In contrast, maturation of monocytes and dendritic cells leads to PrP^C up-regulation [16]. Dendritic cells (DC) display the highest expression levels of PrP^C, in both humans and mice [16]. PrP^C was found to be present on murine epidermis Langerhans cells [115], on DC in extrafollicular areas, including T cell zones, of the gut mucosa [31], and DC of the splenic white pulp [16]. PrP^C was also found on the surface of bone marrow derived human and mouse DC generated in vitro in the presence of GMCSF, at levels that increased with LPS stimulation and were correlated with that of MHC II and the costimulatory molecule CD86 [16]. In lymph nodes, the highest PrP^C level was observed in the CD8int subset, which are strong stimulators of Ag-dependent delayed-type hypersensitivity. This was interpreted as a possible involvement of PrP^C in T cell activation leading to Th1 responses [8]. Studies in mice show a trend towards downregulation of PrP^C during B and T cell maturation, and mature T lymphocyte expression during quiescence is low, yet, high expression of PrP^C is seen in erythroid cells and maturing granulocytes. Approximately 50% of the cells in the region of small lymphocytes and progenitor cells also express PrP^C . Most of these PrP^C+ cells are CD43(+), but B220(-), surface IgM(-) (sIgM(-)), and IL-7R(-), a phenotype that belongs to cells not yet committed to the B cell lineage. [66]. However, there are significant species differences in the reported expression profile on immune cells: in humans and sheep PrP^C expression on mature blood and lymphoid cells remains high [65], with levels increasing further with ageing [90]. In various non-human primates, the expression level of PrP^C is reported to be very variable: all examined species displayed PrP^C on white blood cells (WBCs), with the highest levels found on human cells. Only humans, chimpanzees, and to a lesser degree rhesus macaques expressed PrP^C on platelets [49]. In the hamster, however, PrP^C has been observed in very weak quantities on various peripheral blood cell sub-populations [48]. This expression and subtype discrepancy among mice, humans and other species suggests that any reported functional properties of PrP^C, mostly investigated in mice, should be interpreted cautiously.

1.4.2. Peripheral immune organs function as prion replication machinery prior to neuroinvasion

Experiments in mice have shown that after oral or intraperitoneal inoculation with PrP^{Sc}, prion accumulation/replication occurs in many sites of the immune system, including the spleen, lymph nodes, Peyer's patches and tonsils. After peripheral prion inoculation of wildtype mice with RML, PrP^{Sc} load increases in the spleen and lymph nodes at approximately 30 to 50 days post inoculation (dpi), reaching a plateau after 6 to 9 weeks. However, brain PrP^{Sc} accumulation is only detected 4 to 5 months after inoculation. Even after intracerebral inoculation with the RML strain, PrP^{Sc} accumulation is found in spleens of wild-type mice at 4 dpi. High PrP^{Sc} titres in lymphoid organs are not accompanied by significant histoarchitectural changes; this rules out a damaging effect of PrP^{Sc} in peripheral lymphatic organs.

Splenectomy prior to peripheral prion challenge prolongs the lifespan of scrapie-infected mice whereas thymectomy or athymia has no effect. However, the tropism to peripheral lymphatic organs is species- and prion-strain specific. Splenic prion replication does not occur in all rodent TSE models: analysis of Syrian hamsters that were splenectomized and subsequently infected with the 236K strain showed that neuroinvasion occurred without substantial prion replication in the lymphoreticular system [59]. Additionally, splenectomy had no influence on incubation times after infection with a mouse-adapted CJD prion strain [83], [118].

Separation of splenic pulp from the stroma revealed that approximately ten times more infectivity was present in the stroma than in the pulp fraction. Moreover, infectivity in the stromal fraction was directly correlated with both whole spleen weight and the weight of the stroma [2]. It was concluded that the stromal compartment is the site of replication of the scrapie agent [20], and that the cells involved in scrapie replication are not mitotically active [32]. Accordingly, sublethal irradiation, which preferentially targets mitotically active cells, failed to alter the incubation period of the disease [33].

Prp^C itself is involved in transporting prion infectivity from peripheral sites to the CNS. Adoptive transfer of wild-type bone marrow into $Prnp^{-/-}$ mice reconstitutes the ability of the spleen to accumulate high titres of prion infectivity up to 300 dpi [58], [15]. However, this process was insufficient to restore prion neuroinvasion. Therefore, hematopoietic cells (for example, B and T cells, macrophages and dendritic cells) facilitate the transport of prions from the peripheral entry site to secondary lymphoid organs, where prions can accumulate and/or replicate. However, the primary cellular reservoir for prion neuroinvasion seems to be non-hematopoietic, because this phenotype cannot be restored by bone marrow reconstitution [58], [15], [60]. Nevertheless, other publications speak against the hypothesis of an exclusively stromal prion replication competence and claim that neuroinvasion is not dependent on a stromal reservoir such as follicular dendritic cells [106]. Inducing ectopic chronic inflammation in organs that normally do not possess lymphoid follicles restores prion replication in these organs and impressively highlights the importance of lymphoid organs in prion pathogenesis [45].

1.5. Modeling a human adaptive immune system in mice for studying prion diseases

1.5.1. Historical overview and perspectives

"Humanized mouse models" for studying infectious and immunological phenomena in a more realistic manner have been developed and steadily improved over the last few decades. The main applications for modeling the human immune system in a small animal environment include

1. testing of virulence/pathogenicity of various pathogens in a near-real human-like environment
2. determination of genetic susceptibility variations of donor-specific immune reactions
3. replacement of current animal models previously used in the pharmaceutical industry in preclinical trials
4. diagnostic assay development tool, e.g. blood tests
5. circumvention of ethical limitations in clinical research

Most, if not all, of the models currently available are based on the observation that hematopoietic stem cells can differentiate *in vivo* into different lineage committed cells in the presence of a permissive microenvironment. The term "humanized mouse" therefore stands mainly for a "humanization" of the immune system, and a considerable proportion of mouse organs and most cellular populations of innate immune cells still originate from the mouse. Advances in the ability to generate humanized mice have depended on a systematic progression of genetic modifications to develop immunodeficient host mice. Three major breakthroughs have occurred in this field as depicted in the timeline established by Shultz et al (Figure 1.3).

First, the discovery of the Prkdc^{scid} mutation (protein kinase, DNA activated, catalytic polypeptide; severe combined immunodeficiency, abbreviated scid) in CB17 mice was soon followed by the observation that human PBMCs [85], fetal haematopoietic tissues [79] and HSCs [64] could engraft in these mice. However, engraftment occurred at only a very low level, and the engrafted human cells failed to generate a functional human immune system.

The second breakthrough was the development of immunodeficient non-obese diabetic (NOD)-scid mice [108]. Crossing the scid mutation onto different strain backgrounds led to the observation that NOD-scid mice supported higher levels of engraftment with human PBMCs than did any of the other strains that were tested, including C3H/HeJ-scid and C57BL/6-scid mice [46]. Furthermore, it was observed that NK-cell activity, which is one of the main impediments to the engraftment of human hematopoietic cells [19], was lower in NOD-scid mice than in CB17-scid mice [108]. NOD-scid mice also have additional defects in innate immunity [108] that allow higher levels of human PBMC [46] and HSC [69], engraftment.

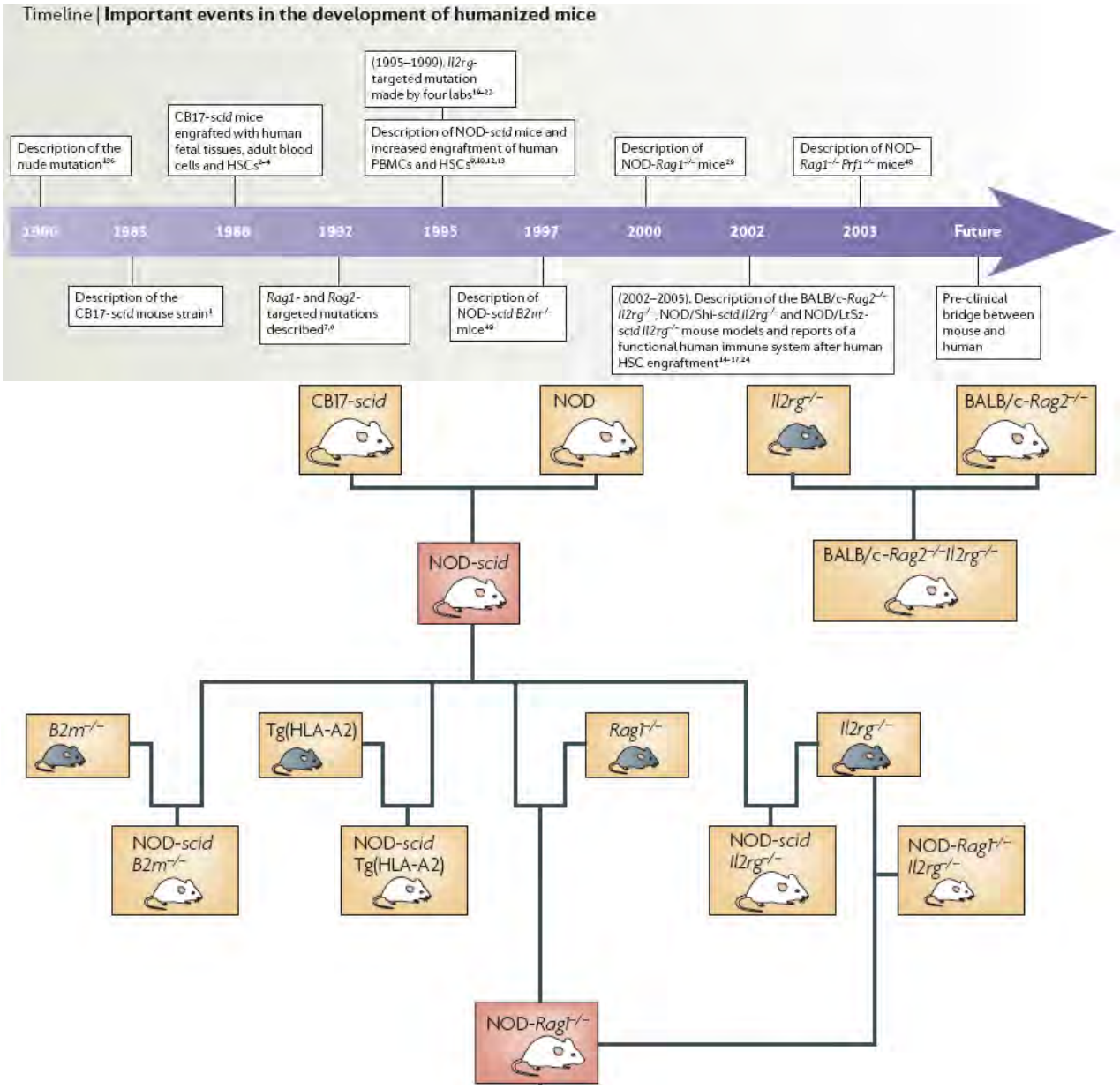

Figure 1.3.: History of humanized mice.
The timeline depicts the most prominent steps in the development of "humanized mice". The lower chart shows current mouse strains and their genetic modifications utilized for "humanization". Adapted from Shultz [109]

The third breakthrough was the humanization of immunodeficient mice homozygous for targeted mutations at the interleukin-2 receptor (IL-2R) gamma-chain locus (*Il2rg*; also known as the common cytokine-receptor gamma-chain, γc) [56], [119], [110], [55].

These mice support greatly increased engraftment of human tissue, HSCs and PBMCs compared with all previously developed immunodeficient humanized mouse models.

1.5.2. Generation of a humanized mouse model suitable to study prions

We therefore decided to design a humanized mouse model to study prions because of the evidence that acquired prion diseases, at least in a majority of cases, start their way to the brain long before in the peripheral immune system. In order to make the model really "human compatible" and because of the fact that the cellular components responsible for prion replication are yet to be defined, we also wanted the model to contain no endogenous murine Prp^{C}. Having this model in our hands, we would be able to test various pathogenic prion species for their ability to replicate in a human immune system. Further, this model would enable us to do genetic susceptibility testing of the engrafted cells as soon as PrP^{Sc} accumulation within the humanized compartments could be identified. The whole repertoire of prion replicating cells in this mouse would be of human origin since absence of murine Prp^{C} expression renders the mouse cells incapable of de novo generation of any kind of prion (a mouse is capable of replicating all kinds of pathogenic prions, including CJD-prions, if Prp^{C} is present). A further step in our plan to achieve an optimal model for prion-humanization was to re-express a human sequence on most of the remaining mouse-cells to study neuroinvasion and not only peripheral prion replication.

Exploiting the historical advances in the development of humanized mouse models, we decided to implement a modified version of the model published by E. Traggiai et al, based on "humanization" of newborn BALB/c $Rag2^{-/-}Il2rg^{-/-}$ mice with CD34(+) selected pluripotent stem cells from fresh human cord blood [119]. Modification means introducing a $Prnp^{-/-}$ allele into this mouse and, in a later phase, complementing this via expression of a human *PRNP* transgene. However, this modification approach is combined with genetic background effects that are likely to affect the outcome of our "humanization" protocol since it is known that xenografting can only be performed in a distinct genetic environment (see also section 1.5.1).

1.6. Influence of genetic background effects on mouse experimentation and experimental outcome

Since we knew that the genetic background issue might be of major impact to our strategy, some introductory words need to be said in order to explain background effects in mouse genetics.

More than 100 different inbred mouse strains are commercially available, each of which has distinct physiological and behavioral hallmarks. There are vast differences in the reaction or resistance of those strains to pathogens, in hematological, biochemical and serological parameters as well as in transplantation issues.

The process of backcrossing a genetically modified genomic region from knockout or transgenic strain onto a different inbred strain is complicated by the problem that linked genetic material from the original strain accompanies the manipulated genomic region.

The amount of this genetic material can be dozens of megabases and can be minimized only by monitoring and selection of the random meiotic recombination events that occur in the DNA flanking the targeted gene. Even eight to ten generations of backcrossing is no guarantee that the flanking region will be substantially reduced [97]. An illustrative example to this represents a study where CD38 in 129Sv/J mice was "knocked out" and the knockout mice were backcrossed ten generations onto the C57Bl/6 strain. Even after ten generations of backcrossing, at least 20 centimorgans (cM) of linked 129-derived DNA remained associated with the disrupted CD38 allele. On average, 1 cM corresponds to approximately 2 Mb of DNA, and the average gene density in mice is ten genes per megabase; therefore, an additional 400 genes may have been carried along with the mutated CD38 allele [29].

These considerations had to be taken seriously into account when planning immunological and xenografting experiments, and a large part of my thesis is therefore committed to apply tools for controlling and describing the genetic background of our acceptor mice.

1.7. Experimental plan and outline of the work

A simplified scetch of the experimental setup that serves as a project outline is depicted in Figure 1.4.

- First, we wanted to reproduce published data by Traggiai et. al. [119].
- Second, we wanted to establish humanized mice devoid of *Prnp* and therefore only expressing human PrP on the repertoire of the differentiated human immune cells, i.e. exhibiting all genetic cofactors involved in pathogenesis.
- Third, stromal expression of a human *PRNP* transgene on a $Prnp^{-/-}$ background should reinstall neuroinvasion and serve as a complete model for human-like prion pathogenesis.

All our reconstituted animals are intended to serve as "bioreactors" that possibly may replicate prions of different species such as CJD, CWD, BSE and scrapie exclusively in their human cells. Accumulation of the pathological PrP^{Sc} would later be assessed and novel diagnostic tests and correlation studies to the genetic variability of the human donor could be developed.

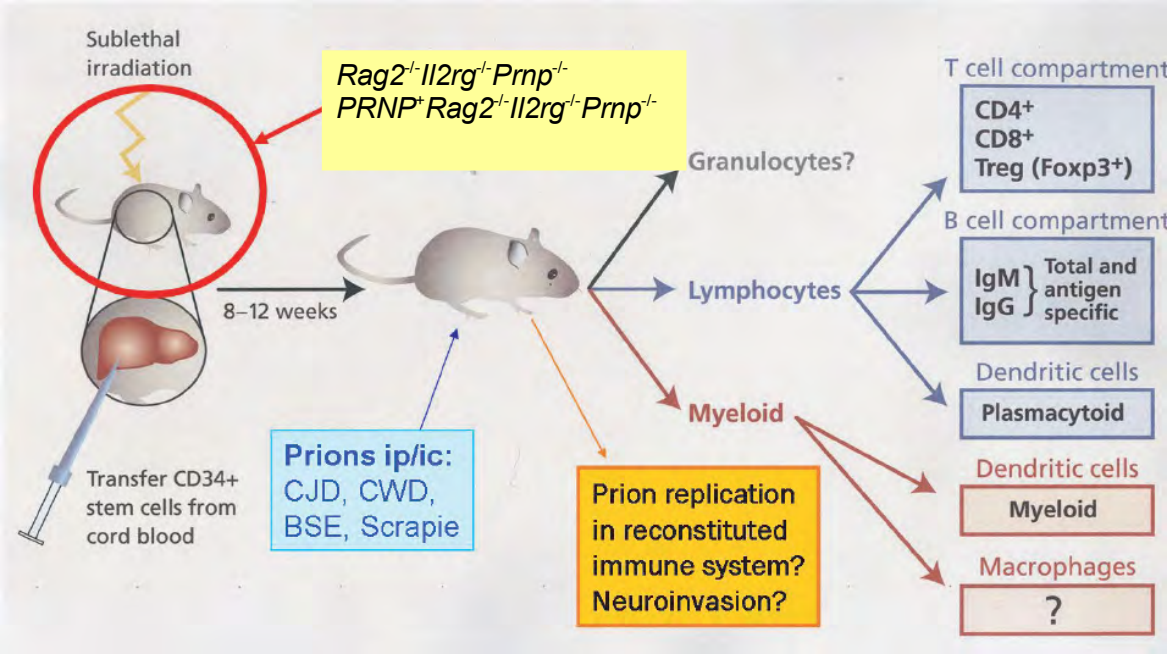

Figure 1.4.: Experimental plan.
Humanized mice will be generated according to the protocol of Traggiai et al. [119] with the difference that our mice lack endogenous *Prnp* and might express transgenic *PRNP*. 6 to 8 weeks after intrahepatical transplantation of sorted stem cells from cord blood, the efficiency of engraftment will be assessed. Successfully reconstituted mice and controls will be challenged with prion inocula from various species including CJD, BSE, CWD and Scrapie. Peripheral organs and blood of these mice serve as a diagnostic surrogate for prion replication.

2. Material and Methods

2.1. Genetically modified mice, breeding strategy

Mice were housed in an SPF facility of the Institute for Laboratory Animals of the University of Zurich according to the guidelines of the cantonal veterinary office of Zurich (Kantonales Veterinäramt). All our immunodeficient mouse strains were accommodated in cages with filter covers and received autoclaved drinking water and food pellets. *Rag*1$^{-/-}$ *Prnp*$^{-/-}$ mice on a mixed C57Bl/6-Sv129 background were available in house [60]. *Rag*2$^{-/-}$ *Il2rg*$^{-/-}$ mice on a BALB/c background were kindly provided by Dr. Markus Manz. Mice carrying transgenically the sequence of the human prion protein in its 129M-form (Tg*PRNP*129M mice) were kindly provided by Prof. John Collinge [6]. Mice harboring the *Prnp*$^{-/-}$ allele on a BALB/c background (10 times backcrossed to BALB/c) were also obtained from John Collinge. The structure and function of the modified/deleted genes as well as the targeting constructs with the respective references and possible genotyping outcomes are depicted in Fig. 2.2.

2.1.1. Rag1$^{-/-}$ and Rag2$^{-/-}$ mice

*Rag*1$^{-/-}$ and *Rag*2$^{-/-}$ mice were described by Mombaerts [84] and Shinkai [105]. They lack functional B- and T- cells because of a deficiency in the generation of functional immunoglobulin and T-cell receptor structure which is mediated by genomic V(D)J recombination through *Rag*1 and *Rag*2 enzymes in a coordinated way (Figure 2.2). Therefore, only precursor B-cells and T-cells can be seen in these mice, the splenic architecture is highly disturbed and an adaptive immune response is impossible. However, these mice can be kept at an SPF-facility with no further impact on their lifespan and do not suffer from major infectious complications. The *Rag*1 and *Rag*2 genes are both closely linked at the same locus on chromosome 2 at 56 cM (genetic map) or in the region of 101439121-101450340 bp(-strand) and 101425557-101433367 bp(+strand) according to the VEGA annotation of NCBI Build 36 (http://www.vega.sanger.ac.uk).

2.1.2. "Zurich1"-Prnp$^{-/-}$ mice

"Zurich1"-*Prnp*$^{-/-}$ mice were constructed by Büeler and Weissmann [13] in the early 90s and have since been a very important tool in prion disease research. Mice devoid of PrP^{C} are resistant to scrapie and other pathogenic prion strains but seem not to exhibit other strong or uncontested phenotypes (refer also to the introduction of this part). Like most of the knockout mice available, these mice were initially designed in 129Sv ES cells and the genetically modified offsprings were mainly maintained on a 129Sv-C57Bl/6 mixed

background or further backcrossed to BALB/c or C57Bl/6. The gene for *Prnp* is located on mouse chromosome 2 at 75 cM (genetic map) or 131601369-131629870 bp (+ strand) according to the VEGA annotation of NCBI Build 36 (http://www.vega.sanger.ac.uk).

2.1.3. Il2rg$^{-/-}$-mice

Il2rg$^{-/-}$-mice were implemented by Ohbo et al. [86] and carry a truncated version of the common gamma chain of the interleukin receptor 2. A sequence fragment containing portions of exon 7 and 8 was replaced with a neo cassette inserted by homologous recombination. The deleted region encoded the majority of the SH2-like domain which abrogates the cytoplasmic signalling part of the protein (see also Figure 2.2). The interleukin-2 (IL-2) receptor gamma chain is indispensable for IL-2-, IL-4-, IL-7-, IL-9-, and IL-15-mediated signaling. Mice carrying the truncated gamma-chain mutant show a decrease in the number of lymphocytes and an increase in monocytes; the number of T and B cells is profoundly reduced and no natural killer cells are detected. Further, Peyers's patches cannot be found in these mice. The gene for the common gamma chain is located X-chromosomally at 38 cM (genetic map), 97467097-97470925 (- strand) respectively according to the VEGA annotation. *Il2rg*$^{-/-}$-mice will develop an autoimmune/lymphoproliferative disease and are not viable for more than 3 months because of a deregulation of regulatory T-cells. In combination with a deletion of *Rag* (*Rag*1 or *Rag*2), the induction of autoimmunity does not occur and *Il2rg*$^{-/-}$-*Rag*$^{-/-}$ mice have a near-normal lifespan despite their profound adaptive immunodeficiency with a total abscence of functional B-/T- and Nk-cells.

2.1.4. TgPRNP129M mice

Transgenic mice harbouring multiple copies of a human *PRNP* transgene were constructed in the lab of John Collinge [6]. We utilized mice expressing the 129M variant of the human sequence on a mouse *Prnp*$^{-/-}$ background and crossed them further to the specific immunodeficient background (see also "breeding strategy"). These mice, when inoculated with either bovine spongiform encephalopathy (BSE) or variant CJD prions, may develop the neuropathological and molecular phenotype of vCJD. These findings are consistent with the hypothesis that these diseases are caused by the same prion strain.

2.1.5. Breeding strategy

Our complex breeding strategy to yield reconstitutable mice either deficient for the mouse prion protein or - alternatively - expressing the human prion proten transgenically on a mouse *Prnp*-deficient and additionally reconstitutable background is depicted in Figures 3.1 (primary strategy) and 3.2 (alternative strategy) and is described in more detail in the Results section of my thesis.

2.2. Genotyping of genetically modified mice

After weaning, mouse tail biopsies were taken and tails were incubated for 5 to 16 hours at 55°C under constant agitation in lysis buffer (10mM TRIS/HCl pH 9.0; 50mM KCl; 0.45% NP-40; 0.45% Tween 20 and 0.1 mg/mL proteinase K). Proteinase K was inactivated by incubation at 95°C for 10 min. After short centrifugation, the lysate was used for PCR or stored at 4°C.
1μL crude tail lysate was added to a PCR mastermix containing 10μL 2x Gotaq green mastermix (Promega), 0.1μL of the respective desalted primers to yield a final concentration of 1μM per oligonucleotide (desalted, genomics scale, all synthesised at Microsynth, Switzerland) and varying amounts of nuclease free water. Normally, DNA isolated as described above resulted in good PCR results. In case of poor DNA quality, samples were purified using standard ethanol/chloroform precipitation or an EZ1-tissue kit (Qiagen). For the various wildtype and knock-out alleles we utilized the primers listed in table 2.1.

PCR cycling was performed on Perkin Elmer and Biolabo thermal cyclers using the following setups per run: *Prnp*: 5 min 95°C, 35 cycles (45 s 95°C, 45 s at 62°C, 1 min 72°C) followed by 7 min 72°C. *Rag*2 (previous method with large amplicons): 5 min 94°C, 32 cycles (1 min 94°C, 1 min 30 s 60°C, 2 min 72°C) followed by 7 min 72°C.*Rag*2 (actual methods with smaller amplicons): 5 min 94°C, 35 cylces (45 s 94°C, 45 s 55°C, 45 s 72°C) followed by 7 min 94°C. *Il2rg*: 5 min 94°C, 35 cylces (45 s 94°C, 45 s 55°C, 45 s 72°C) followed by 7 min 94°C.
Subsequently, amplicons were loaded on a 2% agarose gel containing 5μL ethidium bromide per 500mL of agarose and electrophoresed at 120V for about 1 h. Images of the gel were taken under UV-illumination and results registered in our mouse database (http://irats.unizh.ch).

2.3. Microsatellite mapping

Whole genome microsatellite mapping was performed with fluorescently labeled oligonucleotides specific for defined informative, strain-specific short-tandem repeat regions scattered over the whole mouse genome (see table 2.2). For the first set of experiments, we used commercially available mouse mapping primers (Applied Biosystems, Rotkreuz, Switzerland) and performed PCR amplification of genomic DNA from various mouse strains to calibrate our system. To this purpose, genomic DNA was extracted from tail biopsies as described above, but the resulting lysate was routinely subjected to DNA purification using a Qiagen biorobot EZ1-tissue kit (Qiagen, USA). DNA amount and quality was checked with a nanodrop spectrophotometer. For a single PCR reaction, 1-5 ng of gDNA served as a template. PCR-procedure was performed in a either simplex, duplex or triplex 96-well assay setup per mouse. Per well of a 96 reaction plate, 1-5 ng of template DNA, 7.5μL of 2x PCR colorless Taq-mastermix (Promega, USA), 1.5μL of fluorescently labeled primer mix (FAM, VIC, NED, all from Applied Biosystems) and a variable amount of PCR-grade water to result in a total reaction volume of 15μL was calculated to be an effective way for medium-throughput assay setup. After setting up the reaction plate, PCR amplification was performed with Perkin-Elmer thermocyclers

Gene ID	Primer ID	Sequence and amplicon info
Prnp	P3	5'ATTCGCAGCGCATCGCCTTCTATCGCC
	P10	5'GTACCCATAATCAGTGGAACAAGCCCAGC
	3'NC	5'CCCTCCCCCAGCCTAGACCACGA
		362bp (mutant allele)
		546 bp (wildtype allele)
Rag2, old	Neo	5'CCAACGCTATGTCCTGATAGCGGT
	RAG2-1	5'TTAATTCAACCAGGCTTCTCACT
	RAG2-3	5'GCCTGCTTATTGTCTCCTGGTATG
		1107 bp (mutant allele)
		973 bp wildtype allele)
Rag2, new	Rag1	5'GGGAGGACACTCACTTGCCAGTA
	Rag2	5'AGTCAGGAGTCTCCATCTCACTGA
	Ragneo	5'CGGCCGGAGAACCTGCGTGCAA
		350 bp (mutant allele)
		263 bp (wildtype allele)
Il2rg	P5	5'CTGCTCAGAATGCCTCCAATTCC
	P7	5'GATCCAGATTGCCAAGGTGAGTAG
	pNeo	5'CCTGCGTGCAATCCATCTTGTTCAAT
		350 bp (mutant allele)
		660 bp (wildtype allele)
Rag1	Rag 1 Sense	5'TACCCTGAGCTTCAGTTC
	Rag 1 antisense	5'CAACATCTGCCTTCACGTC
	Rag1 nI	5'CTTGGGTGGAGAGGCTATTC
		280 bp (mutant allele)
		500 bp (wildtype allele)
*TgPRNP*129M	129fw	5'CAGTCATTATGGCGAACCTT
	129rev	5'GACCTTCCTCATCCCACT
		972 bp (presence of transgene)

Table 2.1.: Genotyping PCR primers

(Perkin-Elmer, USA) and the following cycling conditions: 95° 5min, 30 repetitions of 95°C for 30s, 60°C for 30s and 72° for 30s, finally 72° for 7min. PCR reactions were diluted 1:100 in deionized water. Subsequently, 2μL of the diluted reactions were added to 10μL of Hi-Di Formamide (Applied Biosystems) containing 0.04μL GeneScan 600LIZ size standard (Applied Biosystems) per well. The resulting plate was heated at 94°C for 2 min in a Perkin-Elmer thermocycler to denature the DNA and quickly centrifuged (1000 rpm for 1 min). A sequencer assay file was created and the plate was subjected to capillary electrophoresis. This procedure was performed on a in-house 16-capillary sequencer 3130xl (Applied Biosystems) or an 48-capillary sequencer 3730 (Applied Biosystems) at the Institute of Molecular Biology at the University of Zurich. Using the 3130xl-device, two 96well plates could be analysed within 7hrs. The 3730-device was able to handle

12 plates over night. Data acquisition protocols and instrument control were defined in the data collection software of Applied Biosystems. Analysis, allele-calling, binning and calibration of various mouse strains was implemented manually using GeneMapper Software (Applied Biosystems). Alleles were defined to be either non-informative, BALB/c, C57Bl/6, 129Sv or other (table 3.1). We allowed only two alleles per marker. In total, 292 Markers could be checked in one run. In a further set of studies, we designed our own STR-primer library, based on UniSTS (http://www.ncbi.nlm.nih.gov/sites/entrez) ePCR. The respective forward oligonucleotides were either labelled with Yakima Yellow, FAM or ATTO550 and HPLC purified (Microsynth, Balgach, Switzerland), whereas the reverse primers remained unlabeled. Two master plates with 96 primer pairs at 10 μM concentration each were designed that could be multiplexed together to result in one 96well-PCR assay setup per mouse (see table with oligonucleotide sequences and master plate design).

Table 2.2.: Primer sequences for STR analysis (based on UniSTS)

Marker	5'Label	fw Primer	rev Primer
D1Mit132.1	ATTO	TATTGTTTATGGAAATTGGACCC	CATCTCTGAAGGAAAAAGTGCA
D1Mit159.1	FAM	TCTGGGGCCACTATGAGATC	TCACAATCAGAAAATATTATGAGACTC
D1Mit169.1	ATTO	CGCTGACTGCTACTTTATTATATTCC	TCTGATTTACTGTCAATCAAGAGACC
D1Mit17.1	FAM	GTGTCTGCCTTTGCACCTTT	CTGCTGTCTTTCCATCCACA
D1Mit206.1	ATTO	TGAGGCACCTTTGTATTCAGC	CCAGATGTCTTTGAACATTCTCC
D1Mit21.2	FAM	CGCTGGACAATCTTATAATTGCA	TCGAATCCCAACAACCACAT
D1Mit215.1	FAM	GGAGCAGAGTGTGAGAAGGG	CCAGTGTGAGCCCATTCC
D1Mit292.1	FAM	GAACTGGAGGTTTGCTACTGC	GGACATTGTTATCTCAGTTTTCTTC
D1Mit308.1	FAM	GAGGCTATGAGTCAAATGGACC	TTTATGAGGTGCTGAGATGCA
D1Mit411.1	YYE	GGAAACTGGAAAAGGGGGTA	TAGCATTGCTCTTTGGTTTCTG
D1Mit430.1	YYE	TATTAATGTTGAAGCCAGAAGCC	CTTTAATCATCTCTGTGGCAAGG
D1Mit495.1	YYE	CCACCTTGCTCCAAAAGAAA	TCTGAGAGGCTGCCACAATA
D1Mit60.1	ATTO	GGTTTCTGCACTCAGATTTGC	TGCTCTCCTTTCTTCAAAGAAG
D2Mit1.1	YYE	CTTTTTCGTATGTGGTGGGG	AACATTGGGCCTCTATGCAC
D2Mit100.1	YYE	GTGTTCCTAAGGTTGTATTTTGGC	GAAATTTGACAATTGCTAGGTGC
D2Mit113.1	ATTO	CTCACGTGAGGGTCATGAGA	CTTCTCTACCTTCCTCAGAAGCC
D2Mit148.1	YYE	GTTCTCTGATCTACGGGCATG	TTCACTTCTACAAGTTCTACAAGTTCC
D2Mit285.1	ATTO	TCAATCCCTGTCTGTGGTAGG	TATGACACTTACAAGGTTTTTGGTG
D2Mit327.1	ATTO	TAGGGGATCTGATGCCTCTG	GCCCATTGAGCACTTTTGAT
D2Mit365.1	YYE	GAGATCCCACTGATGATACAAGC	AGATGTGCCCAAGGGTCC
D2Mit395.1	ATTO	AGGTCAGCCTGGACTATATGG	AGCATCCATGGGATAATGGT
D2Mit404.1	FAM	GATGGTGATGATGATGATGATG	GACGCGCACAGGAAATAGAT
D2Mit411.1	YYE	ACACTCACAACTACGAGATAAAGCC	AGGTCATTAGGGCTGTCTTCC
D2Mit61.1	ATTO	AAAGTCAACTGCTTTCAGTTACCC	CACAGAAGTGCCCTTGCATA
D3Mit147.1	ATTO	TCTGCCTCTGTTAGATAGATATCCG	TTGTTCATCTATCCTCTGAAGTTCC
D3Mit200.1	ATTO	CAACTTCAGTTTCTCATTTGAATTG	GCAAATGGAAGAGGTTTCTCC
D3Mit203.1	FAM	CTGAATCCTTATGTCCACTGAGG	GGGCACCTGCATTCATGT
D3Mit256.1	ATTO	TACATTGCTTTTTGCTTTGAGTG	GTCGAATGTTATCAGAATTTGCA
D3Mit311.1	YYE	CGCCTGGTGGTAGTGGTG	CAGTGACTTAAGTACCCTTGACTCC
D3Mit320.1	YYE	AATGAAATCTCACGAGAGGCA	AAGCCAGGAGCAGAGTCAAG
D3Mit352.1	YYE	CGCAAAAGGCAGAGGTAAGT	TGCTTGCCTCTCTCCACC
D3Mit51.1	FAM	GGCACTGATAGCAGGCCTAG	TCTCTTCTGGTATTTCCTTCCG248
D3Mit57.1	FAM	TCCAGTTACTTGGTGAACTCCA	ATATGTGTACATGTTCATGGTGTG
D4Mit17.1	ATTO	TGGCCAACCTCTGTGCTTCC	ACAGTTGTCCTCTGACATCC
D4Mit170.1	YYE	TTCCATCGAGTGACTTGATCC	CAGAGTGGCTGTCATCTGGA
D4Mit18.1	FAM	AATTAGCCCGGAGCTTGATT	GCTTCCATACATTTGCTTTTCC
D4Mit196.1	FAM	TTGACTGGTCTTATATATCTCTATCCC	TATATTAAATGCTAACTGCTAAGCACA
D4Mit203.1	YYE	GAATTCTTCCTGGGCCTTTC	CAAGAGCCCAGGTGTGGTAT
D4Mit251.1	YYE	AAAAATCGTTCTTTGACTTCTACATG	TTTAAAAGGGTTTCTTTATCCTGTG
D4Mit256.1	ATTO	CTGGAGAGTTAGAATGGGGTACC	CAACAGAGGCGCTTCCTAAC
D4Mit268.1	ATTO	TAATCTGATCCAAACACTAAATCAGA	GCAGCCTTATGGAAACTTTCA
D4Mit308.1	YYE	TATGGATCCACTCTCCAGAAA	CAAAGTCTCCTCCAAGGCTG
D4Mit348.1	FAM	ACCAAACTTGAGTTCTATGTAAGAACA	TGCTTACATATCAAAACAATACAGACA
D5Mit10.1	FAM	CGAGAAGTTGGAAAGACCCA	GGCACCCATGCCTCTATG
D5Mit146.1	ATTO	TTAAATCTGAAGGTGTGGCTATAGC	GAGATTGCAAGTAAAGTGAGAGAGG
D5Mit158.1	FAM	AAAGACGCTGAGGAGTCACTG	CAGGAGACCTTGTAATAAAGGAAA
D5Mit201.1	YYE	GAGGACTCCTTCGATTTCCC	TTCCTAAGCAGGAACTGACCA
D5Mit309.1	YYE	TAGAGCCTATTTCAAACCCCC	GTTGCATCCATAGCAAGCAA
D5Mit352.1	YYE	CCCAGAGCCCACATCAAG	TAGGTGGGTGTGTCTCTCCC
D5Mit425.1	ATTO	TCGCCTTTCTTTCCCTCC	AAAATTACATTTGCATCTGGGG
D5Mit95.1	YYE	TGTTCTTGTCCATGTCTGATCC	AACCAAAGCATGAAACAGCC
D5Mit98.1	FAM	TCCTTCATTTTATCTTCTGCCC	TGAATTCACTCTCGCACCTG
D6Mit100.1	YYE	CTTGAGTAGGTCTCAGTGCGG	CACATGCACACACAGAAGCA

continued on next page

Table 2.2 – continued from previous page

Marker	5'Label	fw Primer	rev Primer
D6Mit116.1	YYE	ACATTTCTTTGTGAGGTTCCTTG	CAGGTTTTTTGAAAGACACTCTTG
D6Mit123.1	YYE	GGAAGGAGCAGGTCCAATAC	CTCCCAACCACCAAGACCTA
D6Mit138.1	ATTO	GCTCTTATTAATGAAGAAGAAGGAGG	CAAAGAAAGCATTTCAAGACTGC
D6Mit14.1	FAM	ATGCAGAAACATGAGTGGGG	CACAAGGCCTGATGACCTCT
D6Mit209.1	ATTO	CTCCCCCTCTGTGTGATTGT	TTATTACACCAGACCCATGTGG
D6Mit284.1	ATTO	GGCTGCTGAGAAACAACCTC	TGAGTATTGAGCCAAATCCTCC
D6Mit36.1	FAM	ACCATCTGCATGGACTCACA	GTTGAAGAGGACGACCAAGTG
D6Mit374.1	FAM	TTCTGGCTCTTAACAGTCTGTCC	TACATATGCCAATGATATTCTCCC
D6Mit86.1	ATTO	GACCAAACCAGAAGCCCCT	GGAATGTAGCCCTAAGTTGGA
D7Mit101.1	YYE	TACAGTGTGAACATGTAGGGGTG	TCCCAACATGGATGTGCTAA
D7Mit109.1	YYE	TCAACACCAGGAAGTCTCTTCA	CCTCCATCTCCCATCCAATA
D7Mit21.1	ATTO	GGGTTGAACCTTACAGGGGT	ATCAAACCAGCCCAAGTGAC
D7Mit223.1	YYE	ATGCACATGAGTGTGTGTATGC	TCCTGTGTCTGACGCTCATC
D7Mit228.1	ATTO	ATTCTTGGCCTTTTCTTGTAACA	AAACCTCCACACTGACTTCCA
D7Mit248.1	YYE	AATCAGGCAACTCAGGCACT	TCCTTAGGTCTCCAGTGAAAGC
D7Mit259.1	ATTO	CCCCTCCTCCTGACCTCTT	GTCTCCATGGGAACCACACT
D7Mit294.1	YYE	TAGTGGGAAAGAGAGAAACAATCC	TAATGTTTAATCTTGTCGTCTTAGTGG
D7Mit323.1	YYE	TTTCACCTTCTAATCCTACTTCCTG	TGTCCAGAACAGGAAATAGAGTACC
D7Mit350.1	YYE	TCTGCATCTCACTGTCCCAG	ATCTACAAATGAGTTTCTAAGGACTGC
D7Mit83.1	FAM	GGGAGTTGTCATGGGCAG	TAACCAAAAACCTATGCTATCAGA
D7Mit98.1	FAM	CGCCATAGAACAGATTTGATACC	ATGGGTCTCAGATATCCCACC
D8Mit112.1	YYE	ATATCAGGCATGCATTATGATCC	TCTCTCTAGTGGGATTATCAACACA
D8Mit124.1	ATTO	CAACTGTGTATCATAAACTGGGAA	GAAGAATCACTCAGCAGTGTATGG
D8Mit155.1	FAM	TTGGACAGGGAAAATTCTGC	TGAGGACTTGCTTTAAGAGTACTCC
D8Mit178.1	ATTO	AAAATCAACTGTTTACATTTGAGCC	AGAGCACGCAGTGTGTATGC
D8Mit211.1	FAM	CAGAACACTGTCCTGAAAAGTCC	TACCCACAAACCTGTATTTAAATTAA
D8Mit289.1	FAM	AAAAAGAAAAGAAGGCTTAGTAATGTG	CTTGCTATTCATTGCAAAATTCC
D8Mit292.1	YYE	AGTCAAGGCATTTAAAATTAACTGG	CTGGGTTTGCTAGTGAAAGATG
D8Mit339.2	YYE	ACCTATGGTACACACACATCGC	CAAACATTTTTAGGCATTTAGATCC
D8Mit45.1	YYE	GAACAGGACCAATAAAATGAAAGC	CTACCTTACCAAACTTCCCGG
D8Mit46.2	FAM	GCCTGGGCTACATGAGACTC	GGGAATTCCAATACACTAAAGGG
D8Mit47.1	FAM	AAGATGTGCTTACTCTGACTTCCC	GGATCTATCCACATGTGGTGC
D8Mit49.1	FAM	TCTGTGCATGGCTGTGTATG	TGGTGTGCTGCTGATGCT
D8Mit63.1	FAM	TCTGGAACACAGTCCAATTCC	ATATGTGTGAGGGTTTTACCGG
D8Mit92.1	FAM	CTCAGGCTATCTTGGACATGC	TGGCTCACATCTGTGCTTTC
D9Mit129.1	ATTO	TTGTCTTTTAACCTCCTGGAGC	TCCCATCTTTCTCCTTGTGG
D9Mit151.1	YYE	TGGTCAAGGTGTGGTATCGA	AAAACTCAGCATCCAATGGG
D9Mit2.1	FAM	GTGGTCTGCCCTCTTCACAT	CAAAGCCAGTCCAACTCCAA
D9Mit201.1	YYE	CCTGCAAGCCAACTACATGA	GCAAAAATGAAGTTCAAAAGGG
D9Mit250.1	YYE	CCCAAAAACCTATTTGCAGTG	GTGACATGATTCCTTCAGTCTTACC
D9Mit285.1	ATTO	CAAATACATTGCTGATTATATCAGAGA	GGACTCTAGATCTCATCAGGGA
D9Mit336.1	YYE	AAGTGGTTCACAGAAATGTATACAGG	TTTTCTTTCTGTGGTAAAGGGG
D9Mit347.1	YYE	CCTCCACATGTGCACTGCT	CTGTCCATCTATCATCTATCTGTCTG
D9Mit355.1	YYE	CTCATTCACTTCCTGGTCCTG	GAAGGAAAGCCCACACTTTG
D9Mit90.1	ATTO	AGGAGTCTCCCTGTACCTACACC	AAGTAGAGGGGAGGAATGAACC
D9Mit97.1	FAM	TCTCACTACTGCCTGCCAGA	TAGATTTCTCAGGCAAGGAAGC
D10Mit103.1	ATTO	TATGCCGACAATATTTCATTGC	GCCTCTGCATACATACCAATACC
D10Mit14.1	ATTO	AGAGGGGACAAGGAGAGACC	AAGGTTTGGGTTCAGTTCCC
D10Mit20.1	ATTO	CACCCTCACACAGATATGCG	GCATTGGGAAGTCCATGAGT
D10Mit207.1	ATTO	TTTAAGCAAAACACCCATACACA	TCTGAGGGTACCTGTAGTCATGC
D10Mit213.1	ATTO	CTCCTCCTACTGATTGTCCCC	GGGACAAACTTTTAAAAATTGCA
D10Mit230.1	FAM	AGATAGCCTAGGGGGTGCAT	ATCAGTTTCCAATCGCTGCT
D10Mit233.1	ATTO	GTGCTTTATATTGGAGATCATCACA	GTCCCGAATTTCACATACATAGC
D10Mit31.1	ATTO	CATAAGGAGCACAGGCATGA	CCCTCTACGTGCATGCTGTA
D10Mit38.1	ATTO	CGATGAGCCCTAACACCAAT	CCTGTTACAAACTAAACCAAACCC
D10Mit86.1	ATTO	TTTGCCTGTAACAAGCCAGA	TTGAGGCTATCAGTTTAAAATCCC
D10Mit95.1	ATTO	CCAGCCTAGAAAACCAAGCA	ACAGTGCTTCCGGAAAAATG
D11Mit143.1	YYE	TTTATATTTTCAGGCTGTTCAGAGG	AACCTCTTTGCACACAAGAACA
D11Mit186.1	ATTO	AAAACACATTTACATGCATGGTG	TGTGTGCACTTAAGCCCTGA
D11Mit189.1	ATTO	ACCATGTAATCCGATGCCAT	AGATGAATGTAATTGACCTACTTCCA
D11Mit2.1	YYE	TCCCAGAGGTCTCCAAGACA	CCACAGTGTGTGATGTCTTC
D11Mit285.1	YYE	CATGAATCCATCACCAGCAG	TTTTTCAGTCATGCAGGCAG
D11Mit326.1	YYE	CTATGGCAGGCACATGACTG	TTAAAAGTGGTTTCAGGTGTGTATG
D11Mit333.1	ATTO	CATGTGGTTATTTTCTAGCCCC	AGGCATCAATAACTATTTTTCAGTG
D11Mit4.1	ATTO	CAGTGGGTCATCAGTACAGCA	AAGCCAGCCCAGTCTTCATA
D11Mit54.1	ATTO	AGGCTGGTGGCTAGTGTCC	AAGTCTTGCGCTGCATCTTT
D11Mit71.1	FAM	GCCATACCTGGTAGCGTGTT	AATTTTCAGATGTAGCCATAAGCC
D11Mit86.1	YYE	TTGACATTGTGACAAAGACTTTCA	AAGGCATCATGAGGTTTTTAGTG
D12Mit11.1	YYE	TATTAAAAGGCAATGGGAGGG	TTGACTTCAGAGTGATTTCCAGG
D12Mit143.1	ATTO	CCCTATGCATGTACATTGTGAA	CGTGGGCATTTATCTTTCCT
D12Mit158.1	FAM	CATTGGGCAATGGAATTTG	ATGAGAGAAAACCAGAAACAAAGG
D12Mit182.1	ATTO	GTACATACAATACATCACACAAACGG	GGCAAGAAAACAGACCAATAGG
D12Mit285.2	ATTO	GCCTCTTTCTAAATTTTTATGTTGTT	GTCTGTCTGTCTGTCTTTTTCACA
D12Mit59.1	FAM	AGTGAAATTCAGAGCACAAAAGC	ACCCTATATCTCCATGGTACGTG
D12Mit7.1	YYE	CCGGGGATCTAAAACTACAT	TCTAATCTCAGCCCAATGGT
D12Mit91.1	FAM	GATTCAAGACAAGACTCCTGCA	CGCCCCCTCATGTTTTATC
D13Mit151.1	YYE	ACAAATTAAAGACAAAATGTCTGCA	TGTGCACACCAGCATACAAA
D13Mit19.1	FAM	GGTGAGTTGTGTAATGATGGACA	AGCAACAGGGCTACTAAACACA
D13Mit213.1	ATTO	GCCTGAAACTCTACATAAAATACATCC	AGTTTCATTGCTTTAGTTACATTTTCA
D13Mit275.1	YYE	TTAGCAAGGGAACAGAGAGAGG	CAATCAAGGTATCCCTGTCTCC
D13Mit56.1	FAM	CCTGTAACTCCAGATCCTGAGG	CAGTTGACCGAAATAGTCATTCC
D13Mit78.1	FAM	ACAGCACGGGTTTATCATCC	TATGCCTGCCAGGCTTCTAT

continued on next page

Table 2.2 – continued from previous page

Marker	5'Label	fw Primer	rev Primer
D13Mit88.1	FAM	ACTGATGGCTCATGAGACCC	AAAATTAATAGGAACTGCAAGGG
D14Mit126.1	ATTO	CCTGTCCCACAACACCTTTT	TATACATATGGGTAGCACTGAGTGG
D14Mit127.1	FAM	AAACTTTACCTACCAGTGTCAAGTTAG	GTGTTGAACAACTCTATGTCTGTCTG
D14Mit170.1	ATTO	TGTGTATGATTGTGTGGGGG	AGAAAGCAAACTTGCAAATATTCA
D14Mit174.1	ATTO	ACTGCAGAGTCCACACAAGTG	TCTGAGCCACTATGCCTGG
D14Mit263.1	YYE	TGAGCACAGAGCCTATGTGG	ACAGAGAAATACCATGAAAACACC
D14Mit40.2	FAM	TCCCGGGGATCAGTAAAATAT	CAAGGTGGCCTCTGACTTTC
D14Mit44.1	FAM	AGTCACACCTGTAGAGTAAGCACA	GCTACTGCCTCGGTTTGTG
D14Mit48.1	YYE	TTTCTAGCCCTGACCCCC	TCTGTTCACTCTGTGTAATTCTCC
D14Mit5.1	FAM	CACATGAACAGAGGGGCAG	GTCATGAAGTGCCCACCTTT
D14Mit60.1	ATTO	AGGCTGCCCATAAAAGGG	GTTTGTGCTAATGTTCTCATCTGG
D15Mit107.1	FAM	CAACACTTTATACACTTGTGTCAGGG	TCATGGTTGGAACAGCAGAC
D15Mit159.1	ATTO	CACAGGCATACATAGAAATGTGC	CAACTTGTCAGGGTCTACTGAGG
D15Mit242.1	YYE	GGTATACACACACACAATTTCAAGG	GAAAATAGTACCACAGAAGTTTGGG
D15Mit252.1	YYE	CTTCAAACATGTTATCATTGTCACA	CTTCTGTATTCACAGGTGCTCG
D15Mit262.1	YYE	TTTATTAAAGCCAAACAGAGATTGC	AACATTGTATTTGGGTCATTGTG
D15Mit67.1	FAM	AGCTTCAACAGTGAAACATAGCC	CTGCTGTGTGCACTTATGCA
D15Mit70.1	FAM	CATTGAGGGTTTGTAGGTTGG	ACCCCTGCAAGTTGTCTTTG
D15Mit80.1	FAM	TGAAGTCATCTTTCAATTTTCTCC	CGAAGATGCCTGCCAAATAT
D16Mit101.2	FAM	TTATGAAATGTTTTATCTTTTGGGG	CTCCAGATGTAGAAATTAAAATCTTGG
D16Mit131.1	ATTO	TGGTGGTGGTGTTGATGGTA	AAGACCATTTCTAATAAACAACACCC
D16Mit153.1	FAM	CCTTCCAGGACCACAAAGAA	GAAAGAACTAGGAATGGAGAAAAGG
D16Mit189.1	FAM	ACAGTGTTTGTTTGTTTGTTTGTG	CAGTACAGGAAGTCTTTGCATCC
D16Mit52.1	YYE	ACACATGTGCAAGCCTAACC	TTATCCCTGGAATCTGGGG
D16Mit60.1	FAM	AAATGGTCAGCCCTGAAGC	TGCCTCACCCTTTGAAGTGT
D16Mit86.2	ATTO	TAATGTGGCAAGCAACCAAA	GCATGTTTCCATGTGTCTGG
D17Mit1.1	FAM	TGCTTGAAATCCTGGGTTCA	TGCAAAAATGTATGTGCCTG
D17Mit143.2	YYE	GCTTTCTTGAAGACGTGGGA	CACAGGATGCTTGTAAGCACA
D17Mit180.1	ATTO	AGACACTGTCTAAAAACACAAGATGG	TTGTGTTCATATGCATGTGTGC
D17Mit20.1	FAM	AGAACAGGACACCGGACATC	TCATAAGTAGGCACACCAATGC
D17Mit245.1	FAM	TGTGCTCTGGCTAGGGAGTT	CACATTCATATGTACACACACATGC
D17Mit39.1	YYE	CCTCTGAGGAGTAACCAAGCC	CACAGAGTTCTACCTCCAACCC
D17Mit51.1	FAM	TCTGCCCTGTAACAGGAGCT	CTTCTGGAATCAGAGGATCCC
D17Mit81.1	ATTO	CAATCTATCTCATATGCATCTCTGTG	GTCTGGTGCACCTGTCCTC
D18Mit12.1	YYE	TTGTCAGTTTCTTGTGAGGGG	TGTTTAATAAGCCTTTTCCTGAGG
D18Mit177.1	FAM	CTGTAGTTTATCAGTTCACCCTGTG	TGTGCTGTTAAACAAATATCTCTGG
D18Mit186.1	ATTO	AAGTGTTGGGCAAAGGCTAA	CTTTAGTATAGTGTGCATGAGTGTGA
D18Mit194.1	ATTO	CCACCACATAAGGGAGGAAA	GTTTGTTGTTGTTCTATTTTCAAACA
D18Mit208.1	YYE	GACACATTTATGAGTCAGTCAGCC	TGTGAACCCAGGTCATGTGT
D18Mit222.1	FAM	AATCCAAGATTGACATGTGGC	CTTAGATGCCCTGTCTTAAAAAAA
D18Mit48.1	FAM	TTGCACTCACAGGGCACAT	TCAGAGTTTCCAGAAGACACCA
D18Mit64.1	FAM	TCAGATTCACTGCTAAGTCTTTTC	AGCAAGAAAAGCAGGTGAGG
D19Mit103.1	YYE	CCCATGTCCTTTGTTTCCC	GAAGCGCTATCACTGGATCC
D19Mit26.1	ATTO	TTGTTACACAGCAAAATCCTGC	TTGAGGAGTAAGGCAAAAAAGG
D19Mit28.1	ATTO	TCTTCATGCCCAAAAGAGCT	GCATCCTGAATCTCCTGCC
D19Mit33.1	FAM	CCTTTTCAAGAGCATCCTTAAA	GGTGGGACTTGAGAGATGCA
D19Mit6.1	YYE	ATTAGTAAACTGACTCCCATGCG	CTCATGAGTCCCCTGGGTTA
D19Mit68.1	ATTO	CCAATACAAATCAGACTCAATAGTCG	AGGGTCTCCCCATCTTCCTA
D19Mit88.1	ATTO	AACAGTGCAACTTTGGAGGC	TCATTGGAACTGTCTTAACAGTGC
D19Mit90.1	YYE	GTGGGAATCAATTTTAGTATGAACA	GGATGCTTGATATCATGTACATACA
DXMit121.1	FAM	GGACCCCAGTTCTTTCTTACATA	GTAAAACTGGGGGAATGGCTTAG
DXMit132.1	YYE	GTTAGGATTGCTGGTTGCGT	TCAACTCAACTGCAACATACCC
DXMit172.1	ATTO	TACCACAGTTTGAATAAAGATGTGTG	GAAGAAACCATGACTCCTCTTTG
DXMit216.1	YYE	ATTTGGAACAGCAGCGTTG	TGTTTACACAATCTATCCAGTTACAGC
DXMit223.1	YYE	TTGGTTTGGGGTTTTTTTTG	ATTCCTGATAATGTCTTCTGGACA
DXMit64.1	FAM	AATATGTAAGGACAGCCTTCTCAG	AGAGGAGAGACAGGTCCAGGA
DXMit81.1	FAM	GAGGAGCATCAACCTTCTCG	GAGGTGGGGAGAAACAGAGG

2.4. SNP mapping of chromosome 2

For a finer mapping of the region between *Rag*2 and *Prnp* we used taqman-SNP genotyping assays (Applied Biosystems, USA). We chose published SNPs in a 5Mbp distance each. SNP taqman assay primers and identifiers are listed in the table below. 1 ng DNA per well was used for each reaction in a total reaction volume of 5μL, consisting of taqman SNP mastermix (Applied Biosystems) and the respective SNP assay mix. PCR reactions were performed in an 9600 ABI real time PCR device in a 384-well format. A post-read allele-calling and data analysis was acquired with the SDS 3.1 software (Applied Biosystems). Polymorphisms were integrated into the STR-marker profile at the respective genetic map position and data were analysed with Structure software according to ([94]).

Assay ID	SNP ID	pos (Mb)
M_22285663_10	rs13476663	99.9
M_24382337_10	rs29912618	100.8
M_23720601_10	rs13476670	101.9
M_22354457_10	rs6261478	107.0
M_23043361_10	rs13476705	112.9
M_45281514_20	rs3090608	117.8
M_23028483_10	rs33314425	122.3
M_23908236_10	rs13476764	127.8
M_23300050_10	rs13476769	129.7
M_22299775_10	rs13476772	130.6
M_23938758_10	rs13476802	138.5

Table 2.3.: SNP assays for mapping the region between *Rag* and *Prnp*

2.5. Sequencing of the human PRNP coding region for detection of polymorphism on codon 129

DNA from non target fractions for sequencing of the human *PRNP* locus was extracted with the Nucleospin-Blood Kit (Maccherey-Nagel, USA), DNA quality was assessed with a Nanodrop-Spectrophotometer. Subsequent PCR-amplification and gel-extraction was performed with a qiagen gel-extraction kit (Qiagen, USA). PCR-fragments were subjected to the sequencing service of the institue of pathology (Prof. D. Zimmermann). Sequencing reactions for the full length human *PRNP* ORF were performed using the following primer sequences: *PRNP* up: 5'TAT GCA GGA AAC ATT TAG TAA T *PRNP* low 5'TGC CAA GGG TAT TGA TT. Sequence alignment analysis was performed with Sequencher software (USA) in comparison to a reference sequence.

2.6. Sequencing of Sirpa exon 2 in different mouse strains

Genomic DNA from mouse tails was subjected to PCR for amplification of the *Sirpa* exon 2 (IgV domain) using primers SirpExon2fw: 5'TGG CTG CCA TCT TTC TT and SirpExon2rev: 5'TGA AGA AGG CAC AGG CTT ACT using 35 cycles of (95, 55, 72) °C for 1 min each. PCR products were purified with a GelEx-kit (GE-systems, USA) and concentration determined. Fragments were sequenced by our in-house sequencing service with the same PCR primers. Sequence alignment and polymorphism assessment was performed with Sequencher software (USA).

2.7. Histology and immunohistochemistry

Tissues were fixed in 4% buffered formalin and treated with 98% formic acid for 1 hour then fixed for more than 24 hours prior to paraffin embedding. Bone containing tissues such as vertebral bodies were further decalcified with 1% EDTA and sonication. 2μm thick

sections were cut onto positivey charged glass slides and stained with hematoxylin and eosin, or immunostained using antibodies for human CD45 (LCA), for human CD20, or human CD3. Sections were heated to 100°C in a pressure cooker in citrate buffer(pH 6.0), cooled for 3 minutes, then washed in distilled water for 5 minutes. Immunohistochemical stains were performed on an automated Nexus staining apparatus (Ventana Medical Systems) using an IVIEW DAB Detection Kit (Ventana). After incubation with protease 1 (Ventana) for 16 min, sections were incubated with anti-CD45, CD20 or CD3 for 32 min. Sections were counterstained with hematoxylin.

2.8. Cord blood acquisition and preparation of CD34+ hematopoietic stem cells

Fresh human cord blood (30-100 mL) was obtained from healthy full-term newborns with written informed consent of the parents (Department of Gynecology and Obstetrics, University Hospital Zurich, Triemli-Spital, Kantonsspital St. Gallen). Serology testing of the mother beforing cord blood acquisition ensured negativity for HIV, HBV and HCV. Blood was collected in blood bags containing 35 mL of anticoagulants (Macopharma, France) and stored for a maximum of 9 h at room temperature before processing. We took blood from Caesarian sections as well as from spontaneous pregnancies immediately after placentation. The blood was transferred to a biosafety cabinet and filled into 50 mL Falcon tubes containing a filter for density gradient centrifugation (Leucosep, Germany). Usually, the blood was diluted with 1:1 with PBS to obtain a hematocrit of about 25-30% for optimal separation results. After density gradient centrifugation with Lymphoprep (Axon-Lab, Switzerland), 800xg, 20 min, at room temperature, serum was removed, the mononuclear fraction was collected and washed with PBS. Red blood cells were lysed using ACK-lysing solution (Cambrex, USA) for 10 min at room temperature. After a subsequent wash in PBS and centrifugation (300xg, 7 min), cells were incubated with immunomagnetic beads and Fc-blocking reagent in MACS-buffer (1% BSA, 1mM EDTA in PBS) on ice for 30 min according to the manufacturers instructions (CD34+ selection kit, Miltenyi Biotec, Bergisch-Gladbach, Germany). We always performed a magnetic enrichment over two MACS LS-columns. After sorting and washing, the cell count and size of target and non target fraction were evaluated with a CASY-cell counter. Furthermore, samples were evaluated by flowcytometry for CD34 and CD3 cell content using mouse anti-human CD3-PE and mouse-anti-human CD34-APC labelled antibodies (Pharmingen). Cells were either frozen at-80°C or -196°C in heat inactivated fetal calf serum containing 10% DMSO hybrimax (Sigma) or immediately transplanted when newborn mice were available. In case of re-thawing of cells, we checked again for viability and cell count before injection into acceptor mice.

2.9. Cell and tissue culture of hematopoietic stem cells

UCB from full-term deliveries was processed within 10 hours and was diluted with an equal volume of culture medium (Dulbecco's Modified Eagle's Medium (DMEM),

Gibco, USA), layered onto Histopaque (density 1.077g/mL, Sigma-Aldrich, UK) and centrifuged for 30 minutes. Mononuclear cells (MNC) were collected and washed twice with DMEM. Aliquots containing 1x10^7 cells were cryopreserved in DMEM 10% DMSO at a fixed cooling rate (1°C/min) and stored at -80°C. After thawing, the viable cell count, percentage of CD34+ and CD3+ subpopulations, number of colony-forming cells (CFC), number of CFC capable of recloning, cell morphology and growth in in vivo repopulation assays were determined and utilized as day 0 controls.

Cytokines Recombinant human stem cell factor (rhSCF), Flt-3 ligand, rh IL-6 and TPO were purchased from R&D Systems (Switzerland).

Stroma-free long-term cultures For expansion, freshly thawed UCB MNC were seeded at a concentration of 1x10^5 cells /mL in RPMI-1640 and pooled human AB serum (Gibco, USA) used at 10%. Four growth factors were added: these were SCF and Flt-3 (25ng/mL) and TPO and IL-6 (20ng/mL). UCB cultures were grown at 37C in humidified 5% CO_2 in air. Wells were demi-depopulated and fed weekly, and a new 24-well plate was used every week. Cryopreserved UCB MNC (10^6/mL) were also expanded in a closed cell culture system with commercial expansion bags (volume 3mL, VueLife TM Bag, American Fluoroseal Corporation). Similar to wells, MNC were expanded in the same culture medium as above except that the expansion in bags was carried out for 2 weeks only. Cell cultured in bags were split after one week. The harvested cells from wells and bags were counted and suitable aliquots were assayed at week 1 and 2 for bags and 1-3 weeks for wells.

2.10. Immunoblotting

Tissues (brain, spleen, bone marrow) were homogenized with two sets of syringes in 10 volumes of RIPA buffer (3%NP40, 3%Tween 20 in PBS), containing protease inhibitors (Complete Mini, Roche, Switzerland, 1 Tablet per 10 mL), and the resulting homogenates were adjusted to 5 mg/mL protein with a custom BCA assay with respective Albumin standards (Pierce, USA). Total protein (10 to 50μg) was electrophoresed through 12% Bis-Tris Gels (NuPage, USA) in 1x NuPage Running Buffer (NuPage, USA). Proteins were transferred to nitrocellulose (Schleicher-Schuell, Germany) by wet-blotting in transfer buffer (3.3g/L tris, 14.4g/L glycine, 20% methanol). Membranes were blocked with TBS-T (2,42 g/L Tris base, 8g/L NaCl, pH 7.5, 1mL/L tween 20 in H_2O) containing 5% Topblock (Sigma, Switzerland), incubated for 1 hour at room temperature with monoclonal anti-mouse PrP antibody POM1 diluted 1:10'000 in 1% Topblock in TBS-T and washed 3 times with TBS-T. Incubation with secondary antibody HRP-anti mouse IgG1 was performed for 1 hour at room temperature, followed by another 3 washing steps. Detection of the signal was achieved with ECL solution (Pierce, USA) and a Kodak imaging station. Alternatively, blots were developed on films (Kodak) after various exposure times (10s to 5 min). For loading controls, membranes were washed again and re-incubated with antibodies against beta-actin (Zymed, USA) in a 1:7000 dilution. As a secondary antibody an HRP-anti mouse IgG1 antibody (1:10000) was used. Blots were reexposed as previously described.

2.11. Flowcytometry

Detection of human surface antigens CD45, CD20, CD3 and CD34 on mouse peripheral blood leukocytes, spleen or bone marrow: 200μL of peripheral blood from the tail vein was taken directly into ice-cold FACS buffer(PBS, 1mM EDTA, 2% FCS) followed by centrifugation (300xg, 7 min) and incubation for 30 min on ice with 20μL of antibody master-mix in FACS buffer. Lysis of red blood cells was performed using 1-2 mL of BD lysing solution per sample in a 1:10 dilution with millipore H_2O (Becton Dickinson, California, USA). After lysis, cells were washed and centrifuged twice with ice-cold FACS buffer before acquiring them using a FACSCalibur flow cytometer (Becton Dickinson, California, USA) with Cellquest software and appropriate instrument settings and compensation. Postacquisition analysis including gating and statistical analysis was performed with FlowJo software.

The following directly labelled mouse-anti-human antibodies were used (all Pharmingen, Europe): phycoerythrin (PE-) labelled anti-CD20, PE-anti-CD3, APC-anti-CD45, APC-anti-CD34 and the respective isotype controls. Human peripheral blood leukocytes from umbilical cord blood non-target fractions out of the MACS-sorting procedure served as a positive control, unstained and isotype labeled samples defined the negative control.

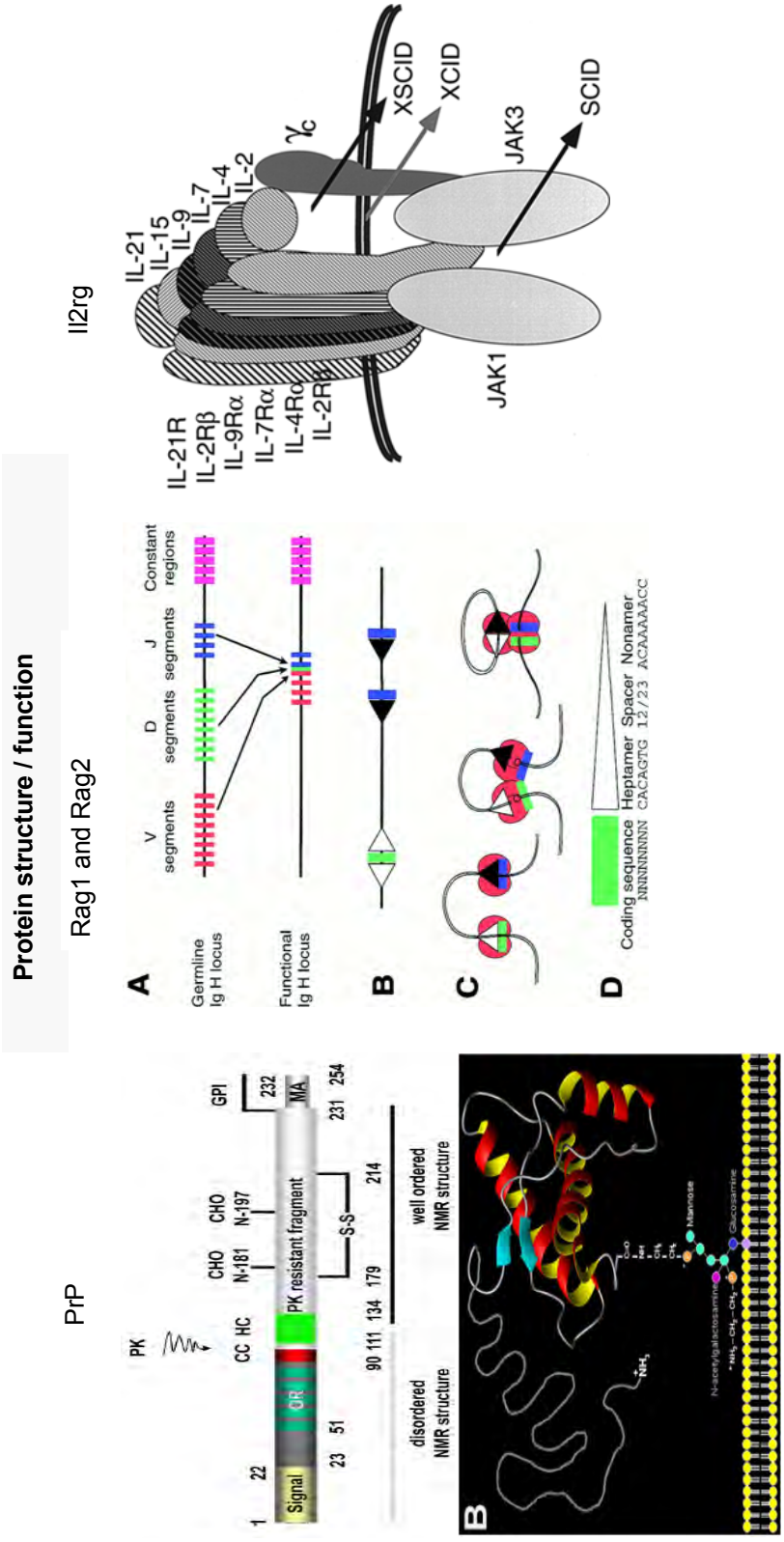

Figure 2.1.: Structure and, if applicable, functions of the deleted proteins

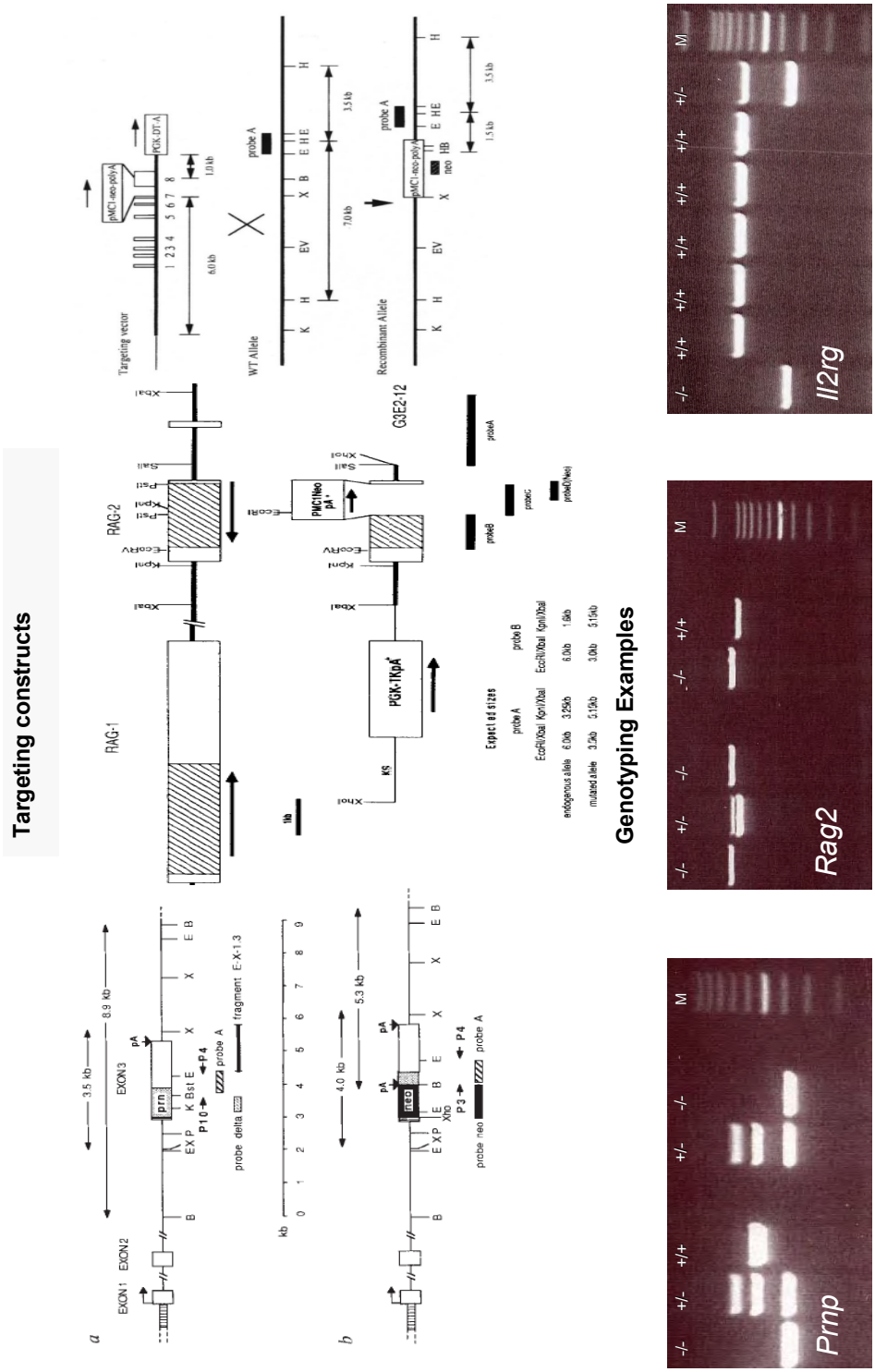

Figure 2.2.: Overview of genetically modified null mice used in this study.
Targeted loci and map of the deletion strategy for *Prnp* [12], *Rag*2 [105] and *Il2rg* [56] the targeting-strategy for deletion of *Rag*1 is not shown here. Representative examples of genotyping PCRs based on the construct design with outcome possibilities for presence or absence of the respective wildtype (+) or knockout (-) alleles.

3. Results

3.1. Breeding of genetically modified mice

A major goal of this study was to yield reconstitutable acceptor mice that would be devoid of the murine prion protein, and, in a later stage of the project, would contain an inserted human *PRNP* transgene. Several bottlenecks accompanied this task:

- The genetic background of the original Zurich1-*Prnp*$^{-/-}$ mice and *Prnp*$^{-/-}$-*Rag*1$^{-/-}$ was not identical to that of the primarily reconstitutable *Rag*2$^{-/-}$Il2rg$^{-/-}$ mice: reconstitution with human CD34(+) cells is only possible on a BALB/c background for reasons that are unknown to date, whereas our in-house *Prnp*$^{-/-}$ mice displayed a mixed C57Bl/6 and Sv129/J background.
- Recombination between *Prnp* and *Rag* genes is limited because of spacial proximity of the two genetic loci: both genes reside on chromosome 2, between the genomic regions 100 and 130 Mbp.
- Breeding of *Il2rg*$^{-/-}$ mice on their own is impossible due to the development of an autoimmune phenotype soon after birth resulting in a markedly reduced lifespan.

Therefore, our breeding strategy became more complicated than initially intended since we had to intercross *Rag*2$^{-/-}$*Il2rg*$^{-/-}$ mice (BALB/c) with already available *Rag*1$^{-/-}$ *Prnp*$^{-/-}$ animals (mixed B6-129Sv background) to yield "triple knock-out" *Rag*1$^{-/-}$ *Prnp*$^{-/-}$*Il2rg*$^{-/-}$ and, in case of a recombination between *Prnp* and *Rag*2, *Rag*2$^{-/-}$ *Prnp*$^{-/-}$*Il2rg*$^{-/-}$ mice. Further, the resulting strains had to be backcrossed with *Rag*2$^{-/-}$*Il2rg*$^{-/-}$ mice to a maximally pure BALB/c genetical background to render them susceptible for reconstitution. However, backcrossing would result in the loss of the *Prnp*$^{-/-}$ allele and had to be performed over several generations to minimize variation and genetic artifacts in experimental outcome. A conventional backcrossing experiment to generate inbred mice contains at least 10 backcrossing cycles, a procedure that would last about two years.

"Speed congenics" was the method of choice to accelerate our backcrossing efforts (see section 3.1.4.

The offsprings of our breeding pairs where genotyped by PCR for the absence or presence of the following genes: *Prnp*, *Il2rg*, *Rag*2, *Rag*1 and the *PRNP* transgene. Figure 3.3 shows a typical outcome of a screening genotyping PCR.

3.1.1. Rag1$^{-/-}$ Prnp$^{-/-}$ Il2rg$^{-/-}$ mice

Since *Il2rg* is located on the X-chromosome, we obtained "triple knockout" *Rag*1$^{-/-}$ *Prnp*$^{-/-}$*Il2rg*$^{-/-}$ mice with the right genotypic constellation for our intended experiment

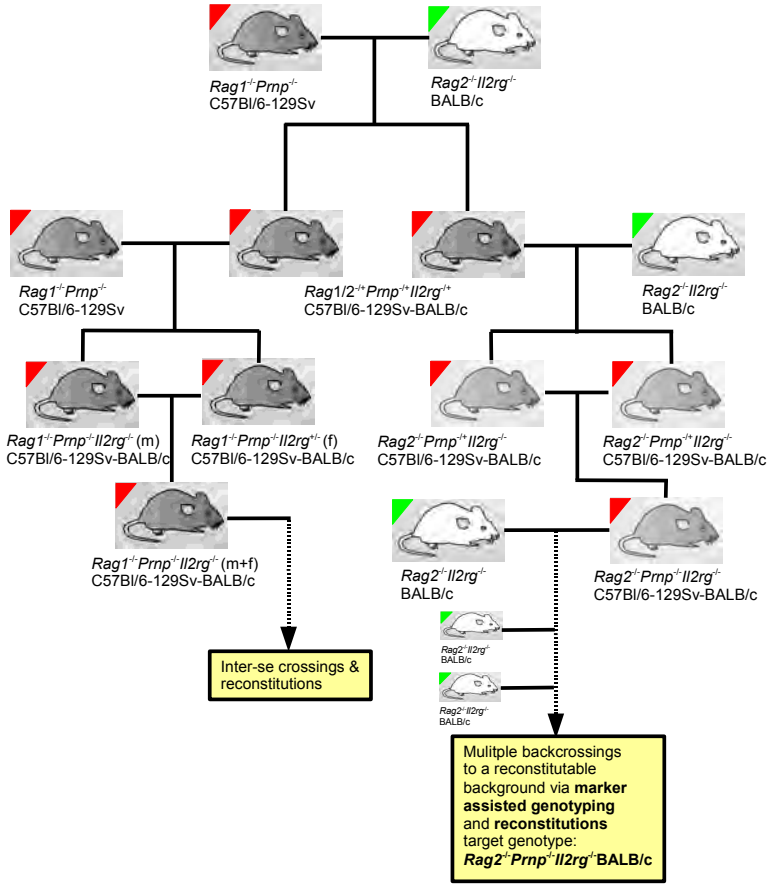

Figure 3.1.: Breeding strategy.
Our "classical" breeding strategy between our mixed $Rag1^{-/-}$ $Prnp^{-/-}$ and BALB/c $Rag2^{-/-}Il2rg^{-/-}$ to yield "triple knockout" $Rag1^{-/-}$ $Prnp^{-/-}Il2rg^{-/-}$ (low BALB/c) and $Rag2^{-/-}$ $Prnp^{-/-}Il2rg^{-/-}$ (high BALB/c) and the subsequent speed congenic backcrossings is depicted.

after two breeding generations. Besides of the genotype, we verified the immunotpye of these mice per FACS and the absence of PrP^C by western blot which clearly showed that these mice were devoid of B-, T- and NK cells and devoid of PrP^C-expression. However, these mice had a mixed genetic background and could possibly not be used for reconstitution experiments from the very beginning.

3.1.2. $Rag2^{-/-}$ $Prnp^{-/-}$ $Il2rg^{-/-}$ mice

Klein et al. needed to analyse about 1000 offsprings to finally find a mouse that exhibited a recombination between *Prnp* and *Rag*1 [60]. *Rag*1 and *Rag*2 are closely linked on chromosome 2 (both at 56 cM), whereas *Prnp* is located upstream, 19 cM or 30 Mb apart from those two genes. Surprisingly, we found the constellation "$Rag2^{-/-}$ $Prnp^{+/-}$ in one

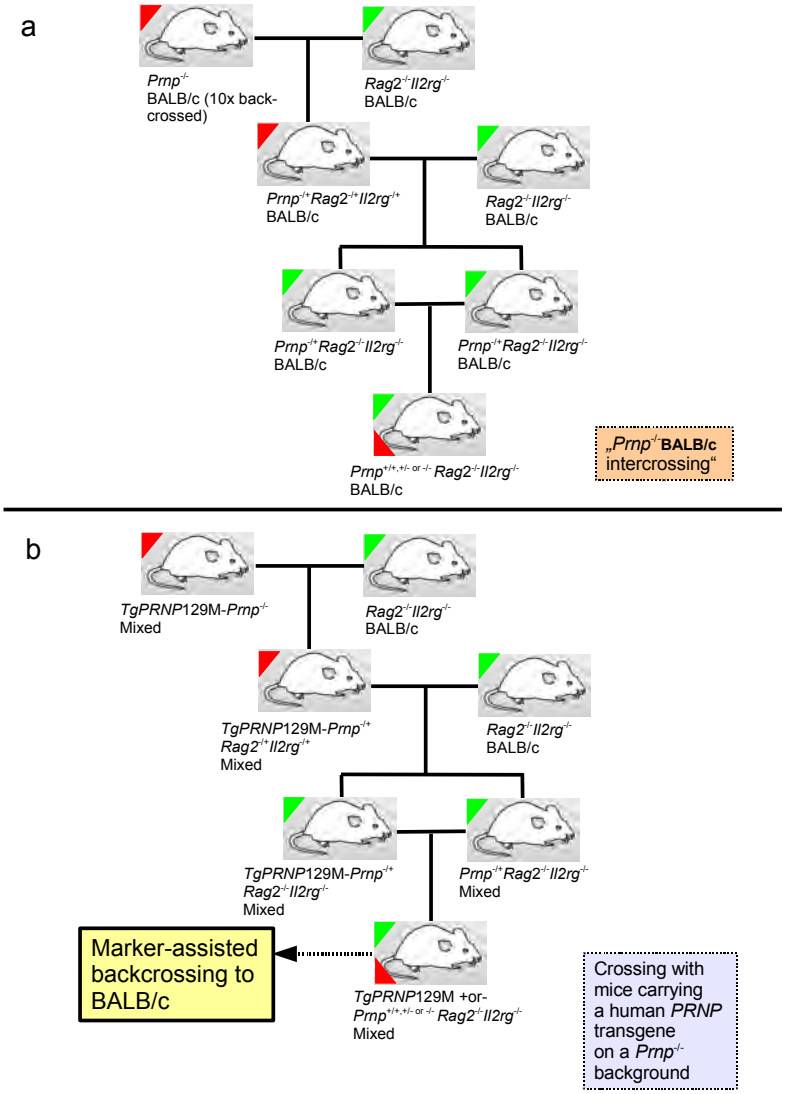

Figure 3.2.: Alternative breeding strategy.
a shows a breeding setup between $Prnp^{-/-}$(BALB/c) and $Rag2^{-/-}Il2rg^{-/-}$(“BALB/c”) mice to yield triple ko reconstitutable $Rag2^{-/-}$ $Prnp^{-/-}$ $Il2rg^{-/-}$ mice. b depicts the strategy applied to yield mice carrying a human *PRNP* transgene (Tg*PRNP*129M) and the respective reconstitutable genetic background. The original Tg*PRNP*129M transgenic mice were described in [6].

mouse already in the 2nd breeding generation which indicated that the probability of a recombination event between *Prnp* and *Rag* is possibly higher than initially expected and follows the calculated probability of 20% (10% for each cross-over possibility). We also saw the reverse case, i.e. recombinations of a *Rag*2(+)-allele to a *Prnp*(-) chromosome. Since those mice could thereafter be backcrossed with the original $Rag2^{-/-}Il2rg^{-/-}$ mice,

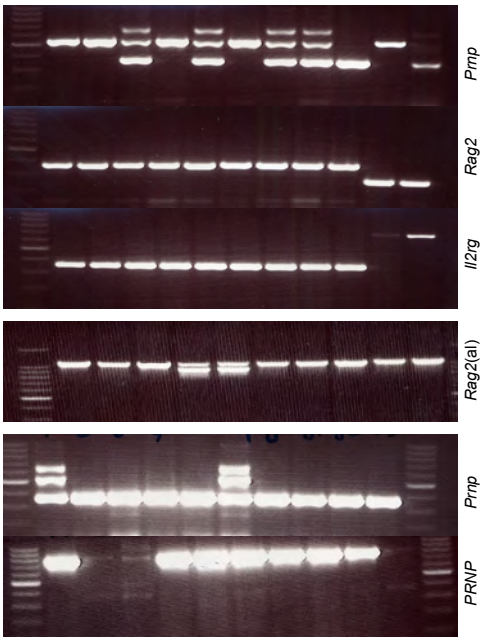

Figure 3.3.: Agarose Gel with specific PCR products.
PCR amplicons were loaded on a 2% agarose gel containing ethidium bromide and visualised under UV-light. For *Prnp*, a 546 bp fragment for wt and a 362 bp fragment for knockout alleles could be detected. The *Rag*2-PCR resulted amplicons of 1107 bp for mutant and 973 bp for wild type alleles in one primer set, or in amplicons of 350 bp and 263 bp in a alternative primer set. Primers for the deleted region within Exon 7 and Exon 8 of *Il2rg* resulted in PCR products of 350 bp (mutant) and 660 bp (wildtype allele). The human *PRNP* transgene sequence was detected with a PCR resulting in a fragment length of 900 bp. Genotyping of the *Rag*1-locus which tests for presence or absence of the wildtype allele is not shown here.

yielding automatically a more elevated percentage of BALB/c specific alleles, we decided to primarily concentrate on these mice for further backcrossings.

Additionally we also decided to intercross $Rag2^{-/-}Il2rg^{-/-}$ with $Prnp^{-/-}$ that already have been backcrossed several times to BALB/c to have those mice primarily on a BALB/c background. This breeding was initiated a little later during the project, but also in this case we could observe a recombination between *Prnp* and *Rag*2 and obtained suitable "BALB/c" triple knockouts within about half a year (see also 3.2)

3.1.3. $Rag2^{-/-}$ $Prnp^{-/-}$ $Il2rg^{-/-}$ - TgPRNP129M mice

Further, we started to backcross Tg*PRNP*129M mice, carrying a human *PRNP* transgene on a mouse *Prnp* knockout background with BALB/c $Rag2^{-/-}Il2rg^{-/-}$ mice. In this case, we also observed several recombination events between *Prnp* and *Rag*2 as early as in

the 2nd breeding generation which facilitated the process of generating "triple knockout" mice carrying a human transgene sequence. However, the genetic background of these mice is already known from published reports to be different from BALB/c, B6 and Sv129, which also necessitated the need to backcross these mice to BALB/c, thereby controlling for the presence of the human transgene and absence of the mouse *Prnp* allele.

3.1.4. STR-marker assisted backcrossing

In order to control for the genetic background of our various mouse strains and to yield reconstitutable mice quicker, we established a "speed congenics" strategy. This technique allows the production of congenic strains on clearly defined genomic intervals in less than half the number of generations required by the classic protocol and enabled us to create a baseline profile for our various mouse strains [121]. Additionally, we could select for mice with the highest number of favorable markers of the target strain and utilize them for further breedings. The results reported here are based on the assays we established from markers available in the public domain through the mouse genome informatics consortium (http://www.informatics.jax.org), all map distances are derived from NCBI build 37.1. In order to achieve medium- to high throughput typing of our mice, we developed a multiplex PCR strategy that allowed us to genotype one mouse per 96 well plate and to assess it for 192 polymorphic microsatellite markers on a 16-capillary sequencer from Applied Biosystems. In such a way, we could analyse 6 mice in 24 hours (or 14 mice per day when using another capillary sequencer localized at another site of the university). In order to save on reagents, our setup would be easily robotizable and could then even be performed on 384 well plates since much smaller volumes could be pipetted with high accuracy. A typical readout of the capillary electrophoresis unit is depicted in 3.4

As a baseline, we typed our original mixed *Rag*$1^{-/-}$*Prnp*$^{-/-}$, the "BALB/c" *Rag*$2^{-/-}$ *Il2rg*$^{-/-}$, the laboratory reference strains C57Bl/6 and BALB/c (Harlan), and the Tg*PRNP*129M mice.

Even if a mouse is stated to be "pure" BALB/c, there was always a certain degree of variation within our markers, especially the *Rag*$2^{-/-}$*Il2rg*$^{-/-}$ mice proposed to be "BALB/c" showed a considerable degree of variation in different individuals. Our experimentally determined allele lengths for the our tested strains are listed in table 3.1 where we classified the alleles according to the main strains and some substrains (not all, the list is therefore a little simplified). It was important to identify C57Bl/6 and BALB/c specific markers in the first line, but we noticed a large amount of polymorphisms in mice carrying a "novel allele" which is in most cases attributed to the Tg*PRNP*129M-mice, but in some respect also to 129Sv-mice which showed a significant overlap there.

Table 3.1.: Experimentally determined allele lenghts

Chromosome	Marker	Pos cM	129Sv	B6	B6a	B6b	BalbC	BalbCa	BalbCb	nodiff	novel
1	D1Mit430	7	110					114	106		
	D1Mit169	12					122				
	D1Mit411	16		97						105	
	D1Mit132	44		144			161				

continued on next page

Table 3.1 – continued from previous page

Chromosome	Marker	Pos cM	129Sv	B6	B6a	B6b	BalbC	BalbCa	BalbCb	nodiff	novel
	D1Mit215	47	136	142				150			144
	D1Mit54	59					139				
	D1Mit60	59		141			139	143			
	D1Mit308	65		143			151				
	D1Mit495	70		115			110				
	D1Mit159	82	172	152	165			118	130		176
	D1Mit206	94		125			117				
	D1Mit17	110		162	196		166				145
	D1Mit292	112		197			195				193
2	D2Mit1	2	121							117	131
	D2Mit365	22		97			103	142			69
	D2Mit61	36		125	136		141				
	D2Mit327	40		125				128			
	D2Mit100	50					105				
	D2Mit395	56		125			134				
	D2Mit404	67					189				
	D2Mit285	72		139	131		146				156
	D2Mit411	78		98			91				101
	D2Mit113	87		143			142				123
	D2Mit148	92	106	108			123				
3	D3Mit203	10	141							150	
	D3Mit51	26	115		107						
	D3Mit311	34	112	119			109			201	
	D3Mit57	40	155	152			150				171
	D3Mit256	46	149				122				
	D3Mit320	50		114			106				112
	D3Mit200	56								117	128
	D3Mit147	59	126	131			139				118
	D3Mit352	63		144			151	128			123
4	D4Mit196	16		187			195				
	D4Mit268	22					124				
	D4Mit17	30	139		130						
	D4Mit348	34	171	173			191				
	D4Mit308	55		60			107				79
	D4Mit203	60		104			114				116
	D4Mit251	67					120			106	
	D4Mit170	70		96			114				107
	D4Mit256	82		136					134		
5	D5Mit146	0	118								
	D5Mit352	15	109	108			116				122
	D5Mit201	28		107			104				87
	D5Mit309	31	109					114			99
	D5Mit10	37	191	187			179				185
	D5MIt158	48						296			329
	D5Mit425	55		122			115				
	D5Mit95	58			103	116	130				
	D5Mit98	67		153			160	178			
6	D6Mit86	0		130				117	142		
	D6Mit138	2		114	93		135	131	108		127
	D6Mit116	6		116			107				91
	D6Mit123	18		107				119	111		
	D6Mit209	22	131	142	128			124			
	D6Mit100	30		82			80				95
	D6Mit284	31		122	128			118	131		135
	D6Mit36	40		191			171				164
	D6Mit14	63		157			153				172
	D6Mit374	67	155							138	146
7	D7Mit21	0		134							
	D7Mit294	6		97					113		
	D7Mit228	16		145			139				
	D7Mit83	25	151		149	103		144	85		
	D7Mit248	26		121	102		99			105	
	D7Mit350	31		118			140				124
	D7Mit323	37		137			104	114			
	D7Mit101	46		111			88				107
	D7Mit109	62		114							
	D7Mit223	68		99	79			75	94		
	D7Mit259	68	146	149	127		110				128
8	D8Mit155	0		120			118		132		
	D8Mit63	3		107	116	207		110	226		
	D8MIT124	4		116	126		132				118
	D8Mit289	9		147			152				
	D8Mit292	20	109	97				104			
	D8Mit339	25		114			97				
	D8Mit46	30		225			197				
	D8Mit178	35	158	152			162				142
	D8Mit45	40									124
	D8Mit211	50	130	121		149		127	159		
	D8Mit112	56		121				119	126		109
	D8Mit47	56		194			192				
	D8Mit49	69	110	151	105		126				153

continued on next page

Table 3.1 – continued from previous page

Chromosome	Marker	Pos cM	129Sv	B6	B6a	B6b	BalbC	BalbCa	BalbCb	nodiff	novel
9	D9Mit250	2	144	107				124			
	D9Mit90	8	135	137			133				139
	D9Mit2	13		168			171				
	D9Mit285	16		125			119				113
	D9Mit129	21		143		117		125	147		
	D9Mit97	24		145			154				128
	D9Mit336	34	113	102	114		99				85
	D9Mit355	49		100			124				
	D9Mit201	63		101			97				80
	D9Mit151	70		103	114		110				95
10	D10Mit213	7		129	149		134				122
	D10Mit86	12		133				149	127		155
	D10Mit38	21		165			149				
	D10Mit20	25		226			221				215
	D10Mit31	31									
	D10Mit207	40								141	
	D10Mit230	47		110				106	137		
	D10Mit95	50		196			176				156
	D10Mit233	63		125			109				
	D10Mit14	70		188			185				
	D10Mit103	77	135	145	116			118	151		
11	D11Mit71	0		209			220	226			
	D11Mit2	4		100			92				102
	D11Mit186	14		128			134				
	D11Mit189	21		134	119		137				
	D11Mit86	25	126	100				118	150		
	D11Mit143	30	107							90	88
	D11Mit4	36		251			244				
	D11Mit326	45	90							87	
	D11Mit285	49	129	116			120				
	D11Mit333	70		123			106				87
12	D12Mit182	2	146	129			143				122
	D12Mit11	6	115	107	111		110				
	D12Mit59	10	143	144			146	122			128
	D12Mit285	20			122		139	129			
	D12Mit91	23			127		146				123
	D12MIt143	30		142			145				148
	D12Mit158	33		139	152		150				135
	D12Mit7	45		104			120	150			97
13	D13Mit56	2	228								198
	D13Mit275	8	117	94			115				
	D13Mit88	13		142				175	122		
	D13Mit19	14	137	127			151				
	D13Mit213	40	155	145			159				
	D13Mit151	50		117			311				111
	D13Mit78	59		221			202				
14	D14Mit48	0	122	113			108				
	D14Mit40	1		136					134		132
	D14Mit126	7	131	127					135		
	D14Mit127	16	139	129			149				
	D14Mit44	16		142					141		
	D14Mit174	18			121				145		
	D14Mit60	24	140	133			112				
	D14Mit5	32		167					157		
	D14Mit263	53		121			114				
	D14Mit170	70		142				148			
15	D15Mit80	4					160				
	D15Mit252	10	128	119			112				
	D15Mit67	30		186							189
	D15Mit70	35		146	149		133				
	D15Mit107	42	162	148			142				127
	D15Mit262	46		116			108				115
	D15Mit159	49	144	138	128		116				142
	D15Mit242	54	99	97			82				98
16	D16Mit131	7		143			181				175
	D16Mit101	18	141					142	155		
	D16Mit60	24	199	202							
	D16Mit189	40		203			196				199
	D16Mit153	46		265			267				269
	D16Mit52	51		191						109	
	D16Mit86	51		125			119				112
17	D17Mit245	3		180			172				
	D17Mit180	29					141				121
	D17Mit39	45		102			85				
	D17Mit143	5		124	105		130				
	D17Mit81	17		123				107	121		134
	D17Mit51	23	159	131	153		150				138
	D17Mit20	41		174			162				
	D17Mit1	57	190	194			188				168
18	D18Mit64	0		150			168				
	D18Mit222	4		88	148	189	98	130			

continued on next page

Table 3.1 – continued from previous page

Chromosome	Marker	Pos cM	129Sv	B6	B6a	B6b	BalbC	BalbCa	BalbCb	nodiff	novel
	D18Mit12	10		171			165			118	
	D18Mit177	14		168			195				160
	D18Mit194	14		115			122				
	D18Mit208	24		120			118				
	D18Mit186	31	126	125				90	108		
	D18Mit48	35	167					188			
19	D19Mit68	3		135	119		120				114
	D19Mit28	10		145			130	153			124
	D19Mit88	24		148			138	142			128
	D19Mit90	28		119			122				128
	D19Mit26	38		129			131				
	D19Mit103	40	130	121			128				
	D19Mit33	46	222	223			255				
	D19Mit347	56	108	119			110				99
	D19Mit6	58									109
X	DXMit64	31		214						209	
	DXMit172	48.7		149			130				
	DXMit132	60						116			
	DXMit216	63		119	112		126	116			122
	DXMit121	67								142	
	DXMit223	74		101			105				87

To visualize better the outcome of a standard STR-typing experiment, we established a color coding system for the most common strains in correlation to their genetic position on the chromosome. This makes it easier to see distinct differences at a glance and simplifies the breeding process by selecting those mice with the highest content of favorable alleles. The STR-profiles of our baseline mice, i.e. a pure BALB/c mouse, a C57Bl/6-Hsd mouse, a "BALB/c" *Rag*2$^{-/-}$*Il2rg*$^{-/-}$ mice that is primarily reconstitutable with hematopoietic stem cells from human umbilical cord blood and a mouse that is expressing human PrP (Tg*PRNP*129M) as a transgene are depicted in Fig.3.5.
Backcrossing to a reconstitutable target strain was achieved in all presented breeding strategies depicted in Figures 3.1 and 3.2. We regained reconstitutability in those mice as soon as about 90% of the markers corresponded to those of the original mice (Section 3.4.2). In retrospective, the quickest strategy was the intercross between between BALB/c *Prnp*$^{-/-}$ mice and the original, reconstitutable mice since most of the markers already overlapped in this paradigm, and even though a spatial proximity between *Rag* and *Prnp* genes was initially thought to be prohibitive to this approach. We decided to stop backcrossing of *Rag*1$^{-/-}$*Prnp*$^{-/-}$*Il2rg*$^{-/-}$ that had a high degree of disambigous STR-markers after detecting recombination events between *Prnp* and *Rag*2 since it might have become very cumbersome to adjust for the right genetic constellation. Reliable reconstitutability was also achieved in mice carrying a human transgene on an immunodeficient background since most of the strain-specific markers of the initial Tg*PRNP*129M were outcrossed with this marker-assisted approach (Fig. 3.6). However, all these observations hold only in the presence of at least one allele of mouse *Prnp* - reconstitutability was not achieved in mice that were deficient for *Prnp*, even though the genetic background monitoring was tight and differences between littermates were minute (please refer to section 3.4.3 for a more detailed description of these experiments). The marker-assisted background evaluation was also applied in other projects in our lab to control for possible genetic background implications in experimental outcome. Briefly, we checked D6$^{-/-}$ mice from Stefan Prokop and Petra Schwarz's tg*a*20 mice for identity to the C57Bl/6 strain.

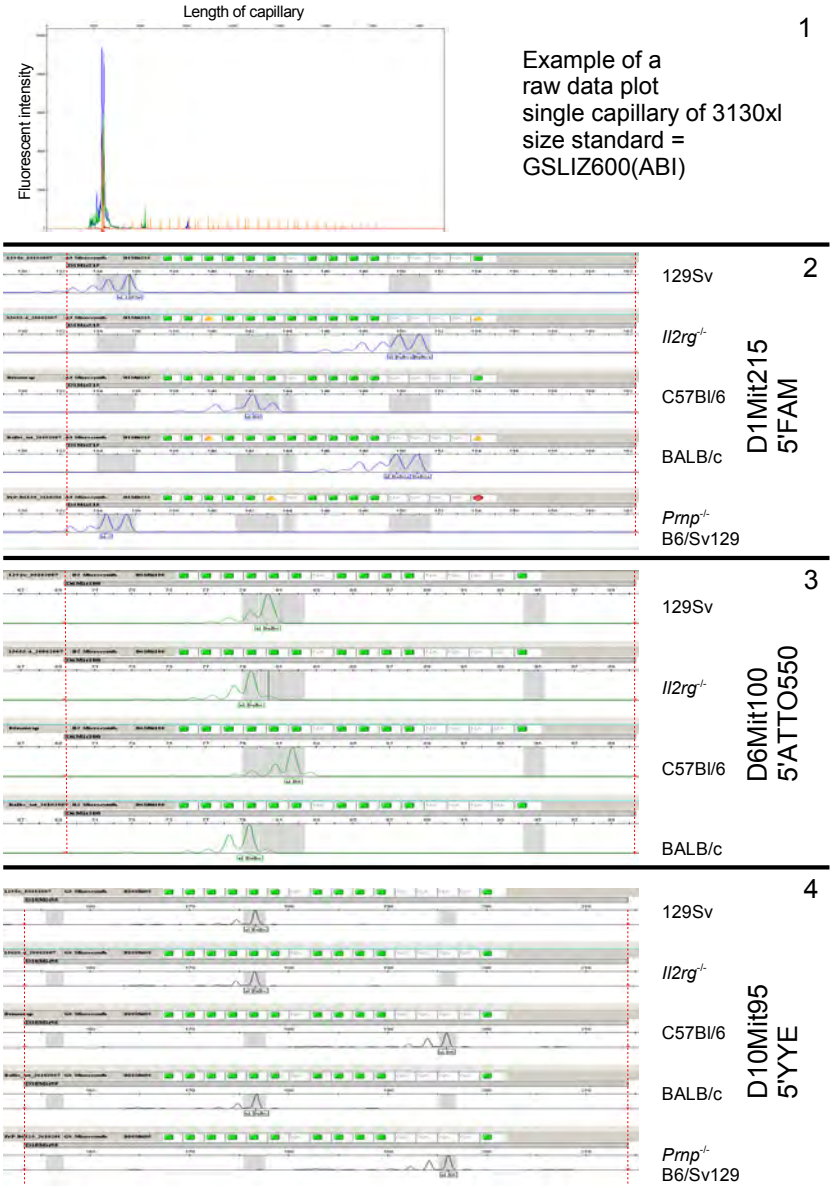

Figure 3.4.: Readout of an STR mapping experiment.
(1) Electrophoresis plot (fluorescent intensity versus size, raw-data readout) of a single capillary within our 3130xl capillary sequencer (ABI) showing the size-standard peaks (orange), and the respective PCR amplicons characteristic for a multiplexed reaction (blue for FAM and green for ATTO550) as well as prominent primer dimers that permanently exist at the small-size end of the plot.
(2-4) representative examples of three differentially labeled STR markers after analysis with gene mapper software. The outcome of FAM-labeled D1Mit215, ATTO550-labeled D6Mit100 and YYE-labeled D10Mit95 in correlation to the respective mouse strain is shown. Dotted red lines indicate the marker size range. Gray boxes indicate the bins that allow to call for identical alleles in further analysis and assign specific names to them.

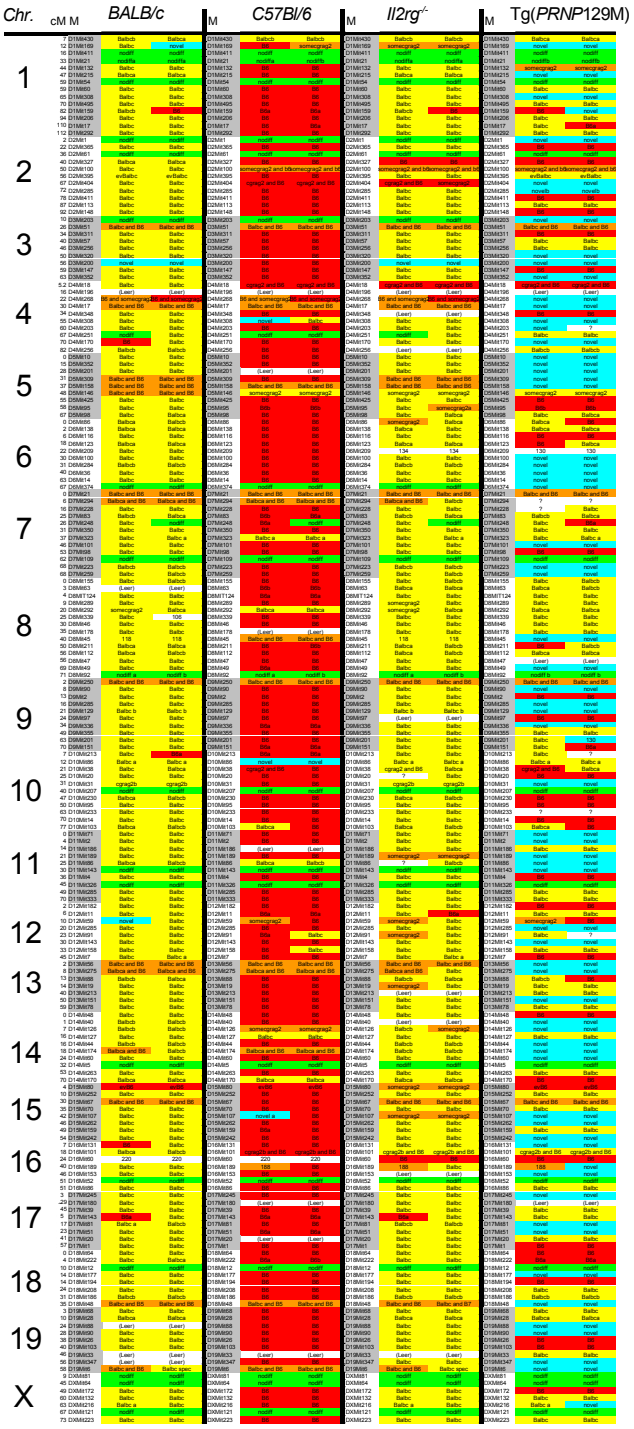

Figure 3.5.: Calibration strains for STR typing.
Depicted are 192 markers per mouse allocated according to their physical location on the 19 autosomes and the X chromosome of the mouse genome. The color code is as follows: yellow for BALB/c and *Il2rg* alleles; red for C57Bl/6 alleles; orange for alleles attributed to either *Il2rg* or C57Bl/B6, but not in any case to BALB/c; green for alleles which are not informative in discriminating those strains but might be polymorphic in other strain types; blue for alleles that are specific for Tg*PRNP*129M-mice and/or 129Sv. In some rare cases, there are empty fields indicating that the PCR reaction in this particular case did not work.

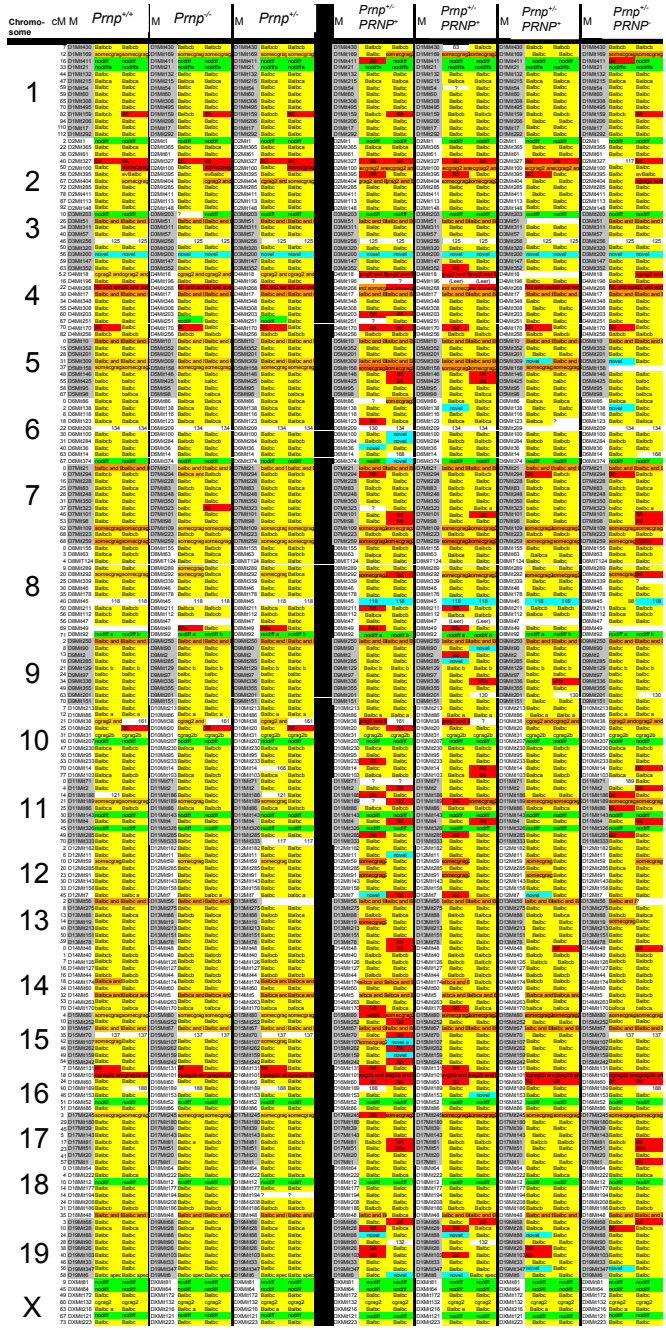

Figure 3.6.: Backcrossed strains.
The first column shows littermates out of a breeding between multiply marker-evaluated backcrossed $Rag2^{-/-}Il2rg^{-/-}Prnp^{+/-}$ parents. A large proportion of the markers correspond to the initial $Rag2^{-/-}Il2rg^{-/-}$ indicated in yellow and depicted in Figure 3.5. No remarkable difference between *Prnp* genotypes can be detected in this medium-resolution setup.
The second column shows a gradual outcrossing of unfavorable markers in mice carrying the human *PRNP* transgene on an immunodeficient background: the left mouse still possesses a fair quantity of blue and red alleles whilst they are gradually eliminated in further breeding generations. For comparison to the original Tg*PRNP*129M constellation, refer to Figure 3.5

3.2. Enrichment of human umbilical cord blood CD34+ hematopoietic stem cells

Despite logistical and other obstacles[1], we succeeded in collecting more than 100 samples from various donors and succeeded in enriching a copious amount of CD34+ stem cells. Usually, cells were directly frozen and stored in liquid nitrogen after enrichment and only thawed when newborn mice were available. The amount of CD34+ cells per sample varied widely depending on the initial cord blood volume: the best result we obtained was 6 million stem cells from a twin pregnancy, but in most cases the numbers ranged between 0.5 to 1.5 million (Figure 3.7).

3.2.1. Sequence analysis for human PRNP polymorphisms in the donor cord blood

The *PRNP*-ORF of all non target fractions was sequenced. We could observe a distribution of 15% MV, 83%MM and 2%VV constellation at codon 129 of the reading frame. However, a correlation between cord blood *PRNP* constellation and behaviour or susceptibility proneness of a CJD-PrP inoculum is yet to established in the humanized mouse model.

[1] Collecting human umbilical cord blood turned out to be one of the most challenging parts of this work, since many groups in the University Hospital Zurich seemed to be interested in physiology/pathology/embryology of the placenta and associated structures. Fortunately we had a very good support from people in the obstetrics department who were willing to provide me with samples during the weekend or on their nightshifts, so we could escape the routine of most other research groups with the drawback of investing a lot of flexibility and patience. Additionally we had great support from other hospitals (mainly St. Gallen) who provided us with samples. The management of the informed consent procedure was greatly facilitated after mid 2006 when a general form for "research purposes" was implemented at the obstetrics department. Before, it was sometimes impossible to fetch the patient at the right time and location to explain a procedure which imposes no risk at all to mother and child. In the course of this work, we also tried a 50/50 strategy to provide the newborn child with half of the enriched sample and store it at our N2 tank if needed whereas the other half could be used for research purposes: installation of a GMP unit, however, would be very cost- and labor intensive and we therefore offered this strategy only to a few patients with the clear caveat that our selected cells would not meet international cord blood banking standards. Research in this field could be generally made much more easier, if big maternity clinics had standard cord blood banking units reserving half of the blood for research and the other half for patient care.

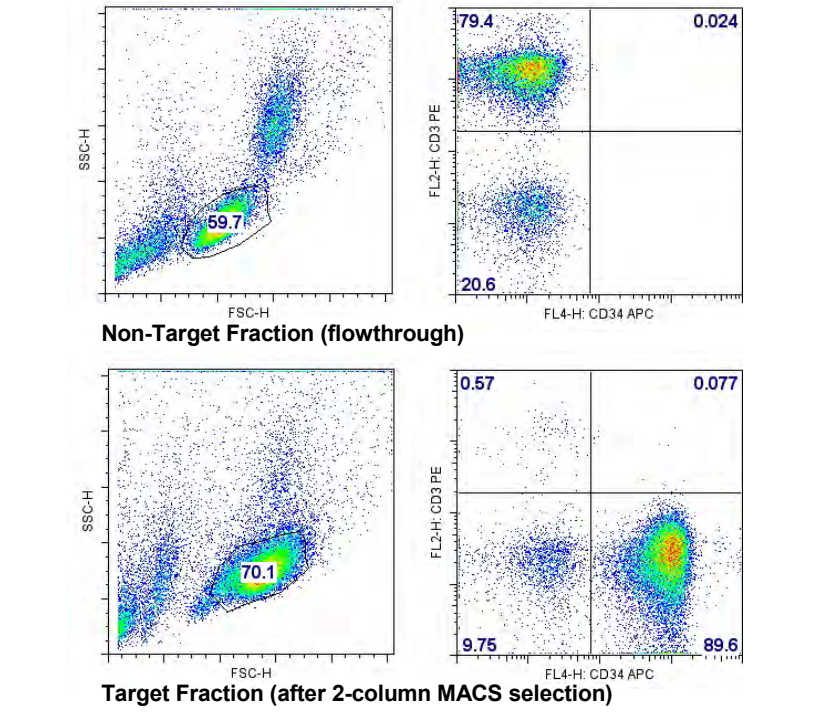

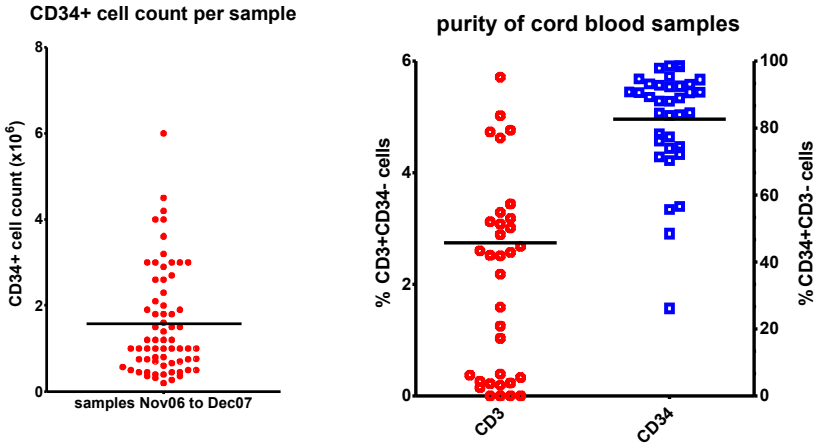

Figure 3.7.: Flowcytometric analysis of enriched CD34+ stem cells (TF) and the respective non target fractions (NTF).
Illustration of our standard cord blood screening flowcytometric analysis after MACS-sorting. We assessed the TF and NTF for the absence/presence and amount of CD34(+) (APC-label, X-axis) and CD3(+)(PE-label, Y-axis) cells. The lower panel shows the distribution of the CD34(+) cell count as well as the purity of the samples indicated by CD34(+) and CD3(+) content. Depicted are samples collected in 2006 and 2007 from various donors (n=100).

3.3. Reconstition of immunodeficient Prnp$^{-/-}$ mice with allogeneic mouse bone marrow

It is known that immunodeficient *Prnp*$^{-/-}$ mice can be engrafted with syngeneic bone marrow from a syngeneic or allogeneic donor. However, reconstitution efforts in *Rag2*$^{-/-}$*Il2rg*$^{-/-}$*Prnp*$^{-/-}$ have never been performed, and to rule out a possible implication of *Prnp* in allografting, we transplanted bone marrow from adult BALB/c mice intrahepatically into newborn and sublethally irradiated *Prnp*$^{-/-}$, *Prnp*$^{+/-}$ and *Prnp*$^{+/+}$ littermates (newborns were genotyped just after birth). Peripheral blood was assessed 6 weeks after transplantation for the presence of mouse B-cell markers. All the littermates showed a positive, stable and equally strong engraftment for a lifelong duration, indicating that the absence of *Prnp* in *Rag2*$^{-/-}$*Il2rg*$^{-/-}$ does not influence the homing of allogeneic cells in a immune-depleted host. Confirmation of the genotypes was complemented by western blot analysis of perfused brains because PrP-expression from the grafted cells migth influence the *Prnp*-genotyping results.

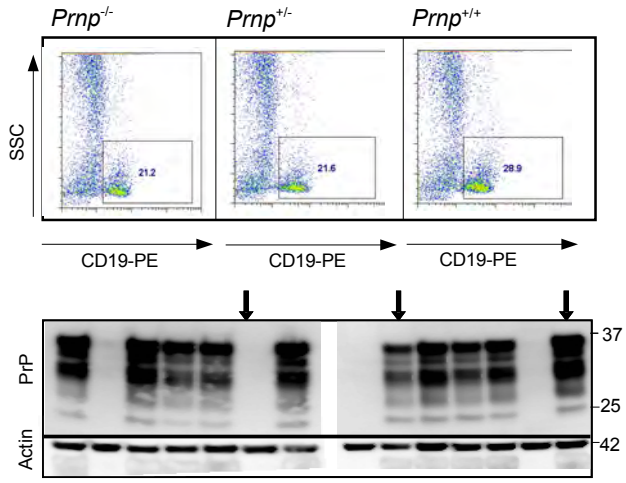

Figure 3.8.: Reconstitution of immunodeficient mice with mouse bone marrow. Reconstitution of newborn *Rag2*$^{-/-}$*Il2rg*$^{-/-}$*Prnp*$^{-/-}$, *Prnp*$^{+/-}$, *Prnp*$^{+/+}$ mice with bone marrow of a wildtype adult BALB/c mouse is equally effective as indicated by re-expression of the B-cell marker CD19 6 weeks after reconstitution. To rule out misleading genotyping results by contamination of donor-related *Prnp*-expression in tail biopsies we performed immunoblot analysis of perfused brains confirming the *Prnp* genotype of the grafted mice.

3.4. Reconstitution experiments with enriched CD34+ hematopoietic stem cells from human umbilical cord blood

3.4.1. Reconstitution of Rag2$^{-/-}$Il2rg$^{-/-}$ mice (BALB/c), prion experiments

Applying the protocol of Traggiai et al.[119], we and others were readily able to reproduce the engraftment of BALB/c *Rag*2$^{-/-}$*Il2rg*$^{-/-}$ mice with sorted stem cells from human umbilical cord blood. Assessment of peripheral blood about 6 weeks after transplantation for human CD45 showed in 50 to 80% of the cases a lymphoid population of human cells which persisted for a period of about 4-6 months and differentiated mainly into the B-cell lineage and to a much lesser proportion into T-cells. Analysis of spleen, lymph nodes and thymus as well as Peyer's patches reproduced the findings of Traggiai et al., yet, a follicular structure of the spleen as depicted in their paper was never observed to this extent. Nonetheless, the same experiment, when performed by Baenziger and Heikenwaelder (personal communication) did not work in a C57Bl/10 strain background. Thus, genetic factors seem to influence the microenvironment for the engraftment of stem cells although both strains were equally devoid of B-cells, T-cells and NK-cells.

Engraftment success in these mice was directly related to the amount and quality of the cord blood cells injected. The best values with nearly 100% human cells in the lymphoid gate were obtained when more than 200'000 fresh cells per mouse were injected; freezing of the cells did not significantly alter the quality but resulted in a loss of viable cells, so that fewer mice could be injected.

I will not report here on the results of ongoing prion inoculation experiments in humanized BALB/c *Rag*2$^{-/-}$*Il2rg*$^{-/-}$-*Prnp*$^{+/+}$ mice, but in the last 2 years, many very well engrafted mice have been grouped and inoculated intraperitoneally with prions from sCJD patients, CWD brains and BSE-brains to see whether the human cells in these mice could replicate those species. These experiments are ongoing and will be dealt with in more detail in the Discussion section of my thesis.

3.4.2. Reconstitution of backcrossed Rag1$^{-/-}$ Prnp$^{-/-}$ Il2rg$^{-/-}$ and Rag2$^{-/-}$ Prnp$^{-/-}$ Il2rg$^{-/-}$ mice

The first reconstitution trials in largely mixed *Rag*1$^{-/-}$ *Prnp*$^{-/-}$ *Il2rg*$^{-/-}$ and *Rag*2$^{-/-}$ *Prnp*$^{-/-}$ *Il2rg*$^{-/-}$ mice were not succesful although reconstitution with the same donor cord blood could be realised in control immunodeficient BALB/c mice. We never detected human cell engraftment in mixed *Rag*1$^{-/-}$ *Prnp*$^{-/-}$ Il2rg$^{-/-}$ mice and since we had mice with a much more favorable STR-marker profile, we decided to lay emphasis on the *Rag*2$^{-/-}$ line.

As soon as a threshold of about 90% in marker-overlap was achieved, we regained reconstitutability in our backcrossed mice. Our goal was to have reconstitutable *Prnp*$^{-/-}$ mice and therefore one marker-assisted backcrossing cycle (thereby loosing one *Prnp*-allele) had to follow intercrossings between *Prnp*$^{+/-}$ mice with a good STR marker profile. In breedings between *Prnp*$^{+/-}$ parents, only 25% of the offsprings were *Prnp*$^{-/-}$, but another experimental approach was not possible.

Interestingly enough, although nearly optimal in terms of the STR profile, reconstitutability seemed to depend on the *Prnp* genotype. We observed this phenomenon in all our breeding strategies, i.e. in the "classical" as well in the "alternative" scheme as depicted in Figures 3.1 and 3.2. In littermates with an equivalent genetic background, we found only positive engraftment in the presence of at least one *Prnp* allele whereas its absence seemed to abolish reconstitutability (Fig. 3.9).
The distribution and differentiation of the engrafted cells as well as the kinetics of the process seemed to be identical to those of the mice published by Traggiai [119] as depicted in Figures 3.10 and 3.11 although the recovery of a near-intact follicular splenic architecture compared to non-reconstituted mice was not demonstrated. The survival of the graft and the relative number of grafted cells related to host cells seemed to depend on the dosage of *Prnp* with $Prnp^{+/-}$ animals displaying a shorter graft survival than $Prnp^{+/+}$ animals. Most of the engrafted cells homed to the bone marrow where they resided for a long time whereas detection in peripheral blood peaked around 8-12 weeks after transplantation.

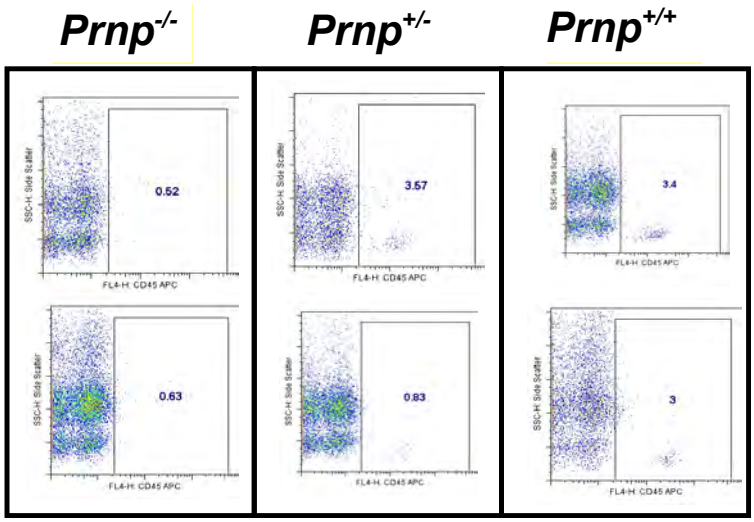

Figure 3.9.: *Prnp*-dependent reconstitutability.
Littermates of a breeding between high-BALB/c or pure BALB/c $Prnp^{+/-}$ parents showed a *Prnp* dependent engraftment behaviour. Human-CD45 positive cells 4 weeks after transplantation are only detectable in mice carrying at least one allele of mo*Prnp*. The effect seems to be gene-dosage dependent since $Prnp^{+/+}$ showed a tendency towards higher engraftment compared to heterozygous littermates.

3.4.3. Reconstitution of backcrossed Rag2$^{-/-}$ Prnp$^{-/-}$ Il2rg$^{-/-}$-TgPRNP129M mice - a transgenic rescue?

Since we also intended to model neuroinvasion more accurately in our model, we backcrossed our reconstitutable mice with mice expressing the human *PRNP* as a transgene as depicted in Fig.3.2b. In parallel, this strategy could also be exploited to evaluate a possible transgenic rescue effect of the observation that *Prnp* itself seemed to influence engraftment capacity of xenogeneic cells in a host mouse. Reconstitutability in immunodeficient Tg*PRNP*129M mice carrying at least one copy of mouse *Prnp* could be established as far as 90% of the STR marker profile overlapped, yet we failed to detect engrafted cells in mice devoid of murine *Prnp* that reexpressed human *PRNP* as a transgene. Moreover, we observed a correlation of mouse *Prnp* expression levels and the number of engrafted cells, i.e. *Prnp* heterozygous mice showed less engraftment than *Prnp* homozygous mice. Analysis of bone marrow and spleen of reconstituted, backcrossed *PRNP*+*Prnp*+ mice showed an equivalent differentiation status of the engrafted cells compared to the other mouse strains evaluated. The profile of engrafted cells in bone marrow and peripheral blood and its histological and immunohistchemical appearance is depicted in Figures 3.10 and 3.11. Of particular interest was the fact that the engrafted cells express PrP and would therefore theoretically be able to replicate prions as shown in Figure 3.10.

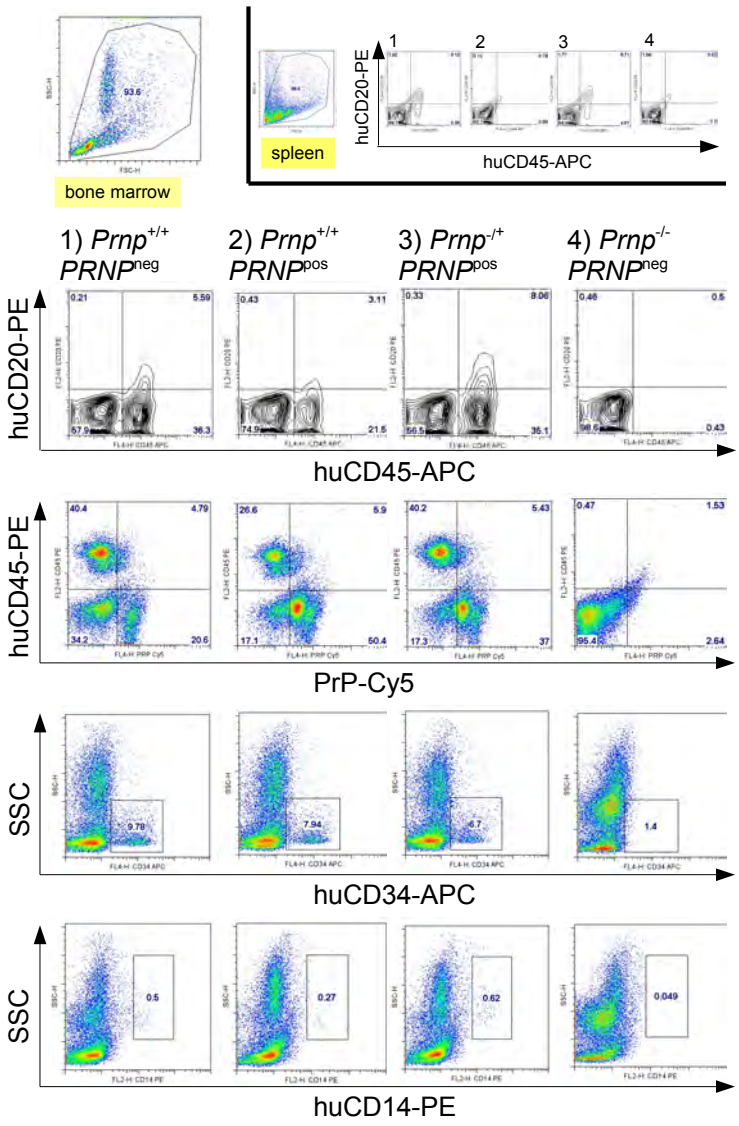

Figure 3.10.: Flowcytometric analysis of engrafted cells in bone marrow 12 weeks after transplantation.
Subtype analysis of engrafted human cells in *PRNP-Prnp+*, *PRNP+Prnp+* and *PRNP-Prnp-* mice. Only live cells are gated. *1* Expression level of human CD45-APC versus human CD20-PE is plotted. *2* PrP-expression of cells positive for human CD45-PE is assessed with a Cy5-labeled antibody against the prion protein (POM2). This antibody binds to mouse and human PrP indicated by a POM2+fraction in the CD45-PE- quadrant in case of presence of mouse andor human PrP. *3* The third panel shows expression of the human stem cell marker CD34, indicating a significant fraction of human self-renewing cells within the bone marrow. *4* Evidence of a myeloid differentiation of a small subset of engrafted cells is indicated with staining against human CD14.

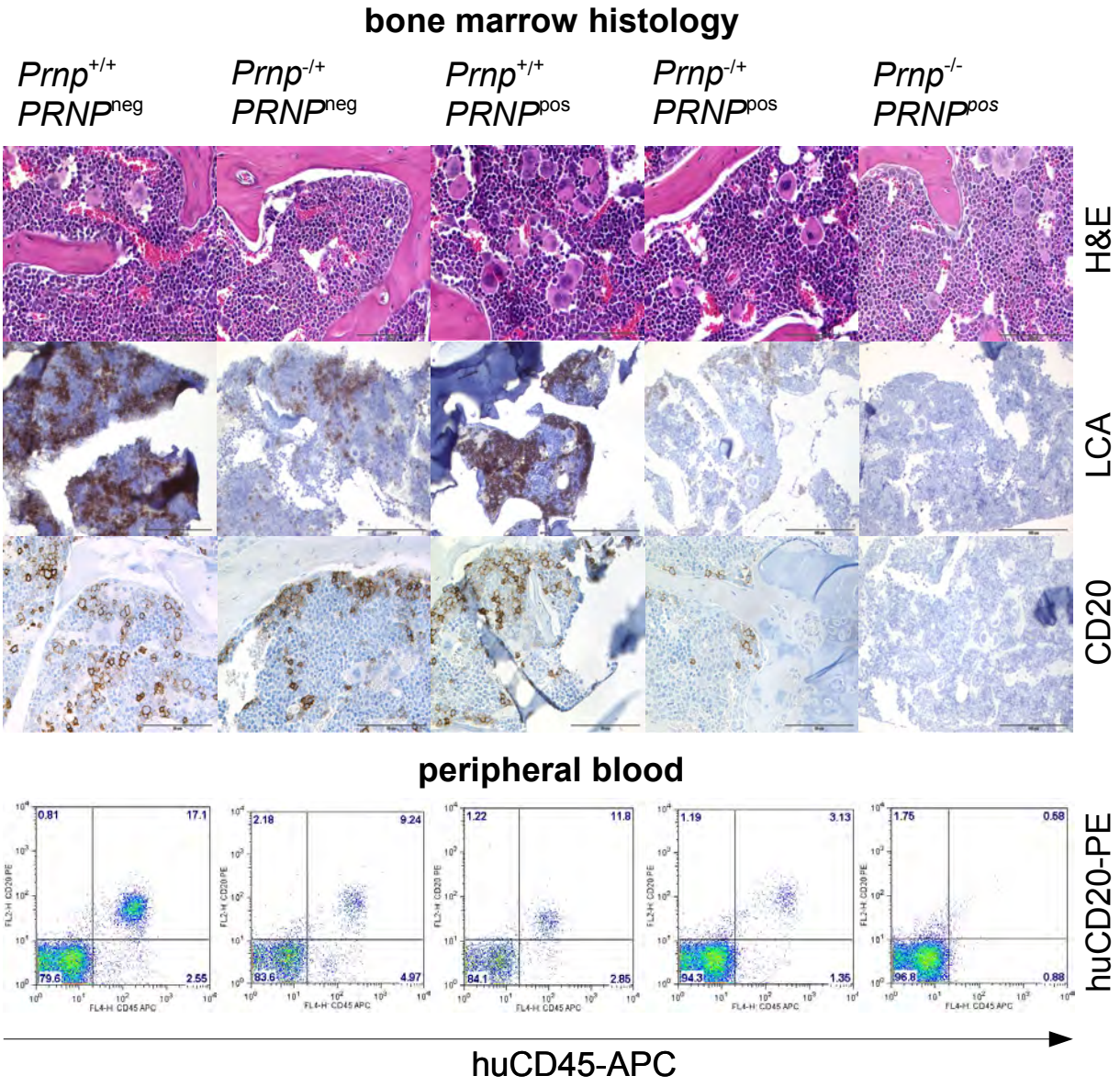

Figure 3.11.: Histology of engrafted mice and flowcytomtric readout in peripheral blood.
Histological sections of the marrow compartment of spinal vertebrae. H&E stains show no overt differences in morphology between the various strains whereas the immunohistochemical stainings with antibodies specific for human CD45 and human CD20 show the presence of human cells indicated by a cytoplasmic immunoperoxidase staining reaction in mice carrying at least one allele of mouse PrP. Expression of a human transgene shows no influence on engraftment behaviour in the absence of *Prnp*. No engraftment is detectable in the absence of *Prnp*. Scale bar 50μm.
Detection of engrafted human cells in peripheral blood 6 weeks after intrahepatic transplantation with antibodies specific for human CD45 and human CD20.

3.5. Reconstitution with cultivated and expanded human umbilical cord blood cells

Based on a collaboration with Dr. R. Peters from the oncology research department, we initiated as a side project an attempt to economize on CD34+ stem cells using *in vitro* expansion of these cells. The motivation behind this was the fact that only a small number of mice could be produced with one batch of identical cord blood. Because of advancements in *in vitro* expansion techniques, however, a significantly increased number of mice would be injected with genetically identical stem cells, which would be advantageous for genetic susceptibility studies. Cord blood leukocytes from frozen samples were cultivated and expanded in cell culture bags or wells and injected into primarily reconstitutable, sublethally irradiated newborn acceptor mice. In parallel, enriched CD34+ samples from the same donor were applied in another set of mice. We achieved an in vitro expansion of up to 20 fold after 3 weeks, yet when we injected these cells intrahepatically, engraftment behaviour was significantly worse compared to the primarily enriched fraction. Expansion with cytokines and subsequent CD34-selection resulted in better engraftment properties, but the expansion technique is cost- and labour intensive and a reasonable cost-benefit-ratio was not obtained.

3.6. Expression analysis of murine PrP in spleen and bone marrow subpopulations

To evaluate whether expression of PrP is a prerequisite for homing of human stem cells into the bone marrow we reevaluated PrP expression in subsets of bone marrow cells using high affinity antibodies specific to PrP to identify possible cellular mediators for this effect. This analysis was performed in six different genotypes of age- and sex-matched 3 month old mice: immunocompetent Tg*PRNP*129M-mice (1), immunodeficient $Prnp^{+/-}$(2), $Prnp^{+/+}$(3), Tg*PRNP*129M(4) and $Prnp^{-/-}$(5) mice as well as a wildtype control (6). Cells were co-labeled with respective subset markers and the amount of double positive cells in the lymphoid, the large lymphoid, the erythroid and the myeloid gate according to the FSC/SSC clustering was assessed. Interestingly, Tg*PRNP*129M mice did not show expression of the transgene in the erythroid population whereas we could detect a strong PrP-expression in this region in all the immunodeficient and wild type mice (Figure 3.12), additionally confirmed by colabeling with the erythroid specific marker ter119. A strong positivity for PrP was further detected in macrophages (CD11b), granulocytes (ly6g), CD14-positive cells and B-cell precursors (Early-B and CD43 positive cells) in the absence of functional B-cells. In the wildtype mouse, we identified B220+PrP+ and CD19+PrP+ as well as CD3+PrP+ cells confirming previous results. A weaker PrP staining was observed in CD34+ cells; no PrP expression was detectable in dendritic cells (CD11c+), regulatory T-cells (CD25+) and Nk cells. A stromal PrP expression in bone marrow could not be detected (data not shown). To pinpoint strong positivity of PrP expression in bone marrow, we additionally performed immunoblotting and qRT-PCR from the same mice and could find consistent evidence for a strong expression of PrP in total mouse bone marrow isolates (Figure 3.12).

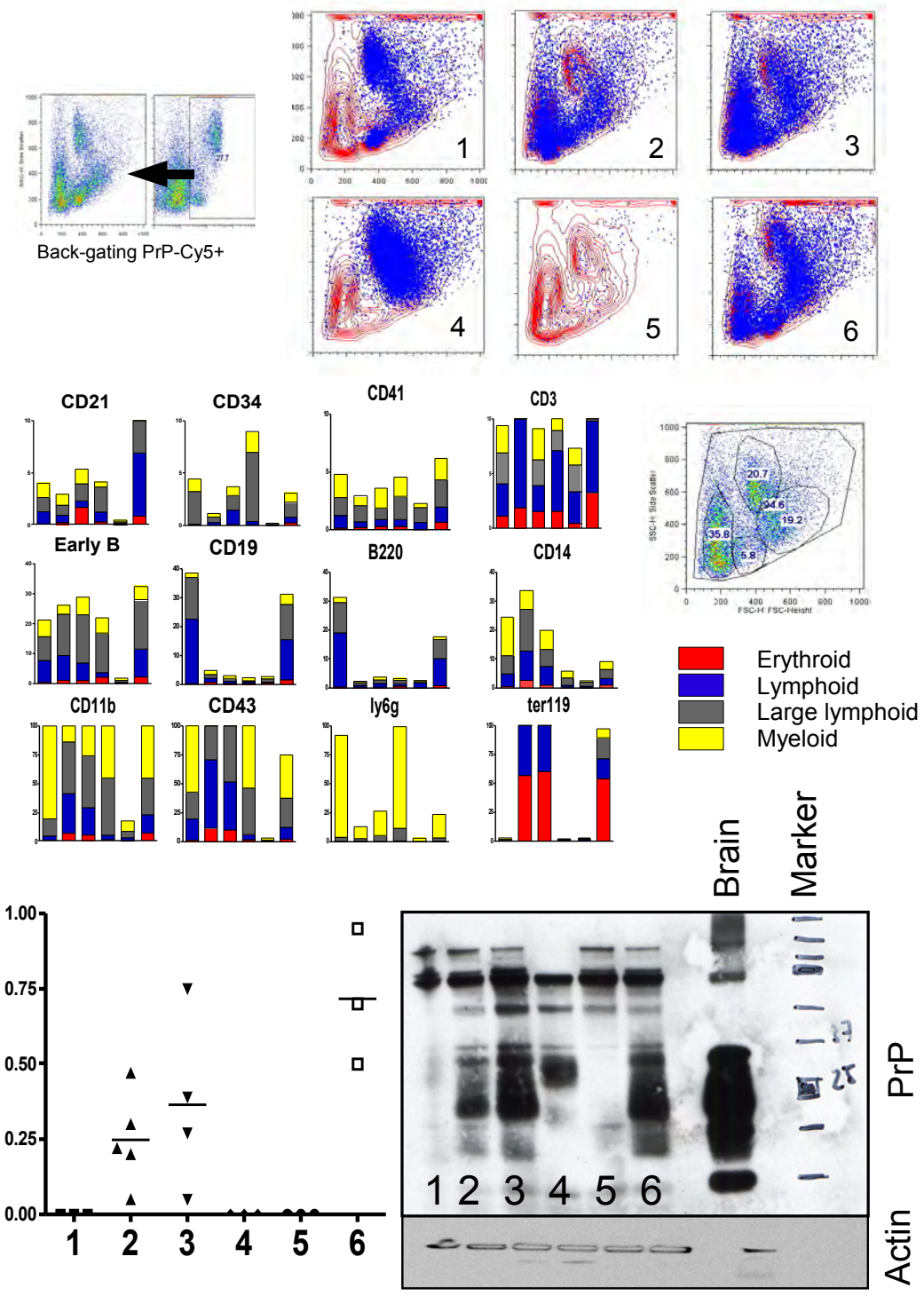

Figure 3.12.: Detailed PrP expression analysis in bone marrow subpopulations by flowcytometry.
Confirmation of PrP expression by qPCR and proof of presence of the protein by western blot. For further explanation to the figure refer to section 3.6

3.7. SNP and STR mapping of the genetic region between Prnp and Rag

Since PrP itself or a genetic determinant around it seemed to modulate the engraftment behaviour of human hematopoietic stem cells in immunodeficient mice, we decided to search for additional genetic markers in the region between *Prnp* and *Rag* (a region spanning over 30 megabases including around 450 known or unknown genes) to map and delimit the recombination breakpoints more accurately. First, we choose additional STR markers near *Prnp* and near *Rag* from the UniSTS database, second, we selected single nucleotide polymorphic markers in a 5 Mb interval deciphering this region. Out of the STR analysis, the markers D2Mit447(128.6 Mb) and D2Mit256(126.4 Mb) were always linked to the *Prnp* knockout allele even in multiply backcrossed *Rag*2$^{-/-}$ *Prnp*$^{-/-}$ *Il2rg*$^{-/-}$ mice to a background very similar to reconstitutable mice, indicating that this region of the original *Prnp*- chromosome and its linked genes cosegregate in most if not all of our backcrossed strains. A linkage to the *Prnp*- allele was also found in some cases in D2Mit395(119.3 Mb) and even D2Mit421(104 Mb). Heterozygosity downstream of D2Mit256 towards *Rag*2 indicated that multiple meiotic recombination events could have taken place at various sites.
Our SNP analysis with a spacing of 5 Mb confirmed that markers next to *Prnp* were linked to the respective *Prnp*-BALB/c or 129Sv-allelotype. However, not all of the applied SNPs were informative in discriminating between 129Sv and BALB/c since they displayed the same nucleotide conformation (Fig. 3.14). The markers just next to *Prnp*, rs13476769(129.7 Mb) and rs13476772(130.6 Mb) were not informative, but the SNPs rs33314425 (122.3 Mb) and rs13476764 (127.8 Mb) clearly cosegregated in most cases with the *Prnp*- allele, which confirmed the additional STR data. The situation in rs33314425 was not in all cases identical since a homozygous "BALB/c" constellation for this marker was found in some *Prnp*$^{-/-}$ mice indicating that different recombination events closer to the *Prnp* locus had occurred. Interestingly, a marker upstream of *Prnp* at 138 Mbp, rs13476802, was only linked to the *Prnp*- allele in mice from the original backcrossing strategy (Fig. 3.1) whereas it displayed a "BALB/c" constellation in mice derived from the alternative breeding strategy starting from multiply backcrossed *Prnp*$^{-/-}$ mice to BALB/c (Fig. 3.2).

The identifiers of possible candidate genes that might influence engraftment of human cells known to have a function assigned to the immune system between *Prnp* and *Rag* are listed in table 3.2.

Table 3.2.: Genes putatively involved in the immune system and stem cell homeostasis between *Rag* and *Prnp*.
The transcriptional start position is based on NCBI build 37.1. of mouse chromosome 2.

Gene start	Gene ID	Gene name
101518597	*Traf6*	Tnf receptor-associated factor 6
102651298	*Cd44*	CD44 antigen
103911167	*Cd59b*	CD59b antigen
103936010	*Cd59a*	CD59a antigen
104839813	*Ga17*	dendritic cell protein GA17
105516602	*Pax6*	paired box gene 6
115688805	*Mrg1*	myeloid ecotropic viral integration site-related gene 1
117937658	*Thbs1*	thrombospondin 1
119577062	*Ltk*	leukocyte tyrosine kinase
120843953	*Epb4.2*	erythrocyte protein band 4.2
120967877	*Adal*	adenosine deaminase-like
121973423	*B2m*	beta-2 microglobulin
127458966	*Mal*	myelin and lymphocyte protein, T-cell differentiation protein
129125346	*Il1a*	interleukin 1 alpha
129190315	*Il1b*	interleukin 1 beta
129419314	*Sirpa*	signal-regulatory protein alpha
130121675	*Ebf4*	early B-cell factor 4

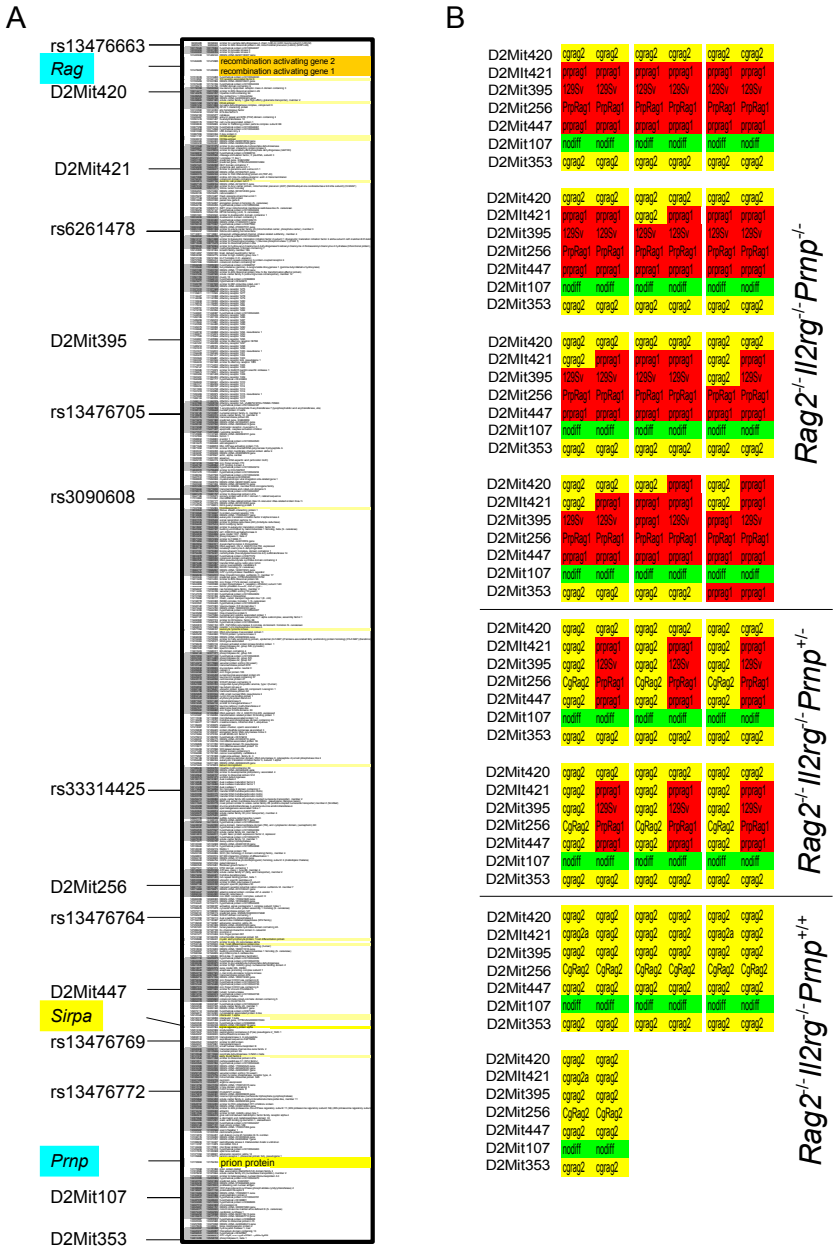

Figure 3.13.: Additional STRs and SNPs between *Rag* and *Prnp*.
A shows the genomic region on chromosome 2 between 99 and 135 megabases according to NCBI build 37.1. This region includes around 450 genes that are irregularly dispersed, in certain spots more than 30 genes reside within a megabase whereas other regions display a gene density of less than 5 genes per megabase (alternating grey and white coloring of one megabase sections). Genes putatively involved in the immune system are highlighted in yellow. Additional SNP and STR markers are placed at the right position of the chromosome.
B STR marker profile of backcrossed immunodeficient $Prnp^{-/-}$, $Prnp^{+/-}$ and $Prnp^{+/+}$ mice. Polymorphic markers D2Mit447 and D2Mit256, in various cases also D2Mit395 remain in the "PrPRag1"-constellation (red) in case of deficiency of *Prnp* and cosegregate with the *Prnp*- allele.

SNP ID	Mb	Rag2-Il2rg$^{-/-}$	Prnp-Rag1$^{-/-}$	Rag2-Il2rg$^{-/-}$Prnp$^{+/+}$ backcrossed	Rag2-Il2rg$^{-/-}$Prnp$^{+/-}$ "Balb/C"	Rag2-Il2rg$^{-/-}$Prnp$^{+/-}$ "Balb/C"	C57Bl/6
rs13476663	99.9	M_22285663_10-T	M_22285663_10-T	M_22285663_10-T	M_22285663_10-T	M_22285663_10-T	M_22285663_10-T
rs29912618	100.8	M_24382337_10-C	M_24382337_10-C	M_24382337_10-C	M_24382337_10-C	M_24382337_10-C	M_24382337_10-T
rs13476670	101.9	M_23720601_10-A	M_23720601_10-A	M_23720601_10-A	M_23720601_10-G	Both	M_23720601_10-A
rs6261478	107.0	M_22354457_10-G	M_22354457_10-G	M_22354457_10-G	M_22354457_10-C	M_22354457_10-C	M_22354457_10-G
rs13476705	112.9	M_23043361_10-A	M_23043361_10-G	M_23043361_10-A	M_23043361_10-A	M_23043361_10-A	M_23043361_10-G
rs33314425	122.3	M_23028483_10-T	M_23028483_10-C	M_23028483_10-T	Both	Both	M_23028483_10-C
rs13476764	127.8	M_23908236_10-C	M_23908236_10-T	M_23908236_10-C	Both	Both	M_23908236_10-T
rs13476769	129.7	M_23300050_10-C	M_23300050_10-C	M_23300050_10-C	M_23300050_10-C	M_23300050_10-C	M_23300050_10-T
rs13476772	130.6	M_22299775_10-C	M_22299775_10-C	M_22299775_10-C	M_22299775_10-C	M_22299775_10-C	M_22299775_10-T
rs13476802	138.5	M_23938758_10-A	M_23938758_10-C	M_23938758_10-A	M_23938758_10-A	M_23938758_10-A	M_23938758_10-C

SNP ID	Mb	Reconstituted Prnp$^{+/-}$ mice			
rs13476663	99.9	M_22285663_10-T	M_22285663_10-T	M_22285663_10-T	M_22285663_10-T
rs29912618	100.8	M_24382337_10-C	M_24382337_10-C	M_24382337_10-C	M_24382337_10-C
rs13476670	101.9	M_23720601_10-A	M_23720601_10-A	M_23720601_10-A	M_23720601_10-A
rs6261478	107.0	M_22354457_10-G	M_22354457_10-G	M_22354457_10-G	M_22354457_10-G
rs13476705	112.9	M_23043361_10-A	M_23043361_10-A	M_23043361_10-A	M_23043361_10-A
rs33314425	122.3	Both	M_23028483_10-T	Both	Both
rs13476764	127.8	Both	Both	Both	Both
rs13476769	129.7	M_23300050_10-C	M_23300050_10-C	M_23300050_10-C	M_23300050_10-C
rs13476772	130.6	M_22299775_10-C	M_22299775_10-C	M_22299775_10-C	M_22299775_10-C
rs13476802	138.5	Both	Both	Both	Both

SNP ID	Mb	Reconstituted Prnp$^{+/+}$ mice			
rs13476663	99.9	M_22285663_10-T	M_22285663_10-T	M_22285663_10-T	M_22285663_10-T
rs29912618	100.8	M_24382337_10-C	M_24382337_10-C	M_24382337_10-C	M_24382337_10-C
rs13476670	101.9	M_23720601_10-A	M_23720601_10-A	M_23720601_10-A	M_23720601_10-A
rs6261478	107.0	M_22354457_10-G	M_22354457_10-G	M_22354457_10-G	M_22354457_10-G
rs13476705	112.9	M_23043361_10-A	M_23043361_10-A	M_23043361_10-A	M_23043361_10-A
rs33314425	122.3	M_23028483_10-T	M_23028483_10-T	M_23028483_10-T	M_23028483_10-T
rs13476764	127.8	M_23908236_10-C	M_23908236_10-C	M_23908236_10-C	M_23908236_10-C
rs13476769	129.7	M_23300050_10-C	M_23300050_10-C	M_23300050_10-C	M_23300050_10-C
rs13476772	130.6	M_22299775_10-C	M_22299775_10-C	M_22299775_10-C	M_22299775_10-C
rs13476802	138.5	M_23938758_10-A	M_23938758_10-A	M_23938758_10-A	M_23938758_10-A

SNP ID	Mb	Triple ko mice (not reconstituted)			
rs13476663	99.9	M_22285663_10-T	M_22285663_10-T	M_22285663_10-T	M_22285663_10-T
rs29912618	100.8	M_24382337_10-C	M_24382337_10-C	M_24382337_10-C	M_24382337_10-C
rs13476670	101.9	M_23720601_10-A	M_23720601_10-A	M_23720601_10-A	M_23720601_10-A
rs6261478	107.0	M_22354457_10-G	M_22354457_10-G	M_22354457_10-G	M_22354457_10-G
rs13476705	112.9	M_23043361_10-G	M_23043361_10-A	M_23043361_10-A	M_23043361_10-A
rs33314425	122.3	M_23028483_10-C	M_23028483_10-C	M_23028483_10-C	M_23028483_10-C
rs13476764	127.8	M_23908236_10-T	M_23908236_10-T	M_23908236_10-T	M_23908236_10-T
rs13476769	129.7	M_23300050_10-C	M_23300050_10-C	M_23300050_10-C	M_23300050_10-C
rs13476772	130.6	M_22299775_10-C	M_22299775_10-C	M_22299775_10-C	M_22299775_10-C
rs13476802	138.5	M_23938758_10-C	M_23938758_10-C	M_23938758_10-C	M_23938758_10-C

Figure 3.14.: SNP analysis of backcrossed and reconstituted mice.
The upper panel shows calibration strains (original strains and C57Bl/6) and *Prnp*$^{+/-}$ mice from both breeding strategies. The lower panels show mice subjected to reconstitution experiments displaying different *Prnp* genotypes. Informative markers rs33314425 (122.3 Mb) and rs13476764 (127.8 Mb) seem to be linked to respective *Prnp* alleles.

3.8. Analysis of signal regulatory protein alpha haplotypes and correlation to reconstitution outcomes

In November 2007, the group of Jayne Danska found a polymorphic gene coding for signal regulatory protein alpha (Sirpa), claimed to modulate engraftment of human hematopoietic stem cells in immunodeficient mice depending on the haplotype configuration of its underlying gene *Sirpa* [116] applying a positional genetic approach. Surprisingly, *Sirpa* is located very close to *Prnp*, 2 Mb apart at 73.1 cM on mouse chromosome 2 between D2Mit447 and *Prnp*. We therefore sequenced *Sirpa* exon 2, the domain known to be most polymorphic within mouse strains and found a clear correlation between *Sirpa* haplotypes and reconstitution outcomes. 3 different haplotypes could be identified within our colony: BALB/c, 129Sv, C57Bl/6 showing many polymorphisms resulting in silent and effective mutations. The *Prnp* knockout allele clearly cosegregated with the *Sirpa* haplotype 129Sv, whereas a BALB/c allele cosegregated with the *Prnp*(+) allele. Even in the case of multiple backcrossings to BALB/c, the *Prnp*(-) mice retained their 129Sv *Sirpa* haplotype. Reconstitution was only possible in mice carrying at least one BALB/c *Sirpa*. Meiotic recombinations between a *Prnp*(-) allele and *Sirpa*-BALB/c took place in one case in a retrospective analysis (Fig. 3.15, we decided therefore to initiate a meiotic recombination screening strategy.

3.9. Meiotic recombination screening between Sirpa and Prnp, subsequent reconstitutions

Using the polymorphic microsatellite marker D2Mit447, we initiated multiple breedings to achieve meiotic recombinations between *Sirpa* and *Prnp* and finally succeeded in identifying mice carrying the constellation $Sirpa^{BALB/c/129Sv}$ - $Prnp^{-/-}$. These mice were further bred to homozygous colonies and subjected to our humanization assay. We could definitely show that $Sirpa^{129Sv}$ recessively suppresses successful engraftment of human stem cells since in a litter of 5 mice, 4 being $Prnp^{-/-}$ and $Sirpa^{129Sv/129Sv}$ had no detectable human $CD45^{+}$ cells in the peripheral blood whereas the only mouse showing the constellation $Prnp^{-/-}$ and $Sirpa^{BALB/c/129Sv}$ had an engraftment of 38% human cells in the lymphoid gate. These data were later confirmed in bone marrow analysis. The long-time survival of the graft seemed to be limited because of a single allele of $Sirpa^{129Sv}$. Currently, the colony of $Sirpa^{BALB/c/BALB/c}$-$Prnp^{-/-}$ mice is being continuously expanded to homozygous littermates which will ensure a longer graft survival.

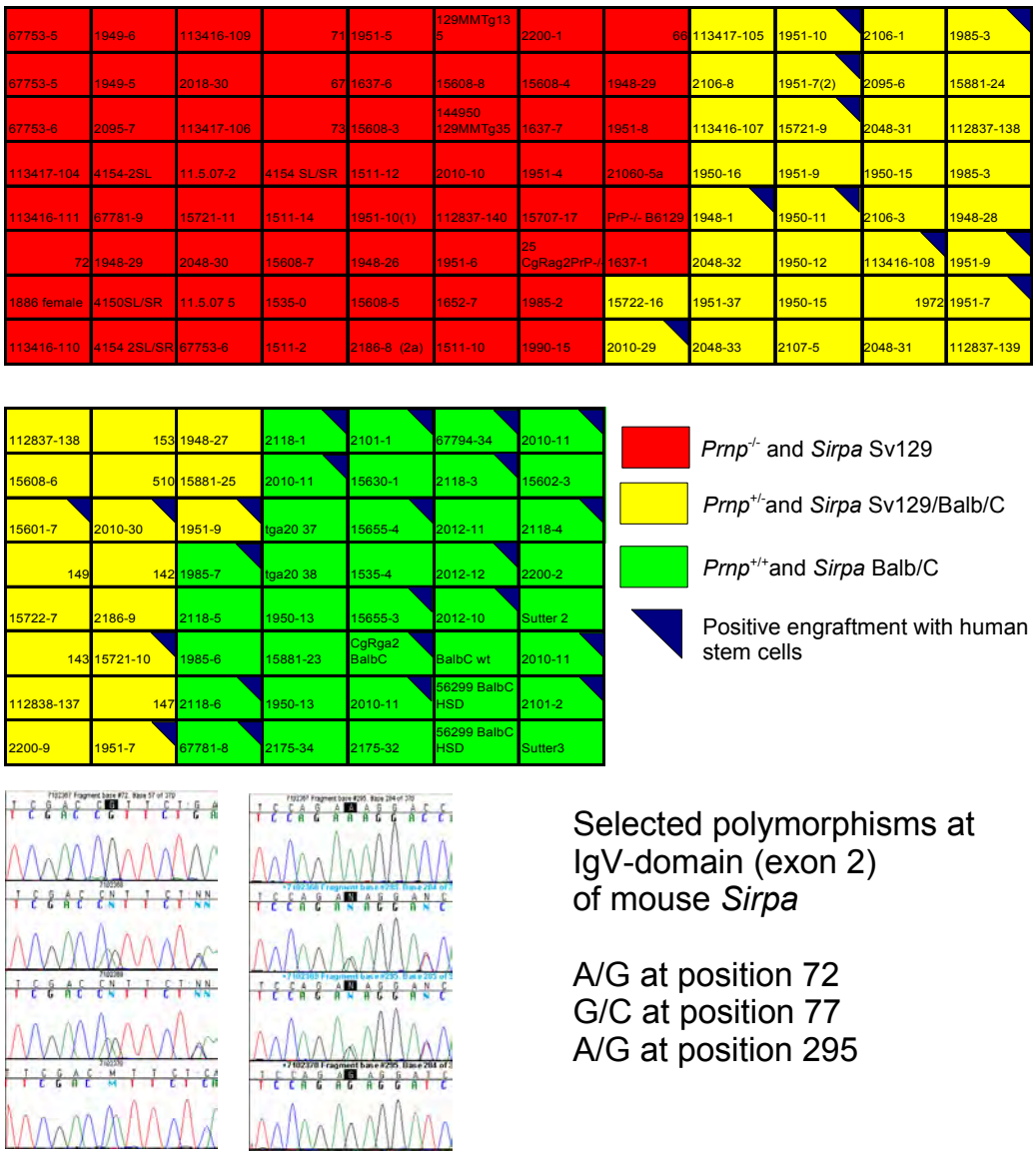

Figure 3.15.: Comparison of *Sirpa* polymorphisms and *Prnp*-allelotype and its correlation to reconstitution outcome.
Retrospective analysis of *Sirpa* haplotypes in mice that were subjected to our humanization assay. All $Prnp^{-/-}$ mice displayed two *Sirpa* alleles of the 129Sv strain, whereas all the $Prnp^{+/+}$ mice carried two alleles of the BALB/c strain. $Prnp^{+/-}$ mice carried both *Sirpa*-alleles. No meiotic recombination event between *Sirpa* and *Prnp* was detected. Only mice carrying at least one *Sirpa*-BALB/c allele were engraftable with human cells, i.e. detection of human CD45+ cells in peripheral blood (n=152).

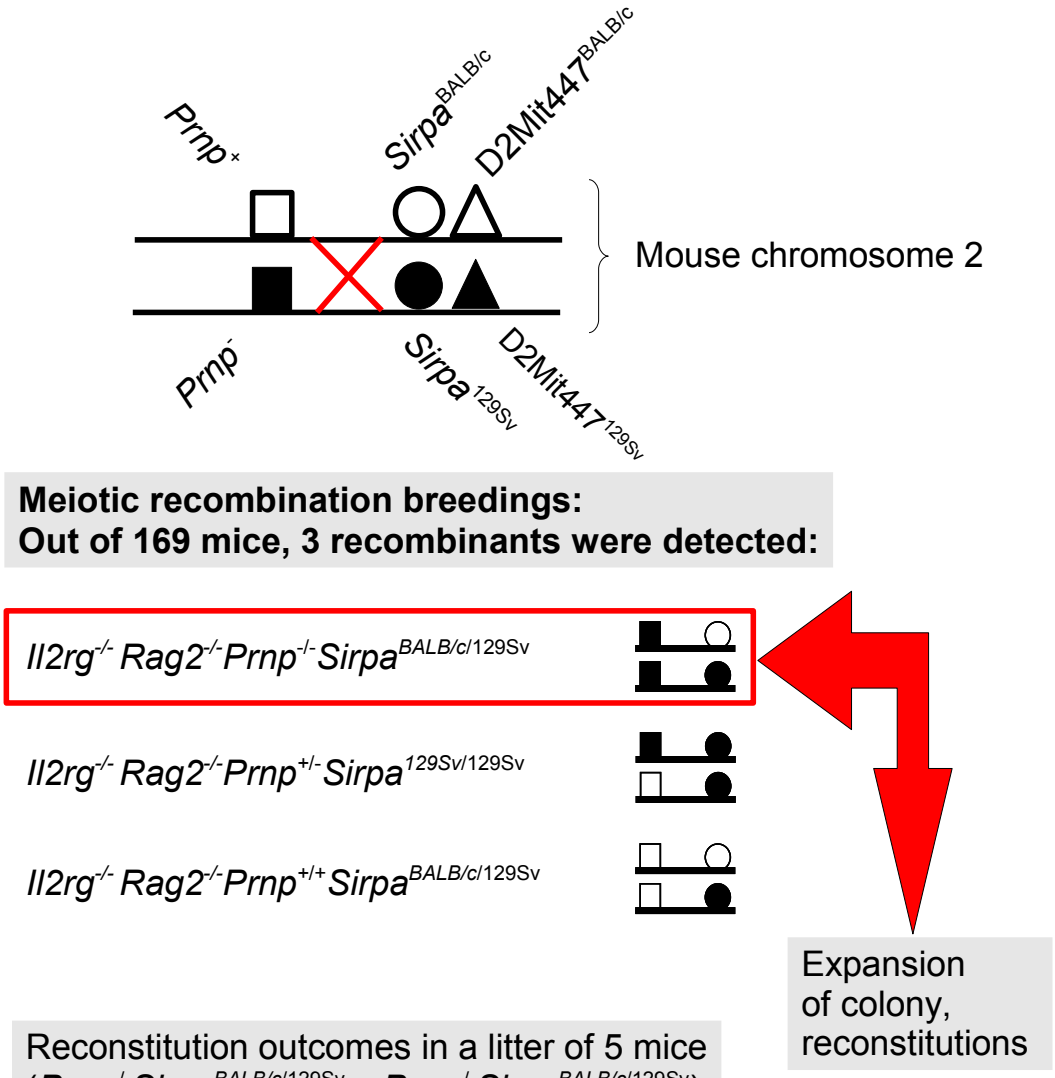

Reconstitution outcomes in a litter of 5 mice
(*Prnp*$^{-/-}$ *Sirpa*$^{BALB/c/129Sv}$ x *Prnp*$^{-/-}$ *Sirpa*$^{BALB/c/129Sv}$)

Mouse	Genotype	% Reconstitution (peripheral blood, 6 weeks)	% Reconstitution (bone marrow, 9 weeks)
1	*Prnp*$^{-/-}$ *Sirpa*$^{129Sv/129Sv}$	0	0
2	*Prnp*$^{-/-}$ *Sirpa*$^{129Sv/129Sv}$	0	0
3	*Prnp*$^{-/-}$ *Sirpa*$^{129Sv/129Sv}$	0	0
4	*Prnp*$^{-/-}$ *Sirpa*$^{129Sv/129Sv}$	0	0
5	***Prnp*$^{-/-}$ *Sirpa*$^{BALB/c/129Sv}$**	**38**	**10**
Control	C57Bl/6	0	0

Figure 3.16.: *Sirpa* meiotic recombination breedings and subsequent reconstitutions.
Meiotic recombination breedings were initiated using primers for *Prnp* and D2Mit447, an informative microsatellite marker closely linked to *Sirpa*. Out of 169 mice, 3 recombinants could be detected, while only one male mouse displayed the genetic constellation *Prnp*$^{-/-}$- *Sirpa*$^{BALB/c/129Sv}$. Further breedings could expand the colony and subsequently lead to reconstitution experiments that pointed out the importance of the *Sirpa*$^{BALB/c}$-allele for xenograft survival and differentiation. The data was controlled by sequencing of *Sirpa* exon 2 in all screened mice.

4. Discussion

The goal of this study was the establishment of a "humanized mouse model" to study the immunology of peripheral prion disease initiation, for reevaluation of the concept of the species barrier and for developing tools to investigate novel diagnostic tests and disease specific genetic susceptibility factors. To impose a realistic model, PrP expression should only be present on the engrafted cells but not on confounding host cells. We succeded in reproducing long-term engraftment with hematopoietic stem cells in immunodeficient mice applying the same protocol as published by Traggiai et al. [119]. Reproducible engraftment success was only possible when high amounts of high-quality CD34+ stem cells were injected, whereas high variability was observed when smaller inocula were applied.

Sirpa$^{BALB/c}$ instead of Sirpa^{129Sv} in Rag2$^{-/-}$Il2rg$^{-/-}$Prnp$^{-/-}$ mice rescues reconstitutability.

*Rag*2$^{-/-}$*Il2rg*$^{-/-}$ mice devoid of *Prnp* could reproducibly be engrafted with bone marrow from *allogeneic* donors (Figure 3.8) However, we failed to reconstitute mice devoid of PrP^C expression with *xenogeneic* hematopoietic stem cells for a long time (Figures 3.9, 3.10) although we implemented a stringent microsatellite-based "speed congenics" strategy to monitor and adjust for the genetic background of the recipient mice (Figures 3.5, 3.6). In fact, *Prnp*(+) littermates with a near-identical genetical profile showed a detectable longterm engraftment whereas this was absent in all our assessed *Prnp*(-) mice.
Since PrP^C is widely expressed in hematopoietic cells, mainly in macrophages and lymphoid precursors, but also in hematopoietic stem cells, we reasoned that PrP^C itself might modulate the homing capacity of xenogeneic cells by a yet to be defined mechanism. We speculated that PrP^C might represent a homing receptor for xenogeneic cells on macrophages or elsewhere in the bone marrow since this observation seemed to be restricted to foreign cells. Expression analysis in bone marrow stroma did not reveal significant PrP^C expression there, possibly ruling out an impact of PrP^C in the stem cell niche compartments (data not shown). However, complementation attempts by expression of a transgenic human *PRNP* on a mouse *Prnp*$^{-/-}$ background did not restore engraftment, even though the genetic background of the tested mice was extremely homogeneous. This suggested a different mechanism for the observed phenomenon (Figure 3.11). A closer analysis of the genetic region around *Prnp* and *Rag* genes using higher resolution STR and SNP mapping revealed that still quite a large portion of the genetic material around and downstream of *Prnp* displayed a configuration of a 129Sv-chromosome and was uniquely present in our *Rag*2$^{-/-}$*Il2rg*$^{-/-}$*Prnp*$^{-/-}$ animals, indicating that other genetic factors might be responsible for the observed phenotype (Figures 3.13, 3.14). This analysis clarified further that more than one meiotic recombination event between these two genes must have occurred.

Very recently published strain polymorphisms in mouse signal regulatory protein alpha (*Sirpa*), a gene that is closely linked to *Prnp* on chromosome 2 less than 2 cM apart from *Prnp*, situated between *Prnp* and *Rag*, were finally able to explain the observed phenomenon [116].

Putative role of Sirpa in innate immunity. Cells of the innate immune system are likely to have other tools determining self and non-self that are being deciphered only recently. Unmasking these functions will strongly enhance the understanding of innate immunity, a field with significant novel discoveries during the last decade. The "Sirpa family" of receptors has been discovered only recently and seems to be a fundamental contributor to innate immune functions [9]. Sirpa is expressed on macrophages and is quoted to be a receptor for foreign or self CD47. In case of efficient binding between Sirpa and human CD47, macrophages are instructed to downregulate their phagocytic machinery via tyrosine-kinase signaling and become tolerant to non-self organisms as described by [116], [54]. As a immunoglobulin-like protein with a hypervariable IgV-domain, Sirpa is reported to be highly polymorphic between different mouse strains and therefore exhibits varying binding properties to CD47 [67]. Its binding site seems to be reminiscent of the T-cell receptor [44] and MHC molecules. The NOD-Sirpa (see also Figure 1.3) seems to have the best binding to its human CD47 counterpart, whereas many other strains, including C57Bl/6 and 129Sv are basically non-binders.

Sirpa haplotypes in *Prnp* deficient mice were of the 129Sv-type, whereas in all our successfully reconstituted and backcrossed mice at least one BALB/c-*Sirpa* allele was present in conjunction with the wild type *Prnp* allele according to our sequence alignment comparison (Figure 3.15). A microsatellite marker closely associated with *Sirpa*, D2Mit447, served as a surrogate for recombination events between *Sirpa* and *Prnp*. In a retrospective analysis of all our reconstituted mice we observed only one favorable recombination event in our mouse colony, and we therefore initiated a screening strategy for meiotic recombinations between *Prnp* and *Sirpa* to yield a BALB/c *Sirpa* on a $Prnp^{-/-}$ (129Sv) chromosome in order to have reconstitutable $Prnp^{-/-}$ mice, an event that statistically should occur in 1 in 100 mice. Applying this screen, we generated as well the reverse situation ($Prnp^{+/+}$-$\text{Sirpa}^{129Sv/129Sv}$) on a basically pure BALB/c background which could easily be used for control and future *in vivo* and *in vitro* experiments, further elucidating the a putative role of *Sirpa* or *Prnp* in phagocytosis. So far a single proof of principle experiment in a well-controlled setting disclosed a clear correlation between the negative impact of $\text{Sirpa}^{129Sv/129Sv}$ and reconstitution outcome: in a litter of solely $\text{Prnp}^{-/-}$ mice with varying *Sirpa* haplotypes, only the mouse with a permissive $Sirpa^{BALB/c}$ allele was positively engrafted and showed sustained engrafting in bone marrow after 9 weeks. We could not detect human engraftment in the other littermates, since binding of the 129Sv-Sirpa to CD47 seems to be less efficient compared to its BALB/c polymorphic counterpart. This confirms the recent publication of [116] in a different way and impressively demonstrates the importance of different *Sirpa* strain polymorphisms in xenografting. Therefore, $\text{Sirpa}^{BALB/c}$ would be placed in between Sirpa^{129Sv} and Sirpa^{NOD} in terms of affinity to xenogeneic CD47 elucidating an all-or-nothing response for macrophage activation. However, other cofactors influencing the activation status

of innate immunity might also contribute to the very variable innate response towards xenografts. So far, Sirpa^{NOD} might bind best to human CD47 and therefore represent the ideal strain for humanization experiments.

Variability of the experiment for other reasons?

Engraftment of human cells sometimes highly varied even in BALB/c *Rag*2$^{-/-}$*Il2rg*$^{-/-}$ mice. Technical reasons or qualitative differences in the stem cell inoculum might have been the cause for this variability, but other genetic factors related to this phenomenon, even on different regions in the genome than the ones described in our work might contribute to the observed variations as well. Other polymorphic or differentially regulated target genes of influence might be identified by application of high-resolution SNP chips for QTL-mapping or microarrays of myeloid cell cDNA with the limitation that the power of the observed phenotype (engraftment versus no/subclinical engraftment) might not be sufficiently strong to identify clear-cut associations. Therefore, one must carefully select the samples and perform a quantitative and kinetic analysis of the engraftment behaviour in a defined cohort of mice and controls before applying these very expensive techniques to identify other factors involved in xenografting.

Steps towards optimization of humanized mouse models - manipulating myeloid cells

It is reported that liposomal clodronate treatment as a preconditioning regimen efficiently depletes macrophages for a certain timeframe [120]. Attempts with clodronate in our triple knockout mice are currently ongoing and in their early days - this might represent another effective but nevertheless harsh way to achieve engraftable mice and reduce variability in our experiments. Another approach to optimize the model would consist in expressing the human Sirpa transgenically in the mouse, either ubiquitously or macrophage-specifically. One might aim at expressing human *Sirpa* cDNA under the control of the CD11b promoter [26] (a macrophage specific promoter) in our *Rag*2$^{-/-}$*Il2rg*$^{-/-}$*Prnp*$^{-/-}$ mice, thereby removing the obstacle of the Sirpa-huCD47 incompatibility. Our screening approach for favorable recombinations between the *Prnp*- allele and *Sirpa*$^{BALB/c}$ was successful although this still will not yield optimal engraftment results, as *Sirpa*$^{BALB/c}$ is inferior to *Sirpa*^{NOD} in terms of binding to human CD47. The making of a transgenic mouse and its breeding into the appropriate genetic environment may take much more time but should finally be the most promising strategy for future directions.

Inoculation studies of humanized BALB/c Rag2$^{-/-}$Il2rg$^{-/-}$ mice - an optimal model?

PrP^{Sc} inoculation experiments with humanized BALB/c *Il2rg*$^{-/-}$*Rag*2$^{-/-}$ mice have been performed in our lab for the last two years, and western blot analysis of spleens 60 days post inoculation revealed PrP^{Sc} deposition in case of a CJD inoculum in reconstituted, but not in unreconstituted littermates. PrP^{Sc} was detected using standard western blotting techniques with an antibody, 3F4, that binds specifically to human PrP^{Sc} because of

a human specific epitope. However, *Il2rg*$^{-/-}$*Rag*2$^{-/-}$ mice express a large amount of endogenous mouse *Prnp* in their hematopoietic compartment, which is well capable of sequestering or replicating CJD prions as reported by others [74], especially in the myeloid and macrophage compartment. In this study, we can reconfirm a high PrP-expression in the hematopoietic and myeloid compartment in mice.
Further, it has been known for more than 20 years that CJD can easily be transmitted in small rodents, thereby circumventing a possible species barrier, and infectivity was detectable in all major lymphatic organs upon intraperitoneal inoculation [117]. In these reported cases, the endogenous mouse PrP^{C} served as a template for the initiation of the replication process, and it might well be that de novo replicated prions carry the human sequence since the nature of the replication process is not yet fully clarified.
According to our observations, *Il2rg*$^{-/-}$*Rag*2$^{-/-}$ mice possess an enlarged macrophage and myeloid compartment in response to their missing adaptive immune sytem. Further, the conditioning regimen includes sublethal irradiation steps which elicit further macrophage activation and accumulation reactions. Additionally, all stromal cells and other organ-specific cells express mouse *Prnp* at a level similar to immunocompetent wildtype mice. Although these mice lack functional FDCs due to impaired cytokine signaling [72], other stromal and hematopoietic cell types could take over prion replication. Moreover, FDC or FDC-like formation might be induced by graft-secreted cytokines. Whether or not FDCs represent a prion replication machinery is still unclear. Reports by our group suggest that the absence of functional FDCs abrogate peripheral prion replication and neuroinvasion of RML-inoculated mice in spleens [93], but others report that the absence of FDCs does not alter the incubation times [87] and suggest that neither FDC nor CD11c(+) cells are essential for neuroinvasion after high doses of RML. A more radical study even claims that neither the absence of FDCs nor the absence of B-cells significantly altered incubation times in case of CJD-inoculated mice [106] and emphasizes the contribution of myeloid cells involved in the replication process. To study the response of a humanized immune system in vivo it is therefore indispensable to have a system available that is devoid of any other PrP-species. The inoculum will exhibit a specific tropism to engrafted and PrP expressing cells and assure that no other entity than human cells is involved in the replication process.

Impact of Sirpa polymorphisms to the prion field

Genetic background artefacts and effects will impact mouse research in the near future to a much larger extent, while many of the described phenotypes of knock-out mice will have to be reevaluated. Also in case of mice devoid of PrP^{C}, most of the phenotypes attributed to a physiological function of the protein might be artefactual since the genetic background was poorly controlled in these studies.
Sirpa and *Prnp* are genetically close in other mammals, especially in humans (on chromosome 20), in cattle (on chromosome 13) and in non-human primates. All the studies describing immunological phenotypes in *Prnp*$^{-/-}$ mice compared to wildtype mice used *Prnp*$^{-/-}$ mice with a *Sirpa*^{129Sv} constellation, whereas in most of the wildtype controls, a different genetic configuration with probably different *Sirpa* haplotypes might

have been used. This holds especially true for the the studies that attribute an enhanced phagocytosis and leukocyte infiltration phenotype to $Prnp^{-/-}$ mice [22] and claim a role for PrP in *Brucella* infection [122] since *Sirpa* polymorphisms with a clear impact on macrophage function could provide a very likely explanation for these observations as well. Another recent study claimed that clearance of splenic endogenous retroviruses upon immune stimulation was *Prnp*-dependent [70], an observation that likewise could be challenged because of the different genetic environment of the mice that were used in the experiment. Further, PrP was claimed to be involved in hematopoietic stem cell self-renewal in a series of transplantation experiments [130] with $Prnp^{-/-}$ bone marrow cells performing worse than wildtype cells - a study that might also be worth reevaluating in the context of polymorphic *Sirpa*. Additionally, mice that overexpress *Prnp* under the control of the *Prnp*-promoter in a *Prnp*-deficient background have often been used for control experiments that are supposed to complement *Prnp*-deficient mice from their immunological phenotype. However, sequence analysis of *Sirpa* in 10 generation backcrossed tg*a*20 mice (to C57Bl/6 or BALB/c) show different *Sirpa* configurations in individual mice, which implies that the observed genetic rescue might equally well be explained by polymorphic *Sirpa*.
Interestingly, *Sirpa* and *Prnp* are co-mentioned in another very recent study investigating the transcriptional response in macrophages of two different cattle breeds to a zoonotic parasite, *Theileria annulata*. Both *Sirpa* and *Prnp* are upregulated upon infection in one breed and the physiological response in the two strains is reported to be highly different expecially in terms of T-cell activation [57]. Bovine *Sirpa* is located on Chromosome 13 at position 53810kB whereas *Prnp* is located at 46690kB on the same chromosome, further apart than in the mouse. Nevertheless, *Sirpa* and *Prnp* seem to be co-regulated on a transcriptional level in myeloid cells upon infection with distinct pathogens which adds another step of complexity to a possible involvment of *Prnp* in innate immune function. This report could give another hint that a polymorphic and co-regulated gene linked to *Prnp* rather than *Prnp* itself plays the major role in phenomena related to innate and specific immune responses.

5. Conclusion

Throughout this work we aimed to solve three specific problems (section 1.7):

- First, we were readily able to reproduce the basic experiment published by Traggiai et. al. exploiting excellent infrastructural and logistical resources.
- Second, despite some natural obstacles, a genetically sound and reproducible basis was laid for a humanized mouse model devoid of murine endogenous *Prnp*. Prion replication in these mice will take place exclusively in the grafted cells and therefore open new frontiers in prion research. Interfering polymorphisms of a genetically linked gene - *Sirpa* - might represent a clue to many artefactual immune-phenotypes described and published in $Prnp^{-/-}$ mice.
- Immunodeficient mice devoid of endogenous murine *Prnp* and re-expressing a human *PRNP* transgene that are equally well reconstitutable with human stem cells have been generated. These mice will soon represent a new model system for human prion diseases, especially neuroinvasion, and will be used as a novel tool for diagnostic and therapeutic purposes.

Part II.

Global Gene Expression Analysis of PrP^{Sc} infected neuronal cells

6. Introduction

Outline

This part of my thesis is a modified version of a manuscript published in November 2007 in the Journal of Molecular Biology with the title

Transcriptional stability of cultured cells upon prion infection

Christian Julius[1,2], Gregor Hutter[1,2], Ulrich Wagner[3], Harald Seeger[1], Veronika Kana[1], Jan Kranich[1], Peter Kloehn[4], Charles Weissmann[5], Gino Miele[6,7], Adriano Aguzzi[1,7]

PII: S0022-2836(07)01463-5 DOI: doi: 10.1016/j.jmb.2007.11.003 Reference: YJMBI 59919 To appear in: Journal of Molecular Biology

Received date: 15 August 2007
Revised date: 30 October 2007
Accepted date: 1 November 2007

Please cite this article as: Julius, C., Hutter, G., Wagner, U., Seeger, H., Kana, V., Kranich, J., Kloehn, P., Weissmann, C., Miele, G. & Aguzzi, A., Transcriptional stability of cultured cells upon prion infection, Journal of Molecular Biology (2007), doi: 10.1016/j.jmb.2007.11.003

[1]Institute of Neuropathology, University Hospital of Zürich, Schmelzbergstrasse 12, CH-8091 Zürich, Switzerland
[2]These autors contributed equally to this study
[3]Functional Genomics Center, Federal Institute of Technology (ETH) and University of Zurich, Winterthurerstrasse 190, CH-8057 Zürich, Switzerland
[4]Medical Research Council Prion Unit and Department of Neurodegenerative Disease, Institute of Neurology, University College London, Queen Square, London WC1N 3BG, United Kingdom
[5]Scripps Florida, 5353 Parkside Drive, Jupiter, Florida 33480, USA
[6]Translational Medicine Research Collaboration, Sir James Black Centre, University of Dundee, Dow Street, Dundee, DD1 5EH, United Kingdom
[7]Correspondence: Adriano Aguzzi (adriano.aguzzi@usz.ch) or Gino Miele (g.miele@dundee.ac.uk

Abstract

Prion infections induce severe disruption of the central nervous system with neuronal vacuolation and extensive glial reactions, and invariably lead to death of affected individuals. The molecular underpinnings of these events are not well understood. In order to better define the molecular consequences of prion infections, we analyzed the transcriptional response to persistent prion infection in a panel of three murine neural cell lines in vitro. Colony spot immunochemistry assays indicated that 65 to 100% cells were infected in each line. Only the *Nav1* gene was marginally modulated in one cell line, whereas those transcripts previously reported to be derailed in prion-infected cells were not confirmed in the present study. We attribute these discrepancies to the experimental stringency of the current study, which was performed under conditions designed to minimize potential genetic drifts. These findings are at striking variance with gene expression studies performed on whole brains upon prion infections in vivo, suggesting that many of the latter changes represent secondary reactions to infection. We conclude that, suprisingly, there are no universal transcriptional changes induced by prion infection of neural cells in vitro.

6.1. Introduction

Prions are the causative agents of transmissible spongiform encephalopathies (TSEs), which include Creutzfeldt-Jakob disease (CJD) in humans, scrapie in sheep, bovine spongiform encephalopathy (BSE) in cattle, and chronic wasting disease (CWD) in cervids [3]. One hallmark of most forms of prion disease is the conversion of the host encoded cellular prion protein (PrP^{C}) to an abnormally folded form, termed PrP^{Sc} [80]. Although prion replication can occur in extraneural tissues prior to neuroinvasion after peripheral challenge, pathological changes have only been observed in the central nervous system (CNS) [32] [92]. These include neuronal vacuolation (spongiosis), neuronal death and pronounced glial reactions, which invariably lead to death of the affected individuals [1]. The molecular mechanisms underlying prion replication and pathways leading to subsequent neural damage are not understood [123]. Transcriptional profiling is a powerful technology that allows for interrogating very large datasets without the need to place the typical constraints of hypothesis-testing experimentation. This inherent lack of bias reflects the strength of the approach. The transcribed genome has been analyzed in whole brains of rodents experimentally infected with various prion strains [99], [100], [129], spleens of prion-infected mice [81], primary cells isolated from tissues [7], and prion-infected cell lines [24], [42]. Studies on whole brain or isolated microglia yielded differentially expressed genes possibly involved in systemic responses to prion infection. Instead, studies on neuronal cell lines may identify cellular responses to prion infection. Also, the use of cell lines highly susceptible to prion infection at high infection rates circumvents potential issues with using either whole or dissected brain, where only a small proportion of the interrogated transcriptome is contributed by prion-infected cells. One such recent study has reported that a number of candidate genes are differentially expressed as a direct result of prion infection [42]. Here we describe the outcome of

transcriptional analyses of cultured cells in vitro under stringently controlled conditions. Our original aim was to identify changes in gene expression after prion infection conserved over different neuronal cell lines. Besides pointing to possible players in the pathogenesis of prion diseases, any robust and consistent transcriptional changes could be utilized for constructing reporter systems, which in turn would allow for identifying and isolating single prion infected cells in intact tissues and in cell cultures. We employed high-density oligonucleotide microarrays analysis of N2aPK1 cells to identify gene expression changes directly resulting from prion infection. After exhaustive interrogation of datasets with several techniques of bioinformatics, we were only able to identify very modest differential expression, even under conditions of low filter stringencies. Subsequent quantitative PCR analyses confirmed modest but statistically significant differential expression of only one transcript (Nav1), which was not differentially expressed in another in vitro cell culture model of prion infection utilized in our laboratory. Our investigations of expression levels in independent cell culture models of prion infection of candidate genes previously reported by others to be profoundly differentially expressed [42] revealed that none of these were differentially expressed in any of the cell culture models of in vitro prion infection utilized here, including those employed by Greenwood et al. [42]. In contrast to reports by others [24], [42], we found no significant changes in the expression profile of our N2aPK1 cells interrogated here as assessed by transcriptional profiling, or in three highly infected neuronal cell lines as assessed by quantitative RT-PCR of several candidate genes recently proposed in the literature [42]. We hypothesize that this discrepancy results from fundamental differences in the experimental design. We conclude therefore that prion agents in cultured neuronal cells infected at high rates do not induce general or specific changes in the transcriptome.

7. Material and Methods

7.1. Cell culture (N2aPK1 cells, CAD cells, GT1 cells)

The N2aPK1 subclone of mouse neuroblastoma N2a cells was selected for high susceptibility to prion infection and kindly provided by Charles Weissmann and Peter Klöhn (MRC Prion Unit, The Institute of Neurology, London, UK) [61]. CAD cells, a subclone of the CNS catecholaminergic cell line Cath.a, were a gift of Dona Chikaraishi (Tufts University School of Medicine, Boston, Massachusetts, USA) [96]. The mouse hypothalamic neuronal cell line GT1 was kindly donated by Ina Vorberg (Institute of Virology, Technical University of Munich, Germany). All cell lines were cultured in Optimem/10% FBS, Pen/Strep. N2aPK1 and CAD cells were split at confluency at a ratio of 1:3 every three or 1:10 every four days. GT1 cells were split at confluency at a ratio of 1:3 every four or 1:10 every five days. For RNA isolation and Western blot analysis, cells were grown to approximately 75% confluence.

7.2. Prion infection of cell lines (N2aPK1RML, CADRML, GT1RML cells)

Prion infection of cells was performed as reported previously [61]. Briefly, 17'000 cells were seeded in six wells of a 96 well plate and after 16h of incubation infected with a 10^{-2} dilution of 10% homogenate of mock CD1 brain homogenate or 10% homogenate of RML infected brain homogenate, respectively. Independent infections were performed in quadruplicate to achieve four true biological replicates of Mock or RML infected cells. After three days of incubation cells were split three times (1:3) and subsequently a further three times (1:10). At that point six wells were pooled and cells were expanded in a T75 cell culture flask. At approximately 75% confluency cells were harvested for RNA isolation or split 1:10 to obtain material for Western blot analysis and clarification of the infection ratio The infection and splitting protocol is visualized in Figure 7.1.

7.3. Assessment of the infection ratio in RML infected cells (N2aPK1RML, CADRML, GT1RML cells)

To assess the proportion of prion infected cells in the N2aPK1RML, CADRML and GT1RML cells cultures we utilized the ELISPOT assay as described previously [61]. A dilution series of cells ranging from aliquots of 2000 to 8 cells per well was performed in a 96 well plate. The cells were transferred to a sterile Multi Screen Immobilon-P 96-well Filtration ELISPOT plate, activated with 70% ethanol (Millipore) and the cell suspension was filtered by vacuum filtration, followed by incubation for 1h at 50°C. Subsequently, 50μL of proteinase K (PK; 0.25 μg/mL in lysis buffer [50 mM Tris·HCl, pH 8.0/150 mM NaCl/0.5% sodium deoxycholate/0.5% Triton X-100]) was added to each well, and the

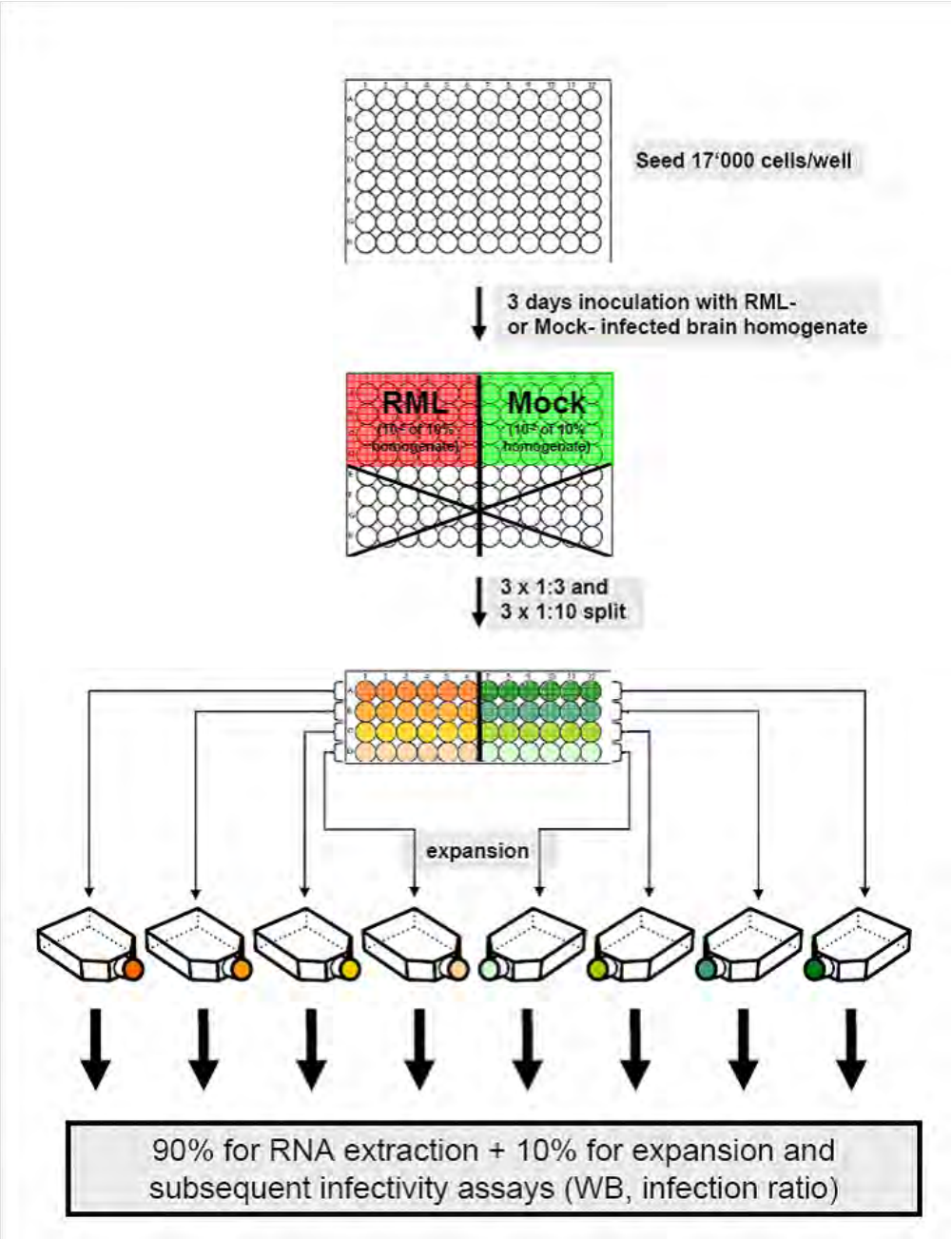

Figure 7.1.: Infection and cell splitting protocol of neuronal cell lines.
17000 cells (N2aPK1, CAD or GT1) were seeded in each of six wells of a 96 well plate. After 16h of incubation cells were infected with a 10^{-2} dilution of 10% homogenate of mock CD1 brain homogenate or 10% homogenate of RML infected brain homogenate, respectively.
Independent infections were performed in quadruplicate to achieve four true biological replicates of Mock or RML infected cells. After three days of incubation cells were split three times (1:3) and subsequently a further three times (1:10). At that point six wells were pooled and cells were expanded in a T75 cell culture flask. At approximately 75% confluency cells were harvested for RNA isolation or split 1:10 to obtain material for Western blot analysis and clarification of the infection ratio.

plates incubated for 90 min at 37°C followed by removal of the proteinase K solution by vacuum filtration. The wells were washed several times with PBS, incubated with 2 mM PMSF for 10 min, and washed again several times with PBS. After incubation with 160 μL of 3 M guanidinium thiocyanate in 10 mM Tris·HCl (pH 8.0) for 10 min, the filters were washed four times with PBS and incubated with 160 μL 5% TopBlock for 60 min. 50 μL of 0.4 μg/ml anti-PrP antibody POM1, in TBST/1% TopBlock, [91] was added and the plates incubated at RT for 1h, followed by removal of the antibody solution. Next, the wells were washed eight times with TBST followed by addition of 50 μL of alkaline phosphatase-conjugated anti-mouse IgG_1 (Southern Biotechnology Associates; 1:4,500 in TBST/1% milk powder) was added for 1 h. Wells were washed eight times with TBST and dried at RT. 50 μL of alkaline phosphatase conjugate substrate (Bio-Rad) was added for 16 min followed by two washes with water. PrP^{Sc} positive cells were counted manually using an Olympus SZX12 stereo microscope. Mock control cells did not give rise to background. The infection ratio was calculated by division of total cells seeded by PrP^{Sc} positive spots counted per well. This was performed for three different dilutions.

7.4. Western blot detection of PrP^{Sc}

To confirm persistent prion infection, cells were screened for PrP^{Sc} content in the different independent biological replicates. For PrP^{Sc} detection, cells were grown on T75 flasks until approximately 75% confluent. Monolayers were rinsed with PBS, harvested and lysed in RIPA lysis buffer (10 mM Tris-HCl (pH 7.5), 100 mM NaCl, 10 mM EDTA, 0.5% (v/v) Triton X-100, 0.5% (v/v) (deoxycholate) followed by three freeze-thaw cycles. Following centrifugation at 1000xg for 5 min the supernatant was removed and protein content quantitated by BCA-protein assay (BioRad) to allow equal amounts of protein to be applied the blot after either treatment with 20 mg/ml of proteinase K for 30 minutes at 37°C for PrP^{Sc} detection or no treatment (for PrP^{C} detection). Proteins were subjected to SDS-PAGE (12.5% Bis-Tris gels, NuPAGE, Invitrogen). PrP^{C} and PrP^{Sc} were detected using the mouse monoclonal antibody POM1 (1:10'000) followed by HRP-anti-mouse IgG1, and blots were developed with ECLplus according to the manufacturer's instructions (Amersham Corporation).

7.5. Preparation of labeled cRNA, microarray hybridization and data analysis

Total RNA was extracted from all samples using TRIzol (Invitrogen Life Technologies) according to the manufacturer's instructions. RNA was subjected to a further clean-up step using RNeasy mini columns (Qiagen). RNA quality was assessed by Agilent 2100 Bioanalyzer. Processing of 15 g of total RNA was continued to cDNA synthesis using a cDNA Synthesis kit (cat. no. 11917-010; Invitrogen Life Technologies) and primer 5'-GGCCAGTGAATTGTAATACG ACTCACTATAGGGAGGCGG(dT)24-3'. Biotin-labeled cRNA was synthesized, using Enzo BioArray HighYield RNA transcript labeling kit (T7) (Enzo Biochem), purified using RNeasy mini columns, quantified by spectrophotometry, and quality was assessed again by Agilent 2100 Bioanalyzer. Labeled

cRNA (15 μg) was fragmented in 40 mM Tris-acetate, 100 mM KOAc, 30 mM MgOAc, pH 8.1, at 95°C for 35 min followed by hybridisation to Affymetrix MOE430A and MOE430B chips. All hybridizations were conducted for 16 h at 45°C at 60 rpm. After hybridization chips were washed and conjugated with streptavidin-PE according to the manufacturer's instructions on the Affymetrix GeneChip Fluidics Station 450 with and scanned using the Affymetrix GS Scanner 2500 in conjunction with Affymetrix Microarray Suite 5.0 software. All experiments were performed in biological triplicates. After hybridization and scanning, probe cell intensities were calculated with the MAS5.0 algorithm of the Affymetrix GCOS software (Santa Clara, CA). Summarization and normalization of intensities for the respective probe sets were carried in two independent approaches using two different algorithms. For the first approach the MAS5.0 algorithms was employed as detailed in [53], present and absent calls were calculated by application of a signed-rank call algorithm [71]. Using the Genespring 7.3 software (Agilent, CA) results were median per-chip and median per-gene normalized. For the second approach, the GCRMA summary algorithm [128] as implemented in Genespring 7.3 was used to generate and normalize raw gene expression data from probe intensities. Independently of each other, genes were filtered out from the two lists of normalized expression values in Genespring 7.3 when not showing an expression value of at least 50 in all replicate measurements of at least one condition. Subsequently, the significance of 1.5 fold changes in expression was tested in Genespring by an equal-variance t-test with a significance threshold of $p < 0.05$. Data sets have been deposited in the Gene Expression Omnibus (http://www.ncbi.nlm.nih.gov/geo/); accession number GSE7229.

7.6. Quantitative Real-time PCR

cDNA of mock and RML infected cells was synthesized using the Quantitect reverse transcription kit (Qiagen, Switzerland) according to the manufacturers description. As negative controls, 1 μg of each RNA was processed without addition of reverse transcriptase. Complete removal of contaminating genomic DNA was confirmed by performing -actin PCR on all samples. Specific primers (supplementary table 1) were designed using primer3-software (http://frodo.wi.mit.edu/cgi-bin/primer3/primer3_www.cgi).

Table 7.1.: Primers designed for quantitative real time PCR reactions

Affymetrix ID	fw Primer	rev Primer
1416759_at	ggctacatgaatcgggaaga	aggtacagcccttgtgatgg
1436448_a_at	gaaggtcctgttcctggtca	gagtccatctgttccctcca
1418539_a_at	gcctccgtaagacacagagc	agtgaccaagagacgcacct
1423946_at	gaaggggtgatagcaggtga	ccatacgctttcgtgtcaaa
1433855_at	gcttgtcagttgtgcaggaa	atgctcgctagctgtggttt
1418175_at	ctgggaggaaaagacagcag	ggtttggactcctcccctac
1418835_at	tcatcacagttgcaggaagc	ctttttctttttggcgagga
1455099_at	gtccctgatgctgcttcttc	cattaaggctggggaaactg
1415834_at	caccaaaattgtgggttcact	cacgaacatcatggagcaag
1417976_at	aggggacttgacaatcatgc	cgcttctgcaggaaagagac
1451386_at	gctgaaatacgtggcagtga	ccacctaggtcagggtgcta
1420737_at	acccgaggatctgtgtcaag	ggggactcaatgtcctctga
1451110_at	cattgttggcagaaggtgtg	ggggttaacggtcctgattt
1416147_at	ttgaatgggacaggatgaga	gtagactggccccaggagta
1450459_at	tgtaccaggcctgttgattg	tgctgcctttccagaacttt
1449275_at	ctcccatggtgcagtctgtat	ctttggctggggacgtaata
1448623_at	gctgctgagaaagccacact	ccccaactcagtggaaatgt
1451385_at	ttgatgctgcgaagaacaag	gccttactcctgggttttcc

Continued on next page

Table 7.1 – continued from previous page

Affymetrix ID	fw Primer	rev Primer
1422136_at	tgtggccacccttttatttgt	agagcatccagtgccagcta
1425140_at	acatggtgctggaaaaggag	aatagaaacggcccccatag
1416922_a_at	tgagaagcaggcttcgtttt	tgtaaggaatgacgccagtg
1451149_at	gcccttgtctccctacatca	gcagatgggagatgcaaaat
1448364_at	gcacctgtgtgaaagcagaa	ccatcaccacacagaattgc
1452444_at	ctctgcctcccagttcagtc	tgcgggattacaagtgttca
1420760_s_at	ggaacttgcttccctctcct	tgactcccaacgatcaagtg
1418709_at	aaaaccgtgtggcagagaag	tttgtccaagtcctccaagc
1416686_at	tctcaggggaagctcatgtc	aggaacaggctcaaaaacca
1451461_a_at	attgctgtacccgagaccac	gagtcagggctggagttcac
1452670_at	accctacaaggagggaccac	ggtgctgagacaactccaca
1423748_at	ggaaaacatgctttgccact	taaggatctgggctgaccac
1420664_s_at	agctcatatgacgccaaaca	cccccaagtctatggtctga
1436004_at	gatggatggatggatggaac	cttcctcaacagggctacca
1436195_at	ttatccaccaaccagcacaa	tggcctgtaaggctgttctt
1455403_at	tgtacctgaagatcattgtgga	tgcaattccagctgtgtttc
1433649_at	cactcttctcccctgtcaaag	agcacacaaagctcaagtgc
1435543_at	ccagggtttctttgcagcta	cctgggtttacagaagtcacg
1428774_at	ctgccagaagagcaaaggag	tctcagtgaagtcccaagca
1429146_at	tttcctttggccatgtcttt	agagagcctttccacagtgc
1441894_s_at	ctttctgccctcccctaaac	tccatcgtggatctcctctc
1440966_at	gttggcgttgctttgttttt	ggcttattaccgctgcatgt
1437414_at	gcaaggtgattgacaccatct	aatctgaaaggccccaaaat
1440739_at	gggaagaagttccaccatca	ccatggtcccacagagtctt
1435822_at	tctgccatacaaaggaatgaaa	gacccttgttcaacctttcc
1438310_at	tttgccattgaaatggacct	cattaacaaagccacccaaa
1434338_at	atttggatcgtggcagtagc	acagccctatcagccttcct
1434969_at	cgcaccgtctagttcatgttt	gatttgccgttgagaagctc
1446550_at	ggcactaaagcgacctgaag	cacgccattcagaaaaagtct
1458232_at	tggttggtgcttttgcctat	aatcacttgcttgggcattc
1437862_at	aacctggagggcagaagagt	cgagtggcaagctactgact
1436907_at	cagagctgggtgttccaact	gaggcagttggaatggaaga
1435033_at	ccccagtgcacttgtaacct	cccagctacagggaactgtc
1456930_at	tctgtgtcgatgtgggatgt	ttcaatgttgcctgaagcag
1432205_a_at	ctcctctggaccctcctctc	taccaggatggtcttgcaca
1455210_at	gctgaaatcttgccaaaagc	cctcagctggcttctcaact
1428517_at	ttggcttcattgctcatctg	tcacacttgcacgctacaca
1456661_at	acagcctgcatgaatcagtt	ggaagaatttgccacatggt
1428767_at	tgtctggtgcttgactctgg	ggattcttttcatcccagca
1453465_x_at	gacaaggccaggtgtgtttt	ggaaagcacaggtttattcca
1435483_x_at	ttgaaatttggggacaatgaa	acctgggagatctgaattgc
1419985_s_at	cccaatcccagatcatcagt	ggctagatgtggtgggacat
1435109_at	gtttgctgctttgacccatc	accttgcagaagccactctc
1432638_at	tgggaacctgtctgagatcc	gtccgacttcatgtccaggt
1434099_at	ccctttttgatggctgtacg	ctcactttccctcttcagca
1424698_s_at	aaacagaagccacaccatga	atgcaccgttgtttgaactg
1426155_a_at	ggcagaacttctagcgaagc	ggtttggaaggggggtagtgt
1426092_a_at	ctggaccctgggagtttaca	ctgtgccctcttcacagtca
1452565_x_at	tctgctgcaaacttggcata	tgaaggacaaagtcggtgtg
1419093_at	cagccgagtacagtgacagc	cctcctaatcgctcaccatc
1438083_at	gagtgaccagggcaggtatc	tgccaacatacatgctgagag
1417835_at	agtgtgtcaggggaaggatg	cagcaatcaccatgttggag
1438642_at	ttgagttttgcctcaacacg	gggatgtgaggtatggatgg
1427026_at	gagctgaagaaggagcagga	gcttacgaagacccttgacg
1458173_at	ctacgtgattctccaggaactt	cccaggattttccattcaag
1459882_at	accccatatcctctggctct	ctcctgtgcatcatcaccat
1438858_x_at	gggcaccatcttcatcattc	acagcctcagggtcaagaga
1457004_at	tccgatacccagcctacttg	atggaaaacgcaaacgagtc
1442146_at	agggcaggaggatcagaaat	gtgtgtgtgcttgtgtgtgc
1447139_at	cgtgtctccctgtgatgtgt	cgcagacgtgacttgtccta
1423603_at	agcagcctgtccacttcat	aagtgtcaagggtcctggtg
1421924_at	cctctgctaggtggagcttg	acctcacacctttccattgc
1416516_at	cctgccctgttggttgta	aggtgtctggagacgtggag
1419157_at	agcattggcatggagaaact	gctactcccagcacatctcc
1430584_s_at	atgtgaaaaggcagggtcac	cccatgaatgcttcaattcc
1456658_at	tgatcaccattggaaacgaa	cttctgcatcctgtcagcaa
1416239_at	tcgcagaggctcgtatacac	ctcatagtcgccctgcacgt
1424492_at	tgggcaacagactgacagag	ccatcaaggccatctcctaa
1417580_s_at	agcactggctcacgagcttc	cagagatgctgctctacaga
1423281_at	gaaccttccaacgtgctgat	taatgcagcaaccagctcac
1420376_a_at	tgaagaagcctcaccgctac	ggcgtggatggcacacagat
1417365_a_at	caacgaagtggatgctgatg	tccgtcgccatcaatatctg
1418626_a_at	gtgaagctgtttgactctga	acactcctacatataggaag
1460214_at	tgatatcgacatggatgcac	tattgagtgaggatgacttc
1416196_at	ctgctgctgagaaggctgtg	agctgctgaccaatcctcag

Quantitative real time PCR analysis (Applied Biosystems Sequence Detection System 9330, Rotkreuz, Switzerland) using SYBR Green (Qiagen) was performed according to manufacturer's instructions. Briefly, reactions consisted of 10μL of cDNA diluted

1:100 out of the primary RT-reaction, 0.5μM forward and reverse primer, 12.5μL of Sybr Green master mix and 2.25μL water. Default PCR conditions of 40 cycles of 15' seconds annealing at 60°C and 1 min denaturing at 95°C were utilized. All primers were assessed for efficiency using SybrGreen conditions prior to being utilized in qPCR studies. Gene expression levels were assessed in four biological replicate samples (and 4 technical replicates of each) from each group using the $\Delta\Delta$CT method and normalization to Gapdh. Standard deviations were calculated in between the biological replicates of mock and RML infected cells.

8. Results

8.1. In vitro cell culture models of prion infection

In view of the potential impact of the choice of the cell culture model onto the transcriptional response to prion infection, we opted to compare results obtained in three distinct cell lines. We used N2aPK1, CAD, and GT1 cells, which are all murine and of neuronal origin. Each of these cell lines can be infected to high rates with the mouse-adapted scrapie prion strain RML [17]; [96]; [104]; [61];(Mahal, pers. communication). GT1 cells have been reported to exhibit mild apoptosis and vacuolarization resembling the pathology in brains of prion infected animals [104]. Instead, prion infection seems to have no impact on cell viability or morphology in N2a or CAD cells (Mahal, pers. communication), although N2a cell subclones have been reported to be more sensitive to caspase-3 /-8 mediated apoptosis [63]. The following measures were taken to avoid the detection of potential clonal or stochastic artifacts. Firstly, prior to prion infection we split the respective parental cell line (N2aPK1, CAD, GT1) into eight batches. Four of these individual batches were infected with RML scrapie prions, and four were exposed to m̈ock(̈uninfected) brain homogenate. Secondly, we strived to minimize the period between establishment of prion infection (or mock infection) of cells and harvesting, since long periods of serial passaging could result in clonal segregation. We opted to use the cells at the earliest time point at which no residual inoculum is detected, but at which the cells show a high degree of infection as measured by Western blot for PrP^{Sc} (Figure 1a-c) and infection ratio as measured by ELISPOT assay (Figure 1d-f) [61]. After eight passages we determined that all cell cultures inoculated with RML showed proteinase K (PK) resistant PrP, whereas this was consistently absent in mock infected control cells (N2aPK1mock, CADmock and GT1mock). In addition, we determined the prevalence of infection within the cell cultures that were studied. We reasoned that the infection rate of the cell cultures would directly impact the sensitivity with which any transcriptional changes would be detected. Whereas the four investigated Scrapie infected N2aPK1 cultures (N2aPK1RML) showed infection ratios of 65-81% (Figure 1d), the GT1RML and CADRML cultures showed ratios close to 100% (Figure 1e-f). Numeric values over 100% represent statistical artifacts: originating from variations in the number of cells seeded in each well. In summary we generated three murine neuronal cell culture models validated for prion infection for a comparison of gene expression with mock infected control cells. Each measurement, therefore, consisted of four true biological replicates for the infected or mock-infected groups, rather than ´technical´ replicates that would result from the splitting of parental infected or mock infected parental lines at the time of harvesting.

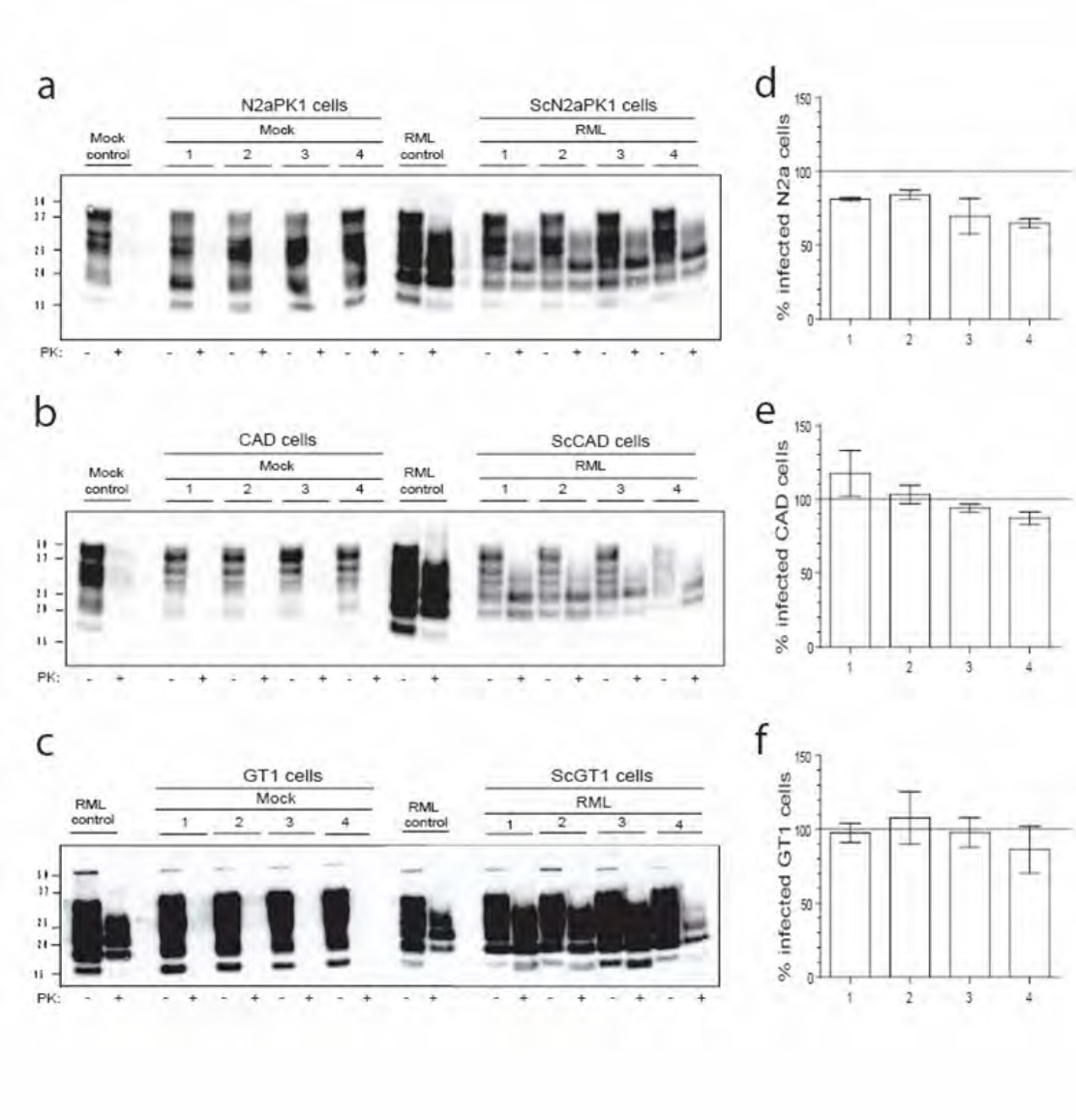

Figure 8.1.: Immunoblot analysis and quantitative infectivity assessment by ELISPOT assay

a) Western blot analysis for PrP^{C} and PrP^{Sc} of monoclonal anti-PrP (POM1) probed protein homogenate of four mock infected and four RML infected biological replicates of N2aPK1 cells are depicted with the respective controls. Proteinase K (PK) digestion visualizes protease resistant and consecutively shifted PrP^{Sc}. 70 mg of protein were loaded for PK+, 35 mg of protein for PK- samples.

b) and **c)** shows equivalent data from mock versus RML infected CAD and GT1 cells respectively.

d-e) The ratio of infected cells per biological replicate as assessed by ELISPOT assay. Data are presented as arithmetic means +/- standard deviation.

8.2. Transcriptional analysis of prion infected N2aPK1 (N2aPK1RML) versus control mock infected N2aPK1 (N2aPK1mock) cells

For the identification of differentially expressed genes as a response to prion infection, we compared the expression profiles of N2aPK1mock vs. N2aPK1RML cells. We utilized the two algorithms, GCRMA and MAS5.0, applying a fold change filter of 2.0 with an equal-variance t-test significance threshold of $p<0.05$. Since this did not result in significant differentially expressed genes, we relaxed the fold change filter conditions and identified a core set of 84 candidates to be differentially expressed more than 1.5 fold in at least one of the two algorithms. Although formally significant, a level of differential expression between 1.5 and 2.2 for 62 out of the 84 candidate genes is indicative of potentially false positives. 22 candidate genes showed differential expression higher than 2.2 fold in at least one of the two algorithms applied. The strongest downregulation of gene expression was observed for *Gca* (grancalcin; 12.7 fold) whereas *Asf1* (anti-silencing function 1 homolog A) was the gene with the strongest upregulation (10.6 fold) as a response to prion infection (Table 1).

Table 8.1.: Candidate genes found in GCRMA and MAS5 algorithms based on RNA microarray chip analysis. M = Mock, R=RML.

Affymetrix ID	Gene name	M/R GCRMA	Stdev	M/R MAS5	Stdev	Gene Id	Cand. identified (X)
1415834_at	dual specificity phosphatase 6	1.601	0.212	1.737	0.47		X
1416147_at	heat shock protein 4	0.665	0.197	0.796	0.291		X
1416196_at	laminin receptor	0.983	0.533	1.414	2.586	lamR	
1416239_at	Argininosuccinate synthetase 1	1.204	0.236	1.402	0.345	ass1	
1416516_at	Fascin homolog 1	0.656	0.674	0.666	0.656	fscn1	X
1416686_at	procollagen lysine, 2-oxoglutarate 5-dioxygenase 2	0.539	0.207	0.683	0.285	plod1	X
1416759_at	NEDD9 interacting protein with calponin homology and LIM domains	2.052	0.461	1.431	0.308		X
1416922_a_at	BCL2/adenovirus E1B 19kDa-interacting protein 3-like	0.621	0.214	0.671	0.301		X
1417365_a_at	calmodulin 1	0.989	0.199	1.171	0.28	calm1	
1417580_s_at	Selenium-binding protein 2	0.824	0.497	0.816	0.347	selenbp2	
1417835_at	murinoglobulin 1	0.987	0.794	7.85	13.518		X
1417976_at	adenosine deaminase	1.585	0.267	1.439	0.346	ada	X
1418175_at	vitamin D receptor	1.634	0.233	1.713	0.388		X
1418539_a_at	protein tyrosine phosphatase, receptor type, E	1.86	0.375	1.411	0.337		X
1418626_a_at	clusterin	1.237	0.229	1.47	0.393	clu	
1418709_at	cytochrome c oxidase, subunit VIIa 1	0.543	0.228	0.556	0.29	cox7a	X
1418835_at	pleckstrin homology-like domain, family A, member 1	1.626	0.214	1.735	0.313		X
1419093_at	tryptophan 2,3-dioxygenase	0.969	1.463	0.15	0.822		X
1419157_at	SRY box containing 4	0.662	0.707	0.645	0.666	sox4	X
1419985_s_at	DNA segment, Chr 11, ERATO Doi 461, expressed	1.884	0.383	0.373	0.183		X
1420376_a_at	histone family 3 B	0.897	0.189	0.906	0.285	hf3B	
1420664_s_at	protein C receptor, endothelial	1.654	0.228	2.178	0.504		X
1420737_at	polyamine modulated factor 1 binding protein 1	1.501	0.221	1.291	0.308		X
1420760_s_at	N-myc downstream regulated 1	0.553	0.208	0.637	0.293	ndrg1	X
1421924_at	Solute carrier family 2	0.479	0.526	0.506	0.522	slc2a2	X
1422136_at	kinase interacting with leukemia-associated gene (stathmin)	0.642	0.216	0.818	0.295		X
1423281_at	Stathmin-like 2	1.054	0.202	1.249	0.342	stmn2	
1423603_at	Zinc finger protein, multitype 1	0.969	0.852	0.941	0.777	zfpm1	X
1423748_at	RIKEN cDNA D530020C15 gene	0.472	0.263	0.481	0.301		X
1423946_at	PDZ and LIM domain 2	1.714	0.299	1.379	0.294		X

Continued on next page

Table 8.1 – continued from previous page

Affymetrix ID	Gene name	M/R GCRMA	Stdev	M/R MAS5	Stdev	Gene Id	Cand. identified (X)
1424492_at	Transient receptor potential cation channel,subfamily C, member 2	1.074	0.191	1.139	0.297	trpc2	
1424698_s_at	grancalcin	0.964	0.639	0.079	1.693		X
1425140_at	lactamase, beta 2	0.632	0.19	0.778	0.287		X
1426092_a_at	tripartite motif protein 34	0.964	0.622	0.098	1.386		X
1426155_a_at	odd-skipped related 2 (Drosophila)	0.96	0.893	0.125	1.21		X
1427026_at	myosin, heavy polypeptide 4, skeletal muscle	0.953	0.624	7.06	12.24		X
1428517_at	WD repeat and FYVE domain containing 3	1.503	0.215	0.668	0.107		X
1428767_at	RIKEN cDNA 1810036L03 gene	1.327	0.209	0.544	0.069		X
1428774_at	12 days embryo male wolffian duct includes surrounding region cDNA, RIKEN full-length enriched library, clone:6720429C22 product:unknown EST, full insert sequence	1.786	0.443	0.882	0.061		X
1429146_at	Adult male testis cDNA, RIKEN full-length enriched library, clone:4931406B08 product:unknown EST, full insert sequence	1.72	0.333	0.682	0.278		X
1430584_s_at	Carbonic anhydrase 3	0.96	0.276	0.499	0.572	car3	X
1432205_a_at	RIKEN cDNA C130038G02 gene	1.526	0.299	0.75	0.235		X
1432638_at	RIKEN cDNA 2810002N01 gene	0.981	3.143	0.241	0.291		X
1433649_at	amine oxidase, flavin containing 1	1.8	0.296	0.709	0.248		X
1433855_at	Transcribed sequence with strong similarity to protein ref:NP_065580.1 (M.musculus) hypothetical protein, I54 (Mus musculus)	1.642	0.276	2.949	1.238		X
1434099_at	RIKEN cDNA A830037N07 gene	0.951	0.451	0.111	3.238		X
1434338_at	18-day embryo whole body cDNA, RIKEN full-length enriched library, clone:1110029E03 product:unknown EST, full insert sequence	1.612	0.284	0.776	0.151		X
1434969_at	CDNA clone IMAGE:5683160, partial cds	1.6	0.246	0.653	0.191	RcDNA	X
1435033_at	RIKEN cDNA 9330140K16 gene	1.54	0.288	0.906	0.185		X
1435109_at	RIKEN cDNA 3010001K23 gene	1.253	0.287	0.188	0.301		X
1435483_x_at	mitochondrial folate transporter/carrier	1.756	0.352	0.53	0.134		X
1435543_at	adenomatosis polyposis coli	1.767	0.34	0.799	0.068	apc	X
1435822_at	16 days neonate heart cDNA, RIKEN full-length enriched library, clone:D830012I24 product:unknown EST, full insert sequence	1.642	0.327	0.584	0.187		X
1436004_at	ubiquitin specific protease 27, X chromosome	2.219	0.513	0.791	0.107		X
1436195_at	cDNA sequence BC046404	1.979	0.44	0.75	0.132		X
1436448_a_at	prostaglandin-endoperoxide synthase 1	2.003	0.337	2.386	0.693	ptgs1	X
1436907_at	neuron navigator 1	1.558	0.226	0.707	0.149	nav1	X
1437414_at	RIKEN cDNA 4933431C08 gene	1.692	0.286	0.63	0.231		X
1437862_at	RIKEN cDNA 2610015J01 gene	1.555	0.333	0.827	0.121		X
1438083_at	Hedgehog-interacting protein	0.995	0.543	7.458	18.137		X
1438310_at	10 days neonate cerebellum cDNA, RIKEN full-length enriched library, clone:B930095L19 product:unknown EST, full insert sequence	1.651	0.356	0.776	0.18		X

Continued on next page

Table 8.1 – continued from previous page

Affymetrix ID	Gene name	M/R GCRMA	Stdev	M/R MAS5	Stdev	Gene Id	Cand. identified (X)
1438642_at	AV278176 RIKEN full-length enriched, adult male testis (DH10B) Mus musculus cDNA clone 4933400E08 3', mRNA sequence.	1.031	0.31	6.987	24.796		X
1438858_x_at	histocompatibility 2, class II antigen A, alpha	0.94	0.477	5.011	1.945		X
1440739_at	vascular endothelial growth factor C	1.688	0.334	0.592	0.212		X
1440966_at	axotrophin	1.689	0.416	0.653	0.085	axot	X
1441894_s_at	BB071890 RIKEN full-length enriched, 15 days embryo male testis Mus musculus cDNA clone 8030499N14 3' similar to AF236099 Mus musculus GRP1-associated scaffold protein GRASP mRNA, mRNA sequence.	1.694	0.346	0.829	0.197		X
1442146_at	H3079F10-3 NIA Mouse 15K cDNA Clone Set Mus musculus cDNA clone H3079F10 3', mRNA sequence.	1.029	0.32	4.126	1.004	cDNAc	X
1446550_at	G1 to phase transition 1	1.601	0.254	0.888	0.33		X
1447139_at	B-cell CLL/lymphoma 7C	1.195	0.286	0.232	0.126		X
1448364_at	cyclin G2	0.592	0.243	0.762	0.324	ccng2	X
1448623_at	RIKEN cDNA 2310075C12 gene	0.65	0.185	0.743	0.309		X
1449275_at	RIKEN cDNA 2310038H17 gene	0.649	0.228	0.77	0.278		X
1450459_at	RIKEN cDNA 2010106G01 gene	0.658	0.219	0.869	0.292		X
1451110_at	EGL nine homolog 1 (C. elegans)	0.662	0.224	0.614	0.309		X
1451149_at	phosphoglucomutase 2	0.6	0.204	0.714	0.314		X
1451385_at	RIKEN cDNA 2310056P07 gene	0.649	0.193	0.74	0.296		X
1451386_at	biliverdin reductase B (flavin reductase (NADPH))	1.549	0.206	1.75	0.416		X
1451461_a_at	aldolase 3, C isoform	0.527	0.246	0.625	0.349		X
1452444_at	N-ethylmaleimide sensitive fusion protein attachment protein beta	0.583	0.225	0.696	0.287		X
1452565_x_at	envelope polyprotein; Mouse endogenous mammary tumor virus (MMTV) RNA, env gene and right LTR.	0.953	0.997	0.116	1.103		X
1452670_at	myosin, light polypeptide 9, regulatory	0.403	0.266	0.494	0.304		X
1453465_x_at	RIKEN cDNA 4930402H24 gene	1.528	0.273	0.415	0.306		X
1455099_at	BB414982 RIKEN full-length enriched, 7 days embryo Mus musculus cDNA clone C430040E04 3', mRNA sequence.	1.624	0.214	1.101	0.297		X
1455210_at	zinc fingers and homeoboxes protein 2	1.499	0.268	0.885	0.136		X
1455403_at	RIKEN cDNA 4932703L02 gene	1.841	0.386	0.658	0.175		X
1456658_at	Actin, alpha 2, smooth muscle, aorta,	0.957	1.289	1.192	0.649	acta2	X
1456661_at	Transcribed sequence with moderate similarity to protein pdb:1JZ5 (E. coli) B Chain B, E. Coli	1.836	0.303	0.515	0.262		X
1456930_at	hypothetical protein 9530003A05	1.521	0.239	0.703	0.073		X
1457004_at	BB698378 RIKEN full-length enriched, 2 days neonate sympathetic ganglion Mus musculus cDNA clone 7120499J15 3', mRNA sequence.	0.937	0.325	4.632	0.298		X
1458173_at	Transcribed sequence with moderate similarity to protein pir:S12207 (M.musculus) S12207 hypothetical protein	1.011	0.876	8.674	28.737		X
1458232_at	dickkopf homolog 1 (Xenopus laevis)	1.558	0.243	0.581	0.209		X

Continued on next page

Table 8.1 – continued from previous page

Affymetrix ID	Gene name	M/R GCRMA	Stdev	M/R MAS5	Stdev	Gene Id	Cand. identified (X)
1459882_at	ASF1 anti-silencing function 1 homolog A (S. cerevisiae)	1.069	0.323	10.582	14.669	asf1	X
1460214_at	Purkinje cell protein 4	0.991	0.206	1.074	0.4	pcp4	

19 candidate genes including *Gca* and *Asf1* out of these 22 were not differentially regulated in the other algorithm. Therefore in a first instance to allow assessment of all 84 candidates we pooled cDNA from four independent biological replicates of N2aPK1mock and N2aPK1RML cells. This pooled cDNA was used to assess gene expression levels by quantitative real time PCR (qPCR) using technical triplicates. 70 of these candidate genes showed no differential expression between N2aPK1mock and N2aPK1RML. A total of 14 candidates showed statistically significant, but less than 5 fold up- or downregulation in the prescreen qPCR analysis. The expression ratios for these as determined by the MAS5.0 and GCRMA algorithms are shown in Figures 2a and 2b respectively. The expression levels of these 14 transcripts in N2aPK1RML cells were analyzed by qPCR, utilizing cDNAs synthesized from RNA obtained from quadruplicate independent biological replicates and three technical replicates of each were analyzed (Figure 2c). Of these 14 candidates, we were only able to confirm statistically significant ($p<0.0005$) downregulation of the Nav1 transcript of less than 1.8 fold in response to prion infection in N2aPK1 cells. We were not able to confirm differential expression of any of the remainder of the potential candidate genes identified in our high-density oligonucleotide microarrays of N2aPK1mock compared to N2aPK1RML cells.

8.3. Analyses of candidate gene expression in prion infected CAD (CADRML) cells.

The expression levels of the 14 candidate genes were also assessed in the CAD cell culture model of prion infection. Again, we could not detect differentially expressed genes as a response to prion infection (Figure 2d). In particular, we could not observe downregulation of *Nav1* in the CADRML cells. Whilst this may certainly be of biological significance relevant to N2aPK1 cells, differential expression of this gene is not a feature common to prion infected neuronal cells in vitro.

8.4. qPCR analyses of candidate differentially expressed genes in N2aPK1RML and GT1RML cell culture models reported by others.

Statistically significant and profound differential expression of several candidate genes has been recently reported [42] as a direct result of prion infection in N2aPK1 and GT1 cell culture models. The expression ratios for nine of those which showed highest levels of differential expression from that study were chosen for validation in our models. This is in stark contrast to the expression ratios determined by MAS5.0 and GCRMA algorithms in our transcriptional profiling analyses of N2aPK1RML and N2aPK1mock cells (Fig. 3a-b). In the latter study, the genes encoding Selenium binding protein 2

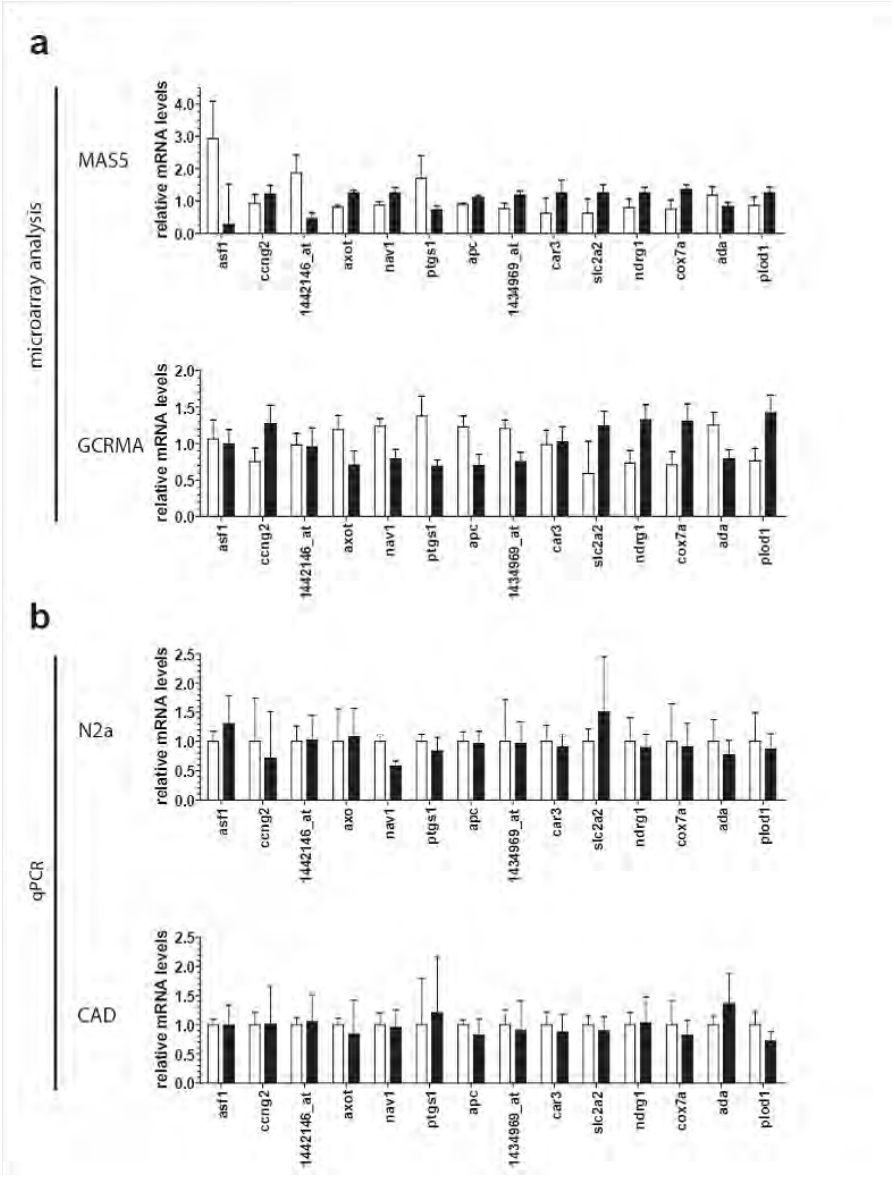

Figure 8.2.: Gene expression analysis of mock versus RML infected N2aPK1 cells.

a) High-density oligonucleotide chip analysis of mock (white bars) vs. RML (black bars) infected N2aPK1 cells as analyzed with MAS5.0 or GCRMA data analysis algorithm. Candidate transcripts originating from one of the two analysis algorithms were later subjected to quantitative real time PCR-analysis (qPCR; see also table 1).

b) Verification of microarray data with qPCR in mock (white bars) versus RML (black bars) infected N2aPK1 cells and expression analysis of candidate genes in mock versus RML infected CAD cells normalized to *Gapdh*. The qPCR-analysis was performed in four biological replicates of each mock and RML infected cell line and three technical replicates per biological replicate. The average of four mock biological replicates was set as one. Data are presented as arithmetic means +/- standard deviation.

(*Selenbp*2), Argininosuccinate synthetase 1 (*Ass*1) and Clusterin (*Clu*) were reported to be profoundly over-expressed in prion infected cell lines; in the case of *Ass*1 up to 40-fold in N2aPK1RML and GT1RML cells, whereas Histone family 3b (*Hf3b*), Calmodulin 1 (*Calm1*) and Purkinje cell protein 4 (*Pcp4*) were reported to be downregulated as a response to prion infection (2-fold, 2-fold, and 5-fold respectively). However, in our own analyses of prion infected neuronal cells, we were unable to validate these findings, neither in the MAS5.0 or GCRMA interrogated microarray data (Figure 3a & b) or by qPCR analyses of our own prion infected N2aPK1RML or GT1RML cell culture models (Figure 3 c & d respectively). Whilst our qPCR studies were performed using *Gapdh* as the housekeeping gene for normalization of expression levels, Greenwood et al. used *Polr2a* (RNA Polymerase II) and *Tbp* (TATA box binding protein) for normalization. Whilst unlikely to account for the discrepancies between these studies, to formally exclude this possibility we investigated the expression levels of *Polr2a* and *Tbp* relative to *Gapdh* in mock and prion infected N2aPK1, CAD and GT1 cell culture models (Suppl. Fig. 1). As expected, the expression levels of these relative to *Gapdh* are not altered in prion infected cells, thereby confirming that using these genes as normalization controls in our study would not alter the conclusions from our data.

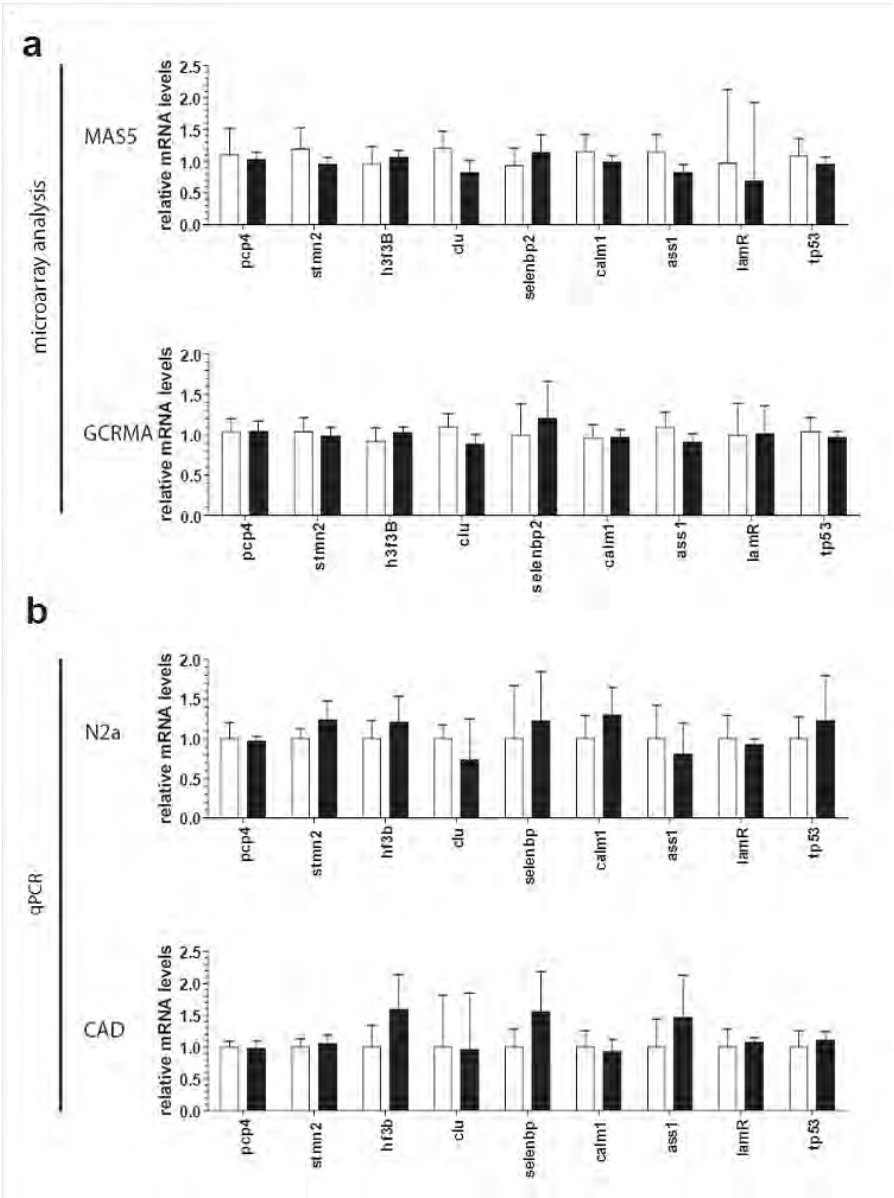

Figure 8.3.: qPCR analysis reported by others

a) High-density oligonucleotide chip analysis of mock (white bars) vs. RML (black bars) infected N2aPK1 cells as analyzed with MAS5.0 or GCRMA data analysis algorithm.

b) Results of qPCR analysis of mock (white bars) versus RML (black bars) infected N2aPK1 or GT1 cells. Relative gene expression levels of published transcripts in N2aPK1 and N2aPK1RML or GT1 compared to GT1RML cells normalized to Gapdh. Analysis was performed in four biological replicates of each mock and RML infected cell line and three technical replicates per biological replicate. The average of four mock biological replicates was set as one. Data are presented as arithmetic means and standard deviations.

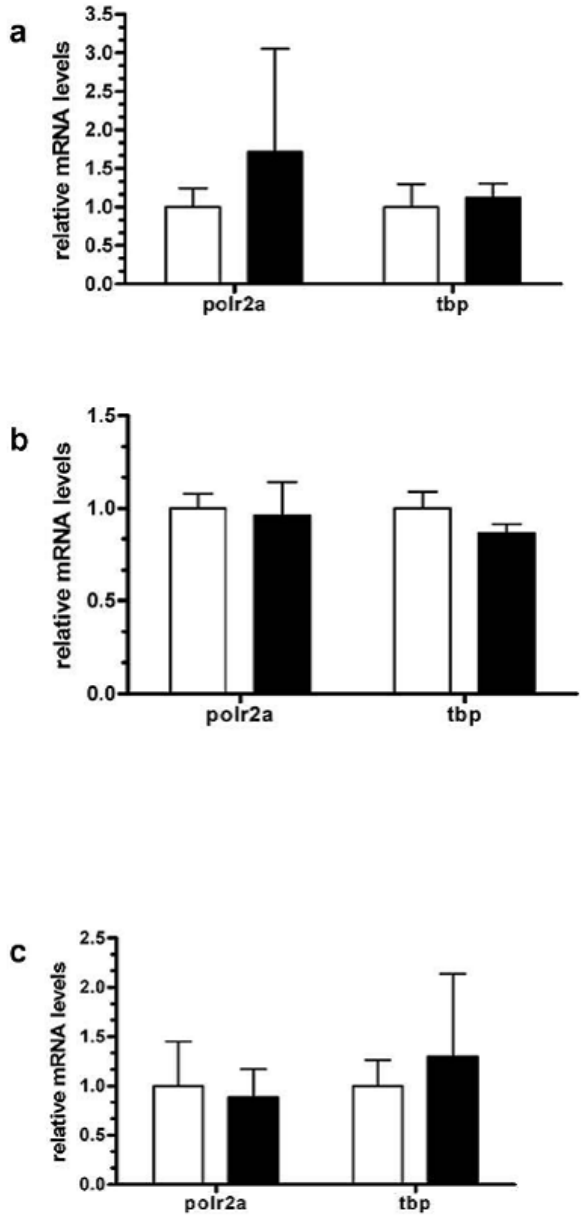

Figure 8.4.: House keeping genes to control for relative cDNA abundance
a-c) expression analysis of housekeeping genes in mock (white bars) versus RML (black bars) infected cells.
The graph shows relative gene expression normalized to *Gapdh* for a) N2aPK1 cells, b) CAD cells and c) GT1 cells. Analysis was performed in four biological replicates of each mock and RML infected cell line and three technical replicates per biological replicate. The average of four mock biological replicates was defined as one. Data are presented as arithmetic means and standard deviations.

9. Discussion

Prion infection does not induce general changes in RNA profiles of cells in vitro.

Here we have investigated the impact of prion infection on the transcriptome of chronically infected N2aPK1RML cells, together with targeted assessment of previously reported differentially expressed candidate genes in three independent neuronal cell culture systems infected with the mouse adapted scrapie strain RML. Despite high concentrations of PrP^{Sc} as assessed by Western blot and infection ratios of 65 to nearly 100% as confirmed by colony spot immunochemistry, we were unable to identify differences in gene expression between prion and mock infected cells that hold true for the three cell lines investigated and therefore represent global responses to prion infection. The only modest but statistically significant changes in expression were identified for the *Nav1* transcript in response to prion infection. The neuron navigator 1 protein is a microtubule-associated protein involved in neuronal migration. However, we could not observe downregulation of *Nav1* in the CADRML cells. Therefore we assume, despite a possible biological significance in N2aPK1 cells, differential expression of *Nav1* is not a feature common to prion infected neuronal cells in vitro. In particular, our investigations of expression levels of previously reported candidate genes [42] revealed that none of these were differentially expressed in any of the cell culture models of in vitro prion infection utilized here. This discrepancy may result from differences in the experimental design of the various studies.

The impact of the cell culture model in studying the transcriptional response of cells to prion infection

The previous studies on the impact of prion infection on gene expression levels had compared subclones or separately passaged prion and uninfected control cells. These cells have been passaged over long periods or subcloning procedures have been performed prior to eventual biological comparisons. Immortalized cells can exhibit alterations in chromosomal composition, leading to profound heterogeneity of gene expression independently of prion infection, with gross differences in morphology or physiology of the cells [24]; [42]. Whereas this issue of clonal segregation of cells is discussed extensively by Doh-ura et al., with reference to the candidate gene subset presented in their study, subsequent publications describing differences in viability, apoptosis, iron regulation or gene expression profiling appear to have neglected this alternative explanation for their findings [104]; [82];[47]; [27]; [28]; [42]. The experiments reported here were designed with the specific goal of avoiding these potential pitfalls. At the beginning of the experiment we split the respective parental cell line (N2aPK1, CAD, GT1) into eight batches and independently infected four of these with RML and four with a mock brain homogenate. This strategy was devised to generate true biological replicates, rather than mere technical replicates as would be the case when parental cell lines are passaged and then split into

groups for comparison. Furthermore, we opted to use the cells at the earliest time point possible, the point at which no residual inoculum is detected, but at which the cells show a high degree of infection as measured by Western blot for PrP^{Sc} and infection ratio as measured by colony spot immunochemistry [61]. This procedure differs from prior studies in that of utilizing a more appropriate biological control; mock infection with healthy brain homogenate rather than uninfected cells, and importantly minimizing the possible clonal segregation of cells of the same parental origin. Our transcriptional profiling data contradict the study by Greenwood et al. [42]. Possibly those results obtained with GT1 and N2a cells may be due to clonal differences. It is striking that the overlap of differentially expressed genes in GT1 and N2a cells as a response to prion infection in that study is restricted to three genes (*Selenbp2*, *Tmsb4x*, *H1F0*), whereas the expression level of one (*H1F0*) is altered in an opposite manner. Furthermore, curing of ScN2a cells by pentosan polysulphate in the Greenwood study did not restore gene expression levels for all differentially expressed transcripts to the level of uninfected cells, which is a further hint of these results being due to clonal variations rather than to prion infection. In conclusion Greenwood et al. describe *Selenbp2* as the only "true" differentially expressed gene in N2a and GT1 cells as a response to prion infection. The reason why we did not identify this candidate in our array study, or were able to confirm differential expression by qRT-PCR in three independent cell lines, could be due to the N2a cells used in the Greenwood study. They overexpress 3F4-tagged murine PrP in addition to endogenous murine wild type PrP and have been generated by stable selection using Zeocine. We are not able to assess the impact on these varieties to the observed differences between our and their studies. What evidence do we have to expect a transcriptional response to prion infection in cells in vitro? By using this experimental design we did not find any statistically significant and convincing differentially expressed gene as a response to prion infection in our microarray approach, using a combination of statistical procedures. Considering previous similar studies by others this was puzzling and also counterintuitive. But what reasons do we really have to expect changes in gene expression provoked by prion infection of neuronal cells? There is no evidence for impaired viability, morphology or physiology in most neuronal cell lines chronically infected with prions under "normal" cell culture conditions [103]; [17]. Also, more recent studies show differences between prion infected and uninfected GT1 cells only after challenge with BOS, a gamma-glutamylcysteine synthetase inhibitor leading to reactive oxygen species induced stress [82], Lactacystin [63] or "in many but not all experiments" [104]. Furthermore Hetz et al., report that Caspase-12 and endoplasmatic reticulum stress mediate neurotoxicity of pathological prion protein [47]. Here again, no differences in viability between ScN2a and N2a cells are observed under normal cell culture conditions in the absence of stressor. In conclusion many studies have shown that prion infected and uninfected cells do not differ in viability under normal culture conditions. It may be surprising to find no alterations in the transcriptional expression profile of cells after challenge with prions as a response to misfolded and aggregated protein in the cell. On the other hand it is very well possible that cells deal with prion infection by post-transcriptional or post-translational mechanisms which do not lead to differences in gene expression profiles. Similar studies in yeast also revealed no transcriptional changes after prion infection [102]. Lastly, it

is conceivable that prion infection in cells in vitro has an entirely benign effect. In conclusion, we propose that prion infection does not alter the mRNA profile of neuronal cells in vitro. We conclude therefore that prion agents in cultured neuronal cells infected at high rates do not induce general or specific changes in the transcriptome. Taking into account that prions represent a unique form of transmissible pathogen that seems to consist of endogenous host protein only, it is conceivable that none of the cellular responses found in virus or bacteria infected cells can be observed in prion infected cells.

A. List of figures

Figure 1.1.	Histologic features of prion diseases.	17
Figure 1.2.	Hypothetical models of conversion from PrP^{C} to PrP^{Sc}	19
Figure 1.3.	History of humanized mice.	23
Figure 1.4.	Experimental plan.	26
Figure 2.1.	Structure and, if applicable, functions of the deleted proteins.	38
Figure 2.2.	Overview of genetically modified null mice used in this study.	39
Figure 3.1.	Breeding strategy.	42
Figure 3.2.	Alternative breeding strategy.	43
Figure 3.3.	Agarose Gel with specifc PCR products.	44
Figure 3.4.	Readout of a STR mapping experiment.	49
Figure 3.5.	Calibration strains for STR typing.	50
Figure 3.6.	Backcrossed strains	51
Figure 3.7.	Flow cytometric analysis of enriched CD34+ stem cells.	53
Figure 3.8.	Reconstitution of immunodeficient mice with mouse bone marrow.	54
Figure 3.9.	Prnp-dependent reconstitutability.	56
Figure 3.10.	Flowcytometric analysis of engrafted cells in bone marrow 12 weeks after transplantation.	58
Figure 3.11.	Histology of engrafted mice and flowcytomtric readout in peripheral blood.	59
Figure 3.12.	Detailed PrP expression analysis in bone marrow subpopulations.	61
Figure 3.13.	Additional STRs and SNPs between *Rag* and *Prnp*.	64
Figure 3.14.	SNP analysis of backcrossed and reconstituted mice.	65
Figure 3.15.	Comparison of *Sirpa* polymorphisms and *Prnp*-allelotype and its correlation to reconstitution outcome.	67
Figure 3.16.	*Sirpa* meiotic recombination breedings and subsequent reconstitutions.	68
Figure 7.1.	Infection and cell splitting protocol of neuronal cell lines.	84
Figure 8.1.	Immunoblot analysis and quantitative infectivity assessment.	90
Figure 8.2.	Gene expression analysis of mock versus RML infected N2aPK1 cells.	95
Figure 8.3.	qPCR analysis reported by others.	97
Figure 8.4.	House keeping genes to control for relative cDNA abundance.	98

B. List of tables

Table 2.1.	Genotyping PCR primers	30
Table 2.2.	Primer sequences for STR analysis (based on UniSTS)	31
Table 2.3.	SNP assays for mapping the region between *Rag* and *Prnp*	34
Table 3.1.	Experimentally determined allele lenghts	45
Table 3.2.	Genes between *Rag* and *Prnp* with a putative immune function	63
Table 7.1.	Primers designed for quantitative real time PCR reactions	86
Table 8.1.	Candidate genes found in GCRMA and MAS5 algorithms	91

C. Abbreviations

AA	amino acid
bp	base pair
BM	bone marrow
BSA	bovine serum albumin
CD	cluster of differentation (for surface antigens)
cDNA	complementary DNA
CJD	Creutzfeldt-Jakob disease
CNS	central nervous system
CSF	cerebrospinal fluid
CT	threshold cycle
Ctrl	control
CWD	chronic wasting disease
DC	dendritic cell
DNA	deoxyribonucleic acid
dpi	days post inoculation
ECL	enhanced chemiluminescence
EDTA	ethylendiamintetraacetic acid
FDC	follicular dendritic cell
FFI	fatal familial insomnia
GALT	gut associated lymphoid tissue
GAPDH	glyceralaldehyde 3-phospate deghydogenase
GFAP	glial acidic fibrilarry protein
GPI	glycosylphosphatidylinositol
GSS	Gerstmann-Sträussler-Scheinker syndrome
H&E	hematoxylin and eosin
HRP	horseradish peroxidase
IHC	immunohistochemistry
IL	interleukin
Il2rg	gene ID for "interleukin receptor 2, common gamma chain" (γc)
ip	intraperitoneal
kD	kilo dalton
LRS	lymphoreticular system
M	molar
Mb	megabases
MRI	magnetic resonance imaging
mRNA	messenger RNA
NK cell	natural killer cell
ORF	open reading frame

PAGE	polyacrylamid gel electrophoresis
PBS	phosphate-buffered saline
PCR	polymerase chain reaction
PK	proteinase K
Prnp	gene ID for the "mouse prion protein"
PRNP	gene ID for the "human prion protein"
PrP^{C}	the cellular prion protein (normal isoform)
PrP^{Sc}	the pathological prion protein (Sc = Scrapie)
Rag	gene ID for "recombination activating gene"
RML	Rocky mountain laboratory (prion strain)
RNA	ribonucleic acid
RT	room temperature
RT-PCR	reverse transcription PCR
SAF84	antibody used to visualize PrP^{Sc} in IHC
SCA	scrapie cell assay
sCJD	sporadic CJD
SDS	sodium dodecyl sulfate
Sirpa	gene ID for "signal regulatory protein alpha"
SNP	single nucleotide polymorphism
STR	short tandem repeat (repetitive non coding DNA)
TSE	transmissible spongiform encephalopathies
TF	target fraction
NTF	nontarget fraction
U	unit
vCJD	variant CJD
wt	wild-type
w/v	weight/volume
-	negative for
+	positive for

D. Curriculum vitae Gregor Andrea Hutter

Home address
Dr. med. Gregor Hutter, MD
Webergasse 29
CH-4058 Basel
Tel 079 353 8771
Email GregorHutter@access.uzh.ch

Current Work address
Neurochirurgische Klinik
Universitätsspital Basel
Spitalstrasse 21
CH-4000 Basel
Phone 061 328 71 72

Email hutterg@uhbs.ch

CV details

23.05.1978	Born in Uznach SG
1985-1991	Primary Schools in Goldach und Rorschach SG
1991-1998	Secondary and High School in Rorschach, Mörschwil and St. Gallen
January 1998	Matura Type B
October 1998	Start of medical school, University of Zurich
1999-2001	Medical pre-diplomas and first part of final exam
2002/3	Experimental work at the lab of Prof. Dr. Adriano Aguzzi Medical elective year in pathology/neuropathology, internal medicine, neurosurgery, pediatrics, gynecology/obstetrics, general surgery (Solomon Islands) and neurooncology (Boston, Massachusetts General Hospital)
January 2004	Pre-diploma in molecular biology (Prof. W. Schaffner/M.O. Hengartner) and informatics (Prof. Stucki/Schauer)
Oct. 2004	Final medical diploma, University of Zurich Medical School
Oct. 2004	USMLE Step 1 and 2
Oct. 2004 to Jan.2005	Swiss Army medical services
Jan. 05 to Dec. 07	PhD-project in the group of Prof. A. Aguzzi
From Jan. 2008	Neurosurgery residency, University Hospital Basel

Publications

Biol Chem 2003 Sep;384(9):1279-85.
No superoxide dismutase activity of cellular prion protein in vivo.
Hutter G[1], Heppner FL, Aguzzi A.

Acta Neuropathol (Berl). 2006 Jan;111(1):56-9. Epub 2005 Nov 23.
Abdominal seeding of an atypical teratoid/rhabdoid tumor of the pineal gland along a ventriculoperitoneal shunt catheter.
Ingold B, Moschopulos M, **Hutter G**, Seeger H, Rothlisberger B, Landolt H, Yonekawa Y, Jochum W, Heppner FL.

J Mol Biol 2007 Nov 12; Epub ahead of print
Transcriptional Stability of Cultured Cells upon Prion Infection.
Hutter G[2], Julius C, Wagner U, Seeger H, Kana V, Kranich J, Klöhn P, Weissmann C, Miele G, Aguzzi A.

Publications, accepted

Proc Natl Acad Sci U S A
A critical protective role for heat shock factor 1 in prion pathogenesis.
Andrew Steele, **Gregor Hutter**, Walker Jackson, Frank Heppner, Andrew Borkowski, Oliver King, Gregory Raymond, Adriano Aguzzi, Susan Lindquist

Grants

MD−PhD−grant of the Swiss National Science Foundation (http://www.snf.ch) for three years since January 2005 (CHF 150'000).

Accepted in the Molecular Life Science Graduate School, ETH and University of Zurich (www.lifesciencezurich.ch).

Member of the Swiss Study Foundation since 1998 (http://www.studienstiftung.ch).

[1] first author
[2] shared first-author with C. Julius

Attended summer schools and conferences

EMBO course/Eumorphia "Mouse Models of Human Disease" September 2005, Strassbourg, France.

ENII-MUGEN Immunology Summer School for advanced PhD students and Postdocs, Mai 2006, Alghero, Italy.

Conference of the Swiss Society of Neuropathology, March 2006, St. Moritz, Switzerland.

Languages

German (mother tongue), French, English, Italian

E. Acknowledgments

First, I would like to thank Adriano Aguzzi for his support and guidance over the last five years throughout my MD-PhD studies, the opportunity to visit exciting summer schools abroad and his enormous generosity in supporting my experimental aims conducted in these projects.

I am very grateful to Adrian Merlo for helping me to manage the challenging combination of clinical medicine and basic research as well as for investing time and effort in writing the second expert opinion on this work ("Zweitgutachten").

Furthermore, I am indebted to Burkhard Becher, Lukas Sommer, Roland Zimmermann and Roberto Speck for their assistance as members of my Ph.D. committee.

I especially would like to thank Knud Nairz for his support in genetics, STR analysis, ski-touring and long and fruitful discussions.

I am very thankful to Cristobàl Tostado who joined in as a "freshmen" and developed very thourough near-roboted pipetting and computer skills.

I am thankful to Rita Moos for her wisdom and experience in the lab.

I would like to thank Rowayda Peters for initiating the cord blood expansion project, her cell-culture differentiating skills and many funny discussions.

Furthermore I would like to thank:

Mirzet Delic, Urs Egli, Walter Ettlin, and Christine Sturzenegger for taking care of the animals and their enormous help in handling, weaning and cleaning and reporting.
Konstantin Dedes, Gero Drack and the crew of the obstetrics departments in Zurich and St. Gallen for providing us with liters of human umbilical cord blood.
Christian Julius and Gino Miele for initiation/collaboration in the RNA profiling project.
Jan Kranich and Veronika Kana and Ulrich Wagner for their help in the RNA profiling project.
Mathias Heikenwälder and Johannes Haybäck for the collaboration in the cord blood project.
Claire Bridel and Jose Barros de Oliviera Martins for various support and scientific as well as not-so-scientific discussions inside and outside of the lab.

The consultant neuropathologists Frank Heppner, Markus Tolnay, Dov Soffer and Michel Mittelbronn, and the medical residents Ekkehard Hewer, Stefan Prokop, Matthias Matter and Felix Geser and various coworkers from the institute of Clinical Pathology for support and discussions from the neuropathological and more clinical viewpoint.
Petra Schwarz for her enormous efforts in keeping the lab and everything in shape.
Marianne König for excellent assistance in preparing histological slices as well as the people from the "Labor für Spezialtechniken", Silvia Behnke and André Fitsche for immunohistochemical stainings.
Norbert Wey for support in informatics and image analyis, Dieter Zimmermann and his crew for sequencing.
Roland Kaelin and Katrin Kuehnle for scientific advice and discussions.
Andrew Steele from MIT, Boston, for various collaborations, input and cultural exchange.

The neurolab people Nike Kräutler, Frank Baumann, Sophorn Chip, Anna Maria-Calella, Nicolas Zeller, Harald Seeger, Jeppe Falsig, Olivier Giger, Giuseppe Manco, Dimitri Gourionov, Audrey Marcel, Christina Sigurdson, Dorothea Rutishauser, Magda Polymenidou, Li-Chun Infanger, Peter Nillson, Sophia Fransson, Ilan Margalith, Antoinette Schuhmacher and Jacqueline Wiedler for discussion and support in various lab and administrative domains.

Susanna Bachmann from the Molecular Life Science Zurich program for a perfectly organized graduate school.

The **Swiss National Science Foundation** for its generous financial support during the MD-PhD studies.

Simon Schmid for critically reading the manuscript in its early phase.

Ethan Taub for his great support in the clinics, for teaching me neurosurgery with great patience and diligence and a fine sense of humor - and especially for reading and correcting my thesis thoroughly to meet real English standards.

This work is dedicated to my parents who supported me throughout my life in an extremely generous and loving manner.

Bibliography

[1] Adriano Aguzzi. Prion diseases of humans and farm animals: epidemiology, genetics, and pathogenesis. *J Neurochem*, 97(6):1726–1739, Jun 2006.

[2] Adriano Aguzzi and Mathias Heikenwalder. Pathogenesis of prion diseases: current status and future outlook. *Nat Rev Microbiol*, 4(10):765–775, Oct 2006.

[3] Adriano Aguzzi and Magdalini Polymenidou. Mammalian prion biology: one century of evolving concepts. *Cell*, 116(2):313–327, Jan 2004.

[4] Adriano Aguzzi and Christina J Sigurdson. Antiprion immunotherapy: to suppress or to stimulate? *Nat Rev Immunol*, 4(9):725–736, Sep 2004.

[5] T. Alper, D. A. Haig, and M. C. Clarke. The exceptionally small size of the scrapie agent. *Biochem Biophys Res Commun*, 22(3):278–284, Feb 1966.

[6] Emmanuel A Asante, Jacqueline M Linehan, Melanie Desbruslais, Susan Joiner, Ian Gowland, Andrew L Wood, Julie Welch, Andrew F Hill, Sarah E Lloyd, Jonathan D F Wadsworth, and John Collinge. Bse prions propagate as either variant cjd-like or sporadic cjd-like prion strains in transgenic mice expressing human prion protein. *EMBO J*, 21(23):6358–6366, Dec 2002.

[7] Christopher A Baker and Laura Manuelidis. Unique inflammatory rna profiles of microglia in creutzfeldt-jakob disease. *Proc Natl Acad Sci U S A*, 100(2):675–679, Jan 2003.

[8] Clara Ballerini, Pauline Gourdain, Véronique Bachy, Nicolas Blanchard, Etienne Levavasseur, Sylvie Grégoire, Pascaline Fontes, Pierre Aucouturier, Claire Hivroz, and Claude Carnaud. Functional implication of cellular prion protein in antigen-driven interactions between t cells and dendritic cells. *J Immunol*, 176(12):7254–7262, Jun 2006.

[9] A. Neil Barclay and Marion H Brown. The sirp family of receptors and immune regulation. *Nat Rev Immunol*, 6(6):457–464, Jun 2006.

[10] K. Basler, B. Oesch, M. Scott, D. Westaway, M. Wälchli, D. F. Groth, M. P. McKinley, S. B. Prusiner, and C. Weissmann. Scrapie and cellular prp isoforms are encoded by the same chromosomal gene. *Cell*, 46(3):417–428, Aug 1986.

[11] Frank Baumann, Markus Tolnay, Christine Brabeck, Jens Pahnke, Ulrich Kloz, Hartmut H Niemann, Mathias Heikenwalder, Thomas Rülicke, Alexander Bürkle, and Adriano Aguzzi. Lethal recessive myelin toxicity of prion protein lacking its central domain. *EMBO J*, 26(2):538–547, Jan 2007.

[12] H. Büeler, A. Aguzzi, A. Sailer, R. A. Greiner, P. Autenried, M. Aguet, and C. Weissmann. Mice devoid of prp are resistant to scrapie. *Cell*, 73(7):1339–1347, Jul 1993.

[13] H. Büeler, M. Fischer, Y. Lang, H. Bluethmann, H. P. Lipp, S. J. DeArmond, S. B. Prusiner, M. Aguet, and C. Weissmann. Normal development and behaviour of mice lacking the neuronal cell-surface prp protein. *Nature*, 356(6370):577–582, Apr 1992.

[14] C. Bernoulli, J. Siegfried, G. Baumgartner, F. Regli, T. Rabinowicz, D. C. Gajdusek, and C. J. Gibbs. Danger of accidental person-to-person transmission of creutzfeldt-jakob disease by surgery. *Lancet*, 1(8009):478–479, Feb 1977.

[15] T. Blättler, S. Brandner, A. J. Raeber, M. A. Klein, T. Voigtländer, C. Weissmann, and A. Aguzzi. Prp-expressing tissue required for transfer of scrapie infectivity from spleen to brain. *Nature*, 389(6646):69–73, Sep 1997.

[16] J. Burthem, B. Urban, A. Pain, and D. J. Roberts. The normal cellular prion protein is strongly expressed by myeloid dendritic cells. *Blood*, 98(13):3733–3738, Dec 2001.

[17] D. A. Butler, M. R. Scott, J. M. Bockman, D. R. Borchelt, A. Taraboulos, K. K. Hsiao, D. T. Kingsbury, and S. B. Prusiner. Scrapie-infected murine neuroblastoma cells produce protease-resistant prion proteins. *J Virol*, 62(5):1558–1564, May 1988.

[18] Byron Caughey and Gerald S Baron. Prions and their partners in crime. *Nature*, 443(7113):803–810, Oct 2006.

[19] S. W. Christianson, D. L. Greiner, I. B. Schweitzer, B. Gott, G. L. Beamer, P. A. Schweitzer, R. M. Hesselton, and L. D. Shultz. Role of natural killer cells on engraftment of human lymphoid cells and on metastasis of human t-lymphoblastoid leukemia cells in c57bl/6j-scid mice and in c57bl/6j-scid bg mice. *Cell Immunol*, 171(2):186–199, Aug 1996.

[20] M. C. Clarke and R. H. Kimberlin. Pathogenesis of mouse scrapie: distribution of agent in the pulp and stroma of infected spleens. *Vet Microbiol*, 9(3):215–225, Jul 1984.

[21] Chelle PJ Cuille J. La "tremblante du mouton est bien inoculable. *Comptes rendus des Seances de lAcademie des Sciences*, 206:78–79, 1936.

[22] Cecília J G de Almeida, Luciana B Chiarini, Juliane Pereira da Silva, Patrícia M R E Silva, Marco Aurélio Martins, and Rafael Linden. The cellular prion protein modulates phagocytosis and inflammatory response. *J Leukoc Biol*, 77(2):238–246, Feb 2005.

[23] V. C. Dodelet and N. R. Cashman. Prion protein expression in human leukocyte differentiation. *Blood*, 91(5):1556–1561, Mar 1998.

[24] K. Doh-ura, S. Perryman, R. Race, and B. Chesebro. Identification of differentially expressed genes in scrapie-infected mouse neuroblastoma cells. *Microb Pathog*, 18(1):1–9, Jan 1995.

[25] P. Duffy, J. Wolf, G. Collins, A. G. DeVoe, B. Streeten, and D. Cowen. Letter: Possible person-to-person transmission of creutzfeldt-jakob disease. *N Engl J Med*, 290(12):692–693, Mar 1974.

[26] S. Dziennis, R. A. Van Etten, H. L. Pahl, D. L. Morris, T. L. Rothstein, C. M. Blosch, R. M. Perlmutter, and D. G. Tenen. The cd11b promoter directs high-level expression of reporter genes in macrophages in transgenic mice. *Blood*, 85(2):319–329, Jan 1995.

[27] Sandra Fernaeus, Jonas Hälldin, Katarina Bedecs, and Tiit Land. Changed iron regulation in scrapie-infected neuroblastoma cells. *Brain Res Mol Brain Res*, 133(2):266–273, Feb 2005.

[28] Sandra Fernaeus and Tiit Land. Increased iron-induced oxidative stress and toxicity in scrapie-infected neuroblastoma cells. *Neurosci Lett*, 382(3):217–220, Jul 2005.

[29] Jonathan Flint, William Valdar, Sagiv Shifman, and Richard Mott. Strategies for mapping and cloning quantitative trait genes in rodents. *Nat Rev Genet*, 6(4):271–286, Apr 2005.

[30] Pascaline Fontes, Maria-Teresa Alvarez-Martinez, Antoine Gross, Claude Carnaud, Stephan Köhler, and Jean-Pierre Liautard. Absence of evidence for the participation of the macrophage cellular prion protein in infection with brucella suis. *Infect Immun*, 73(10):6229–6236, Oct 2005.

[31] M. J. Ford, L. J. Burton, R. J. Morris, and S. M. Hall. Selective expression of prion protein in peripheral tissues of the adult mouse. *Neuroscience*, 113(1):177–192, 2002.

[32] H. Fraser and A. G. Dickinson. Pathogenesis of scrapie in the mouse: the role of the spleen. *Nature*, 226(5244):462–463, May 1970.

[33] H. Fraser and C. F. Farquhar. Ionising radiation has no influence on scrapie incubation period in mice. *Vet Microbiol*, 13(3):211–223, Mar 1987.

[34] D. C. Gajdusek, C. J. Gibbs, and M. Alpers. Experimental transmission of a kuru-like syndrome to chimpanzees. *Nature*, 209(5025):794–796, Feb 1966.

[35] D. C. Gajdusek, C. J. Gibbs, and M. Alpers. Transmission and passage of experimenal "kuru" to chimpanzees. *Science*, 155(759):212–214, Jan 1967.

[36] D. C. Gajdusek, C. J. Gibbs, D. M. Asher, P. Brown, A. Diwan, P. Hoffman, G. Nemo, R. Rohwer, and L. White. Precautions in medical care of, and in handling materials from, patients with transmissible virus dementia (creutzfeldt-jakob disease). *N Engl J Med*, 297(23):1253–1258, Dec 1977.

[37] D. C. Gajdusek, C. J. Gibbs, D. M. Asher, and E. David. Transmission of experimental kuru to the spider monkey (ateles geoffreyi). *Science*, 162(854):693–694, Nov 1968.

[38] Michael D Geschwind, Jennifer Martindale, Deborah Miller, Stephen J DeArmond, Jane Uyehara-Lock, David Gaskin, Joel H Kramer, Nicholas M Barbaro, and Bruce L Miller. Challenging the clinical utility of the 14-3-3 protein for the diagnosis of sporadic creutzfeldt-jakob disease. *Arch Neurol*, 60(6):813–816, Jun 2003.

[39] Markus Glatzel, Eugenio Abela, Manuela Maissen, and Adriano Aguzzi. Extraneural pathologic prion protein in sporadic creutzfeldt-jakob disease. *N Engl J Med*, 349(19):1812–1820, Nov 2003.

[40] Markus Glatzel, Colette Rogivue, Azra Ghani, Johannes R Streffer, Lorenz Amsler, and Adriano Aguzzi. Incidence of creutzfeldt-jakob disease in switzerland. *Lancet*, 360(9327):139–141, Jul 2002.

[41] Markus Glatzel, Katharina Stoeck, Harald Seeger, Thorsten Lührs, and Adriano Aguzzi. Human prion diseases: molecular and clinical aspects. *Arch Neurol*, 62(4):545–552, Apr 2005.

[42] Alex D Greenwood, Marion Horsch, Anna Stengel, Ina Vorberg, Gloria Lutzny, Elke Maas, Sandra Schädler, Volker Erfle, Johannes Beckers, Hermann Schätzl, and Christine Leib-Mösch. Cell line dependent rna expression profiles of prion-infected mouse neuronal cells. *J Mol Biol*, 349(3):487–500, Jun 2005.

[43] J. S. Griffith. Self-replication and scrapie. *Nature*, 215(5105):1043–1044, Sep 1967.

[44] Deborah Hatherley, Karl Harlos, D. Cameron Dunlop, David I Stuart, and A. Neil Barclay. The structure of the macrophage signal regulatory protein alpha (sirpalpha) inhibitory receptor reveals a binding face reminiscent of that used by t cell receptors. *J Biol Chem*, 282(19):14567–14575, May 2007.

[45] Mathias Heikenwalder, Nicolas Zeller, Harald Seeger, Marco Prinz, Peter-Christian Klöhn, Petra Schwarz, Nancy H Ruddle, Charles Weissmann, and Adriano Aguzzi. Chronic lymphocytic inflammation specifies the organ tropism of prions. *Science*, 307(5712):1107–1110, Feb 2005.

[46] R. M. Hesselton, D. L. Greiner, J. P. Mordes, T. V. Rajan, J. L. Sullivan, and L. D. Shultz. High levels of human peripheral blood mononuclear cell engraftment and enhanced susceptibility to human immunodeficiency virus type 1 infection in nod/ltsz-scid/scid mice. *J Infect Dis*, 172(4):974–982, Oct 1995.

[47] Claudio Hetz, Milene Russelakis-Carneiro, Kinsey Maundrell, Joaquin Castilla, and Claudio Soto. Caspase-12 and endoplasmic reticulum stress mediate neurotoxicity of pathological prion protein. *EMBO J*, 22(20):5435–5445, Oct 2003.

[48] K. Holada and J. G. Vostal. Different levels of prion protein (prpc) expression on hamster, mouse and human blood cells. *Br J Haematol*, 110(2):472–480, Aug 2000.

[49] Karel Holada, Jan Simak, Paul Brown, and Jaroslav G Vostal. Divergent expression of cellular prion protein on blood cells of human and nonhuman primates. *Transfusion*, 47(12):2223–2232, Dec 2007.

[50] J. Hope. The biology and molecular biology of scrapie-like diseases. *Arch Virol Suppl*, 7:201–214, 1993.

[51] K. Hoshi, H. Yoshino, J. Urata, Y. Nakamura, H. Yanagawa, and T. Sato. Creutzfeldt-jakob disease associated with cadaveric dura mater grafts in japan. *Neurology*, 55(5):718–721, Sep 2000.

[52] G. Hsich, K. Kenney, C. J. Gibbs, K. H. Lee, and M. G. Harrington. The 14-3-3 brain protein in cerebrospinal fluid as a marker for transmissible spongiform encephalopathies. *N Engl J Med*, 335(13):924–930, Sep 1996.

[53] Earl Hubbell, Wei-Min Liu, and Rui Mei. Robust estimators for expression analysis. *Bioinformatics*, 18(12):1585–1592, Dec 2002.

[54] Kentaro Ide, Hui Wang, Hiroyuki Tahara, Jianxiang Liu, Xiaoying Wang, Toshimasa Asahara, Megan Sykes, Yong-Guang Yang, and Hideki Ohdan. Role for cd47-sirpalpha signaling in xenograft rejection by macrophages. *Proc Natl Acad Sci U S A*, 104(12):5062–5066, Mar 2007.

[55] Fumihiko Ishikawa, Masaki Yasukawa, Bonnie Lyons, Shuro Yoshida, Toshihiro Miyamoto, Goichi Yoshimoto, Takeshi Watanabe, Koichi Akashi, Leonard D Shultz, and Mine Harada. Development of functional human blood and immune systems in nod/scid/il2 receptor gamma chain(null) mice. *Blood*, 106(5):1565–1573, Sep 2005.

[56] Mamoru Ito, Hidefumi Hiramatsu, Kimio Kobayashi, Kazutomo Suzue, Mariko Kawahata, Kyoji Hioki, Yoshito Ueyama, Yoshio Koyanagi, Kazuo Sugamura, Kohichiro Tsuji, Toshio Heike, and Tatsutoshi Nakahata. Nod/scid/gamma(c)(null) mouse: an excellent recipient mouse model for engraftment of human cells. *Blood*, 100(9):3175–3182, Nov 2002.

[57] Kirsty Jensen, Edith Paxton, David Waddington, Richard Talbot, Mohamed A Darghouth, and Elizabeth J Glass. Differences in the transcriptional responses induced by theileria annulata infection in bovine monocytes derived from resistant and susceptible cattle breeds. *Int J Parasitol*, Sep 2007.

[58] P. S. Kaeser, M. A. Klein, P. Schwarz, and A. Aguzzi. Efficient lymphoreticular prion propagation requires prp(c) in stromal and hematopoietic cells. *J Virol*, 75(15):7097–7106, Aug 2001.

[59] R. H. Kimberlin and C. A. Walker. The role of the spleen in the neuroinvasion of scrapie in mice. *Virus Res*, 12(3):201–211, Mar 1989.

[60] M. A. Klein, R. Frigg, E. Flechsig, A. J. Raeber, U. Kalinke, H. Bluethmann, F. Bootz, M. Suter, R. M. Zinkernagel, and A. Aguzzi. A crucial role for b cells in neuroinvasive scrapie. *Nature*, 390(6661):687–690, 1997.

[61] P-C. Klöhn, L. Stoltze, E. Flechsig, M. Enari, and C. Weissmann. A quantitative, highly sensitive cell-based infectivity assay for mouse scrapie prions. *Proc Natl Acad Sci U S A*, 100(20):11666–11671, Sep 2003.

[62] T. K. Koch, B. O. Berg, S. J. De Armond, and R. F. Gravina. Creutzfeldt-jakob disease in a young adult with idiopathic hypopituitarism. possible relation to the administration of cadaveric human growth hormone. *N Engl J Med*, 313(12):731–733, Sep 1985.

[63] Mark Kristiansen, Marcus J Messenger, Peter-Christian Klöhn, Sebastian Brandner, Jonathan D F Wadsworth, John Collinge, and Sarah J Tabrizi. Disease-related prion protein forms aggresomes in neuronal cells leading to caspase activation and apoptosis. *J Biol Chem*, 280(46):38851–38861, Nov 2005.

[64] T. Lapidot, F. Pflumio, M. Doedens, B. Murdoch, D. E. Williams, and J. E. Dick. Cytokine stimulation of multilineage hematopoiesis from immature human cells engrafted in scid mice. *Science*, 255(5048):1137–1141, Feb 1992.

[65] R. Li, D. Liu, G. Zanusso, T. Liu, J. D. Fayen, J. H. Huang, R. B. Petersen, P. Gambetti, and M. S. Sy. The expression and potential function of cellular prion protein in human lymphocytes. *Cell Immunol*, 207(1):49–58, Jan 2001.

[66] T. Liu, R. Li, B. S. Wong, D. Liu, T. Pan, R. B. Petersen, P. Gambetti, and M. S. Sy. Normal cellular prion protein is preferentially expressed on subpopulations of murine hemopoietic cells. *J Immunol*, 166(6):3733–3742, Mar 2001.

[67] Yuan Liu, Qiao Tong, Yubin Zhou, Hsiau-Wei Lee, Jenny J Yang, Hans-Jörg Bühring, Yi-Tien Chen, Binh Ha, Celia X-J Chen, Yang Yang, and Ke Zen. Functional elements on sirpalpha igv domain mediate cell surface binding to cd47. *J Mol Biol*, 365(3):680–693, Jan 2007.

[68] C. A. Llewelyn, P. E. Hewitt, R. S G Knight, K. Amar, S. Cousens, J. Mackenzie, and R. G. Will. Possible transmission of variant creutzfeldt-jakob disease by blood transfusion. *Lancet*, 363(9407):417–421, Feb 2004.

[69] P. A. Lowry, L. D. Shultz, D. L. Greiner, R. M. Hesselton, E. L. Kittler, C. Y. Tiarks, S. S. Rao, J. Reilly, J. H. Leif, H. Ramshaw, F. M. Stewart, and P. J. Quesenberry. Improved engraftment of human cord blood stem cells in nod/ltsz-scid/scid mice after irradiation or multiple-day injections into unirradiated recipients. *Biol Blood Marrow Transplant*, 2(1):15–23, Feb 1996.

[70] Marius Lötscher, Mike Recher, Karl S Lang, Alexander Navarini, Lukas Hunziker, Roger Santimaria, Markus Glatzel, Petra Schwarz, Jürg Böni, and Rolf M Zinker-

nagel. Induced prion protein controls immune-activated retroviruses in the mouse spleen. *PLoS ONE*, 2(11):e1158, 2007.

[71] W m Liu, R. Mei, X. Di, T. B. Ryder, E. Hubbell, S. Dee, T. A. Webster, C. A. Harrington, M h Ho, J. Baid, and S. P. Smeekens. Analysis of high density expression microarrays with signed-rank call algorithms. *Bioinformatics*, 18(12):1593–1599, Dec 2002.

[72] Neil A Mabbott and Moira E Bruce. Prion disease: bridging the spleen-nerve gap. *Nat Med*, 9(12):1463–1464, Dec 2003.

[73] G. R. Mallucci, S. Ratté, E. A. Asante, J. Linehan, I. Gowland, J. G R Jefferys, and J. Collinge. Post-natal knockout of prion protein alters hippocampal ca1 properties, but does not result in neurodegeneration. *EMBO J*, 21(3):202–210, Feb 2002.

[74] L. Manuelidis, I. Zaitsev, P. Koni, Z. Y. Lu, R. A. Flavell, and W. Fritch. Follicular dendritic cells and dissemination of creutzfeldt-jakob disease. *J Virol*, 74(18):8614–8622, Sep 2000.

[75] Laura Manuelidis. A virus behind the mask of prions? *Folia Neuropathol*, 42 Suppl B:10–23, 2004.

[76] Laura Manuelidis. A 25 nm virion is the likely cause of transmissible spongiform encephalopathies. *J Cell Biochem*, 100(4):897–915, Mar 2007.

[77] C. L. Masters, D. C. Gajdusek, and C. J. Gibbs. Creutzfeldt-jakob disease virus isolations from the gerstmann-sträussler syndrome with an analysis of the various forms of amyloid plaque deposition in the virus-induced spongiform encephalopathies. *Brain*, 104(3):559–588, Sep 1981.

[78] I. E. Mazzoni, H. C. Ledebur, E. Paramithiotis, and N. Cashman. Lymphoid signal transduction mechanisms linked to cellular prion protein. *Biochem Cell Biol*, 83(5):644–653, Oct 2005.

[79] J. M. McCune, R. Namikawa, H. Kaneshima, L. D. Shultz, M. Lieberman, and I. L. Weissman. The scid-hu mouse: murine model for the analysis of human hematolymphoid differentiation and function. *Science*, 241(4873):1632–1639, Sep 1988.

[80] M. P. McKinley, D. C. Bolton, and S. B. Prusiner. A protease-resistant protein is a structural component of the scrapie prion. *Cell*, 35(1):57–62, Nov 1983.

[81] G. Miele, J. Manson, and M. Clinton. A novel erythroid-specific marker of transmissible spongiform encephalopathies. *Nat Med*, 7(3):361–364, Mar 2001.

[82] O. Milhavet, H. E. McMahon, W. Rachidi, N. Nishida, S. Katamine, A. Mangé, M. Arlotto, D. Casanova, J. Riondel, A. Favier, and S. Lehmann. Prion infection impairs the cellular response to oxidative stress. *Proc Natl Acad Sci U S A*, 97(25):13937–13942, Dec 2000.

[83] S. Mohri, S. Handa, and J. Tateishi. Lack of effect of thymus and spleen on the incubation period of creutzfeldt-jakob disease in mice. *J Gen Virol*, 68 (Pt 4):1187–1189, Apr 1987.

[84] P. Mombaerts, J. Iacomini, R. S. Johnson, K. Herrup, S. Tonegawa, and V. E. Papaioannou. Rag-1-deficient mice have no mature b and t lymphocytes. *Cell*, 68(5):869–877, Mar 1992.

[85] D. E. Mosier, R. J. Gulizia, S. M. Baird, and D. B. Wilson. Transfer of a functional human immune system to mice with severe combined immunodeficiency. *Nature*, 335(6187):256–259, Sep 1988.

[86] K. Ohbo, T. Suda, M. Hashiyama, A. Mantani, M. Ikebe, K. Miyakawa, M. Moriyama, M. Nakamura, M. Katsuki, K. Takahashi, K. Yamamura, and K. Sugamura. Modulation of hematopoiesis in mice with a truncated mutant of the interleukin-2 receptor gamma chain. *Blood*, 87(3):956–967, Feb 1996.

[87] Michael B A Oldstone, Richard Race, Diane Thomas, Hanna Lewicki, Dirk Homann, Sara Smelt, Andreas Holz, Pandelakis Koni, David Lo, Bruce Chesebro, and Richard Flavell. Lymphotoxin-alpha- and lymphotoxin-beta-deficient mice differ in susceptibility to scrapie: evidence against dendritic cell involvement in neuroinvasion. *J Virol*, 76(9):4357–4363, May 2002.

[88] P. Parchi, S. Capellari, S. G. Chen, R. B. Petersen, P. Gambetti, N. Kopp, P. Brown, T. Kitamoto, J. Tateishi, A. Giese, and H. Kretzschmar. Typing prion isoforms. *Nature*, 386(6622):232–234, Mar 1997.

[89] P. Parchi, R. Castellani, S. Capellari, B. Ghetti, K. Young, S. G. Chen, M. Farlow, D. W. Dickson, A. A. Sima, J. Q. Trojanowski, R. B. Petersen, and P. Gambetti. Molecular basis of phenotypic variability in sporadic creutzfeldt-jakob disease. *Ann Neurol*, 39(6):767–778, Jun 1996.

[90] G. Politopoulou, J. D. Seebach, M. Schmugge, H. P. Schwarz, and A. Aguzzi. Age-related expression of the cellular prion protein in human peripheral blood leukocytes. *Haematologica*, 85(6):580–587, Jun 2000.

[91] Magdalini Polymenidou, Katharina Stoeck, Markus Glatzel, Martin Vey, Anne Bellon, and Adriano Aguzzi. Coexistence of multiple prpsc types in individuals with creutzfeldt-jakob disease. *Lancet Neurol*, 4(12):805–814, Dec 2005.

[92] Marco Prinz, Mathias Heikenwalder, Tobias Junt, Petra Schwarz, Markus Glatzel, Frank L Heppner, Yang-Xin Fu, Martin Lipp, and Adriano Aguzzi. Positioning of follicular dendritic cells within the spleen controls prion neuroinvasion. *Nature*, 425(6961):957–962, Oct 2003.

[93] Marco Prinz, Fabio Montrasio, Michael A Klein, Petra Schwarz, Josef Priller, Bernhard Odermatt, Klaus Pfeffer, and Adriano Aguzzi. Lymph nodal prion

replication and neuroinvasion in mice devoid of follicular dendritic cells. *Proc Natl Acad Sci U S A*, 99(2):919–924, Jan 2002.

[94] J. K. Pritchard, M. Stephens, and P. Donnelly. Inference of population structure using multilocus genotype data. *Genetics*, 155(2):945–959, Jun 2000.

[95] S. B. Prusiner, D. F. Groth, S. P. Cochran, F. R. Masiarz, M. P. McKinley, and H. M. Martinez. Molecular properties, partial purification, and assay by incubation period measurements of the hamster scrapie agent. *Biochemistry*, 19(21):4883–4891, Oct 1980.

[96] Y. Qi, J. K. Wang, M. McMillian, and D. M. Chikaraishi. Characterization of a cns cell line, cad, in which morphological differentiation is initiated by serum deprivation. *J Neurosci*, 17(4):1217–1225, Feb 1997.

[97] William M Ridgway, Barry Healy, Luc J Smink, Dan Rainbow, and Linda S Wicker. New tools for defining the 'genetic background' of inbred mouse strains. *Nat Immunol*, 8(7):669–673, Jul 2007.

[98] R. Riek, S. Hornemann, G. Wider, M. Billeter, R. Glockshuber, and K. Wüthrich. Nmr structure of the mouse prion protein domain prp(121-321). *Nature*, 382(6587):180–182, Jul 1996.

[99] C. Riemer, I. Queck, D. Simon, R. Kurth, and M. Baier. Identification of upregulated genes in scrapie-infected brain tissue. *J Virol*, 74(21):10245–10248, Nov 2000.

[100] Constanze Riemer, Sabine Neidhold, Michael Burwinkel, Anja Schwarz, Julia Schultz, Jörn Krätzschmar, Ursula Mönning, and Michael Baier. Gene expression profiling of scrapie-infected brain tissue. *Biochem Biophys Res Commun*, 323(2):556–564, Oct 2004.

[101] Eric Rivera-Milla, Claudia A O Stuermer, and Edward Málaga-Trillo. An evolutionary basis for scrapie disease: identification of a fish prion mrna. *Trends Genet*, 19(2):72–75, Feb 2003.

[102] Eric D Ross and Reed B Wickner. Prions of yeast fail to elicit a transcriptional response. *Yeast*, 21(11):963–972, Aug 2004.

[103] R. Rubenstein, R. I. Carp, and S. M. Callahan. In vitro replication of scrapie agent in a neuronal model: infection of pc12 cells. *J Gen Virol*, 65 (Pt 12):2191–2198, Dec 1984.

[104] H. M. Schätzl, L. Laszlo, D. M. Holtzman, J. Tatzelt, S. J. DeArmond, R. I. Weiner, W. C. Mobley, and S. B. Prusiner. A hypothalamic neuronal cell line persistently infected with scrapie prions exhibits apoptosis. *J Virol*, 71(11):8821–8831, Nov 1997.

[105] Y. Shinkai, G. Rathbun, K. P. Lam, E. M. Oltz, V. Stewart, M. Mendelsohn, J. Charron, M. Datta, F. Young, and A. M. Stall. Rag-2-deficient mice lack mature lymphocytes owing to inability to initiate v(d)j rearrangement. *Cell*, 68(5):855–867, Mar 1992.

[106] M. J. Shlomchik, K. Radebold, N. Duclos, and L. Manuelidis. Neuroinvasion by a creutzfeldt-jakob disease agent in the absence of b cells and follicular dendritic cells. *Proc Natl Acad Sci U S A*, 98(16):9289–9294, Jul 2001.

[107] D. Shmerling, I. Hegyi, M. Fischer, T. Blättler, S. Brandner, J. Götz, T. Rülicke, E. Flechsig, A. Cozzio, C. von Mering, C. Hangartner, A. Aguzzi, and C. Weissmann. Expression of amino-terminally truncated prp in the mouse leading to ataxia and specific cerebellar lesions. *Cell*, 93(2):203–214, Apr 1998.

[108] L. D. Shultz, P. A. Schweitzer, S. W. Christianson, B. Gott, I. B. Schweitzer, B. Tennent, S. McKenna, L. Mobraaten, T. V. Rajan, and D. L. Greiner. Multiple defects in innate and adaptive immunologic function in nod/ltsz-scid mice. *J Immunol*, 154(1):180–191, Jan 1995.

[109] Leonard D Shultz, Fumihiko Ishikawa, and Dale L Greiner. Humanized mice in translational biomedical research. *Nat Rev Immunol*, 7(2):118–130, Feb 2007.

[110] Leonard D Shultz, Bonnie L Lyons, Lisa M Burzenski, Bruce Gott, Xiaohua Chen, Stanley Chaleff, Malak Kotb, Stephen D Gillies, Marie King, Julie Mangada, Dale L Greiner, and Rupert Handgretinger. Human lymphoid and myeloid cell development in nod/ltsz-scid il2r gamma null mice engrafted with mobilized human hemopoietic stem cells. *J Immunol*, 174(10):6477–6489, May 2005.

[111] Christina J Sigurdson, K. Peter R Nilsson, Simone Hornemann, Giuseppe Manco, Magdalini Polymenidou, Petra Schwarz, Mario Leclerc, Per Hammarström, Kurt Wüthrich, and Adriano Aguzzi. Prion strain discrimination using luminescent conjugated polymers. *Nat Methods*, 4(12):1023–1030, Dec 2007.

[112] T. Simonic, S. Duga, B. Strumbo, R. Asselta, F. Ceciliani, and S. Ronchi. cdna cloning of turtle prion protein. *FEBS Lett*, 469(1):33–38, Mar 2000.

[113] Andrew D Steele, Jason G Emsley, P. Hande Ozdinler, Susan Lindquist, and Jeffrey D Macklis. Prion protein (prpc) positively regulates neural precursor proliferation during developmental and adult mammalian neurogenesis. *Proc Natl Acad Sci U S A*, 103(9):3416–3421, Feb 2006.

[114] B. Strumbo, S. Ronchi, L. C. Bolis, and T. Simonic. Molecular cloning of the cdna coding for xenopus laevis prion protein. *FEBS Lett*, 508(2):170–174, Nov 2001.

[115] Makoto Sugaya, Koichiro Nakamura, Takahiro Watanabe, Akihiko Asahina, Nami Yasaka, Yoh ichi Koyama, Masashi Kusubata, Yuko Ushiki, Kumiko Kimura, Akira Morooka, Shinkichi Irie, Takashi Yokoyama, Keiichi Inoue, Shigeyosi Itohara, and

Kunihiko Tamaki. Expression of cellular prion-related protein by murine langerhans cells and keratinocytes. *J Dermatol Sci*, 28(2):126–134, Feb 2002.

[116] Katsuto Takenaka, Tatiana K Prasolava, Jean C Y Wang, Steven M Mortin-Toth, Sam Khalouei, Olga I Gan, John E Dick, and Jayne S Danska. Polymorphism in sirpa modulates engraftment of human hematopoietic stem cells. *Nat Immunol*, 8(12):1313–1323, Dec 2007.

[117] J. Tateishi, M. Ohta, M. Koga, Y. Sato, and Y. Kuroiwa. Transmission of chronic spongiform encephalopathy with kuru plaques from humans to small rodents. *Ann Neurol*, 5(6):581–584, Jun 1979.

[118] J. Tateishi, Y. Sato, M. Koga, H. Doi, and M. Ohta. Experimental transmission of human subacute spongiform encephalopathy to small rodents. i. clinical and histological observations. *Acta Neuropathol*, 51(2):127–134, 1980.

[119] Elisabetta Traggiai, Laurie Chicha, Luca Mazzucchelli, Lucio Bronz, Jean-Claude Piffaretti, Antonio Lanzavecchia, and Markus G Manz. Development of a human adaptive immune system in cord blood cell-transplanted mice. *Science*, 304(5667):104–107, Apr 2004.

[120] N. van Rooijen and R. van Nieuwmegen. Elimination of phagocytic cells in the spleen after intravenous injection of liposome-encapsulated dichloromethylene diphosphonate. an enzyme-histochemical study. *Cell Tissue Res*, 238(2):355–358, 1984.

[121] E. Wakeland, L. Morel, K. Achey, M. Yui, and J. Longmate. Speed congenics: a classic technique in the fast lane (relatively speaking). *Immunol Today*, 18(10):472–477, Oct 1997.

[122] Masahisa Watarai, Suk Kim, Janchivdorj Erdenebaatar, Sou ichi Makino, Motohiro Horiuchi, Toshikazu Shirahata, Suehiro Sakaguchi, and Shigeru Katamine. Cellular prion protein promotes brucella infection into macrophages. *J Exp Med*, 198(1):5–17, Jul 2003.

[123] Charles Weissmann. Birth of a prion: spontaneous generation revisited. *Cell*, 122(2):165–168, Jul 2005.

[124] G. A. Wells, A. C. Scott, C. T. Johnson, R. F. Gunning, R. D. Hancock, M. Jeffrey, M. Dawson, and R. Bradley. A novel progressive spongiform encephalopathy in cattle. *Vet Rec*, 121(18):419–420, Oct 1987.

[125] R. G. Will, J. W. Ironside, M. Zeidler, S. N. Cousens, K. Estibeiro, A. Alperovitch, S. Poser, M. Pocchiari, A. Hofman, and P. G. Smith. A new variant of creutzfeldt-jakob disease in the uk. *Lancet*, 347(9006):921–925, Apr 1996.

[126] Robert G Will. Acquired prion disease: iatrogenic cjd, variant cjd, kuru. *Br Med Bull*, 66:255–265, 2003.

[127] E. S. Williams and S. Young. Chronic wasting disease of captive mule deer: a spongiform encephalopathy. *J Wildl Dis*, 16(1):89–98, Jan 1980.

[128] Zhijin Wu and Rafael A Irizarry. Preprocessing of oligonucleotide array data. *Nat Biotechnol*, 22(6):656–8; author reply 658, Jun 2004.

[129] Wei Xiang, Otto Windl, Gerda Wünsch, Martin Dugas, Alexander Kohlmann, Nicola Dierkes, Ingo M Westner, and Hans A Kretzschmar. Identification of differentially expressed genes in scrapie-infected mouse brains by using global gene expression technology. *J Virol*, 78(20):11051–11060, Oct 2004.

[130] Cheng Cheng Zhang, Andrew D Steele, Susan Lindquist, and Harvey F Lodish. Prion protein is expressed on long-term repopulating hematopoietic stem cells and is important for their self-renewal. *Proc Natl Acad Sci U S A*, 103(7):2184–2189, Feb 2006.